Heliospheric Tomography used to Provide Velocities, Densities, and Vector Magnetic Fields

B.V. Jackson
and
H.-S. Yu, P.P. Hick, A. Buffington, D. Odstrcil
Center for Astrophysics and Space Sciences,
University of California at San Diego, LaJolla, CA, USA

http://smei.ucsd.edu/ **http://ips.ucsd.edu/**

Heliospheric Tomography

Introduction:

Motive:

Current progress in heliospheric tomography.

Data Set/Analysis:

Interplanetary scintillation (IPS) mainly from STELab, Japan.

Heliospheric Tomography:

3-D Heliospheric Tomography (a fit to data – a time-dependent heliospheric view from a single observer location)

Speeds and densities from the IPS, vector fields from solar surface magnetic field maps.

Current Applications:

Accurate and continuously verifiable forecasts, analysis using 3D-MHD models including ENLIL, Faraday Rotation

Heliospheric Tomography

Interplanetary Scintillation (IPS) Analysis

Heliospheric Tomography

DATA

IPS Heliospheric Analyses (STELab)

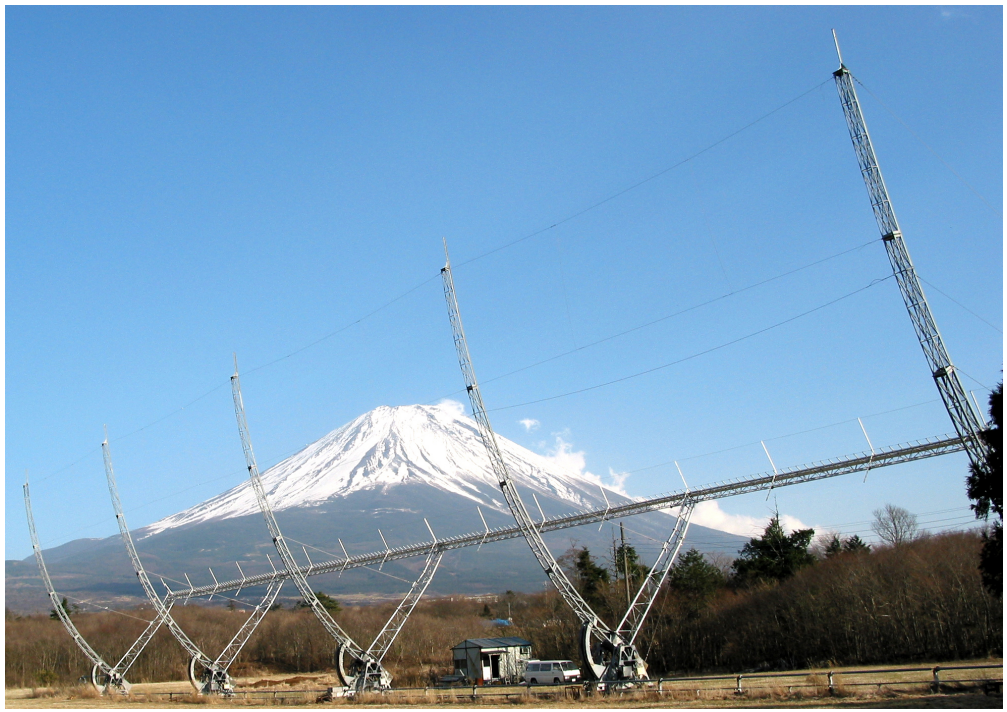

STELab IPS array near Mt. Fuji

STELab IPS array systems

Heliospheric Tomography

DATA

IPS Heliospheric Analyses (STELab)

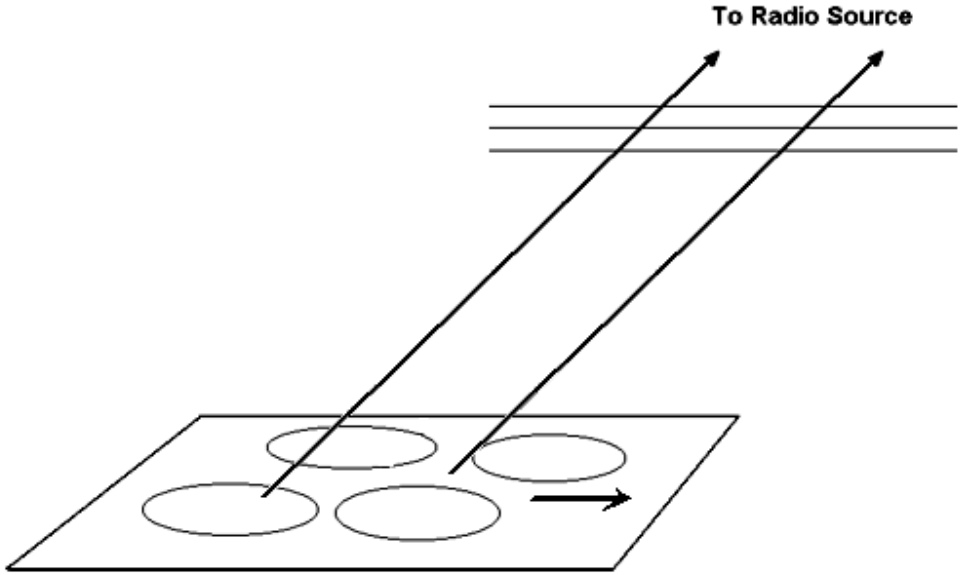

IPS line-of-sight response

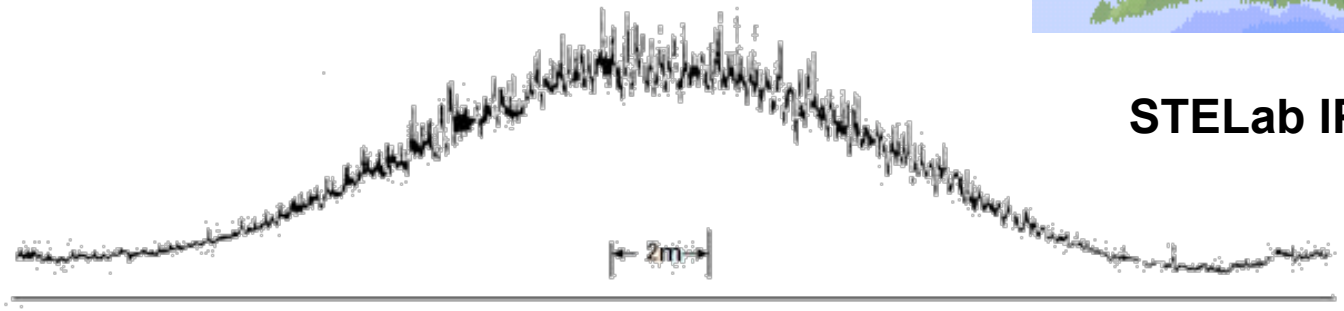

STELab IPS array systems

Heliospheric Tomography

Current STELab Toyokawa IPS System

New STELab IPS array in Toyokawa
(3,432 m^2 array now operates well – year-round operation began in 2011)

Heliospheric Tomography

Other Current Operating IPS Radio Systems

The Pushchino Radio Observatory 70,000 m^2 110 MHz array, Russia (summer 2006)
Now named the "Big Scanning Array of the Lebedev Physical Institute" (BSA LPI).

The Ootacamund (Ooty), India off-axis parabolic cylinder 530 m long and 30 m wide (15,900 m^2) operating at a nominal frequency of 326.5 MHz.

Heliospheric Tomography

Other and Potential Future IPS systems

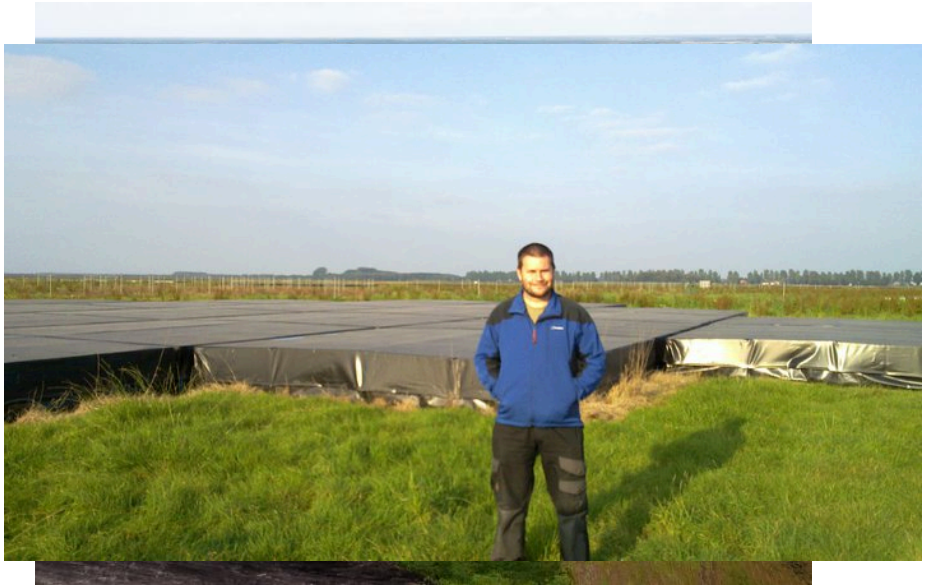

Heliospheric Tomography

IPS line-of-sight response Jackson, B.V., *et al.*, 2008, *Adv. in Geosciences,* 21, 339-360.

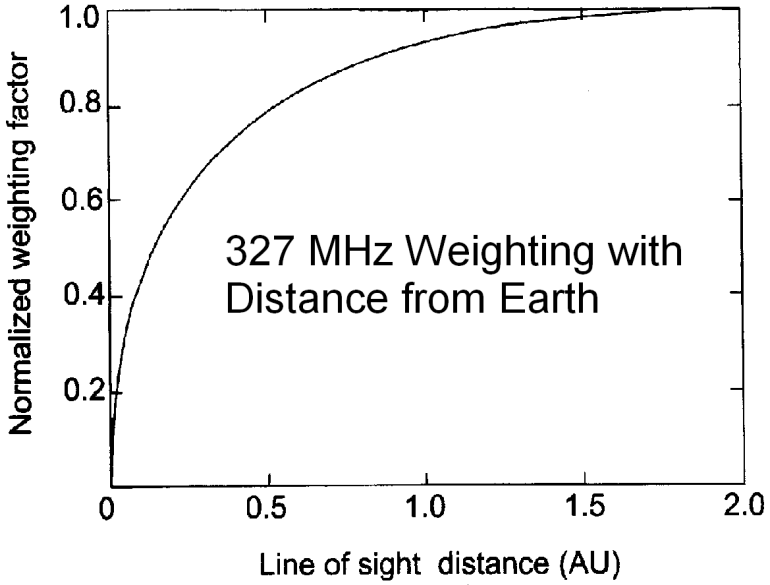

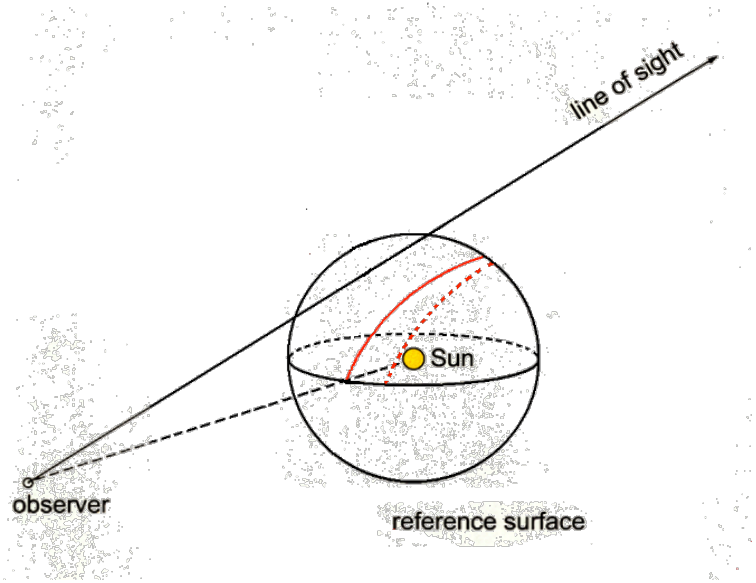

Heliospheric C.A.T. analyses: example line-of-sight distribution for each sky location to form the source surface of the 3D reconstruction.

STELab IPS

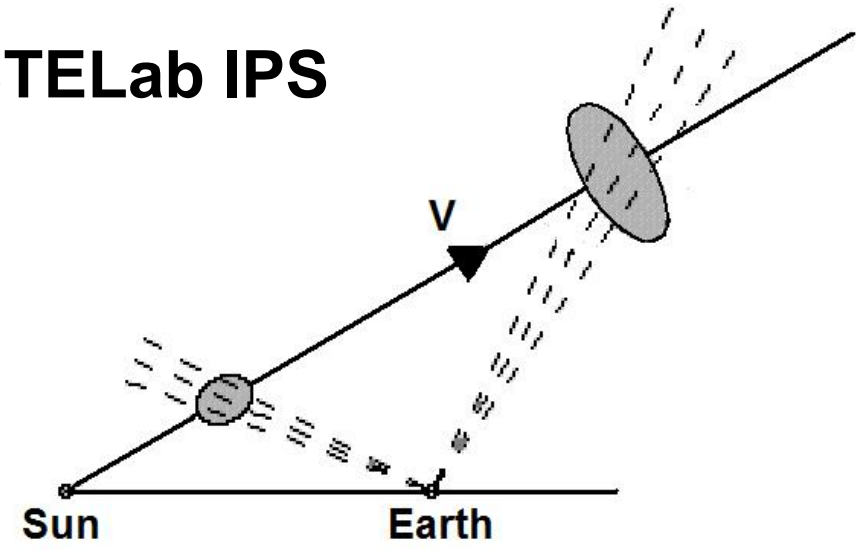

Sample outward motion over time

Heliospheric Tomography

IPS line-of-sight response Jackson, B.V., *et al.*, 2008, *Adv. in Geosciences,* 21, 339-360.

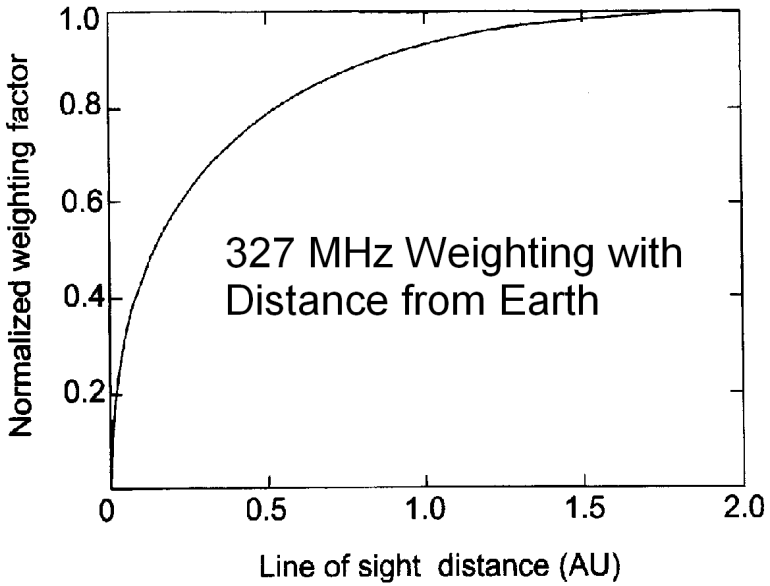

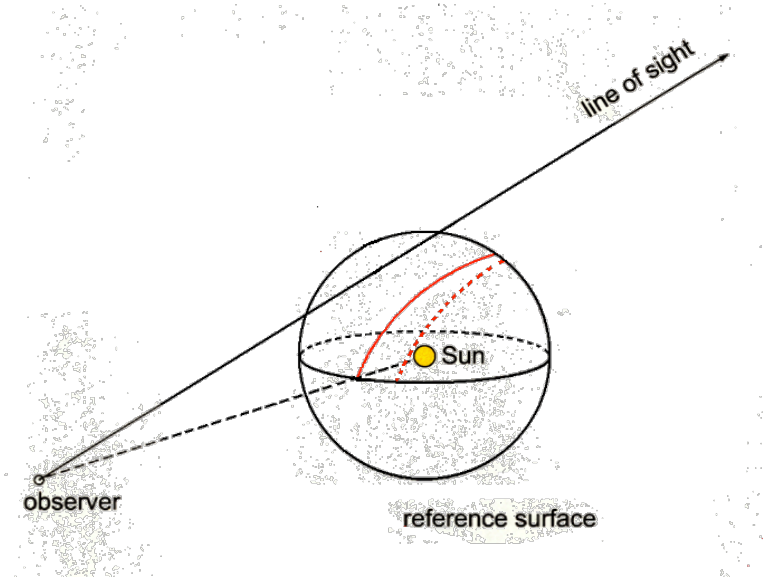

Heliospheric C.A.T. analyses: example line-of-sight distribution for each sky location to form the source surface of the 3D reconstruction.

STELab IPS

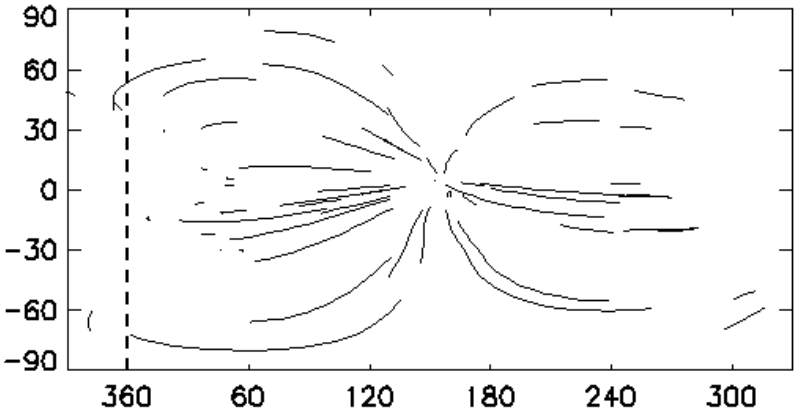

13 July 2000

Heliospheric Tomography

Jackson, B.V., et al., 2002, *Solar Wind 10,* 31

IPS C.A.T. Analysis

Bastille Day Event

14 July 2000

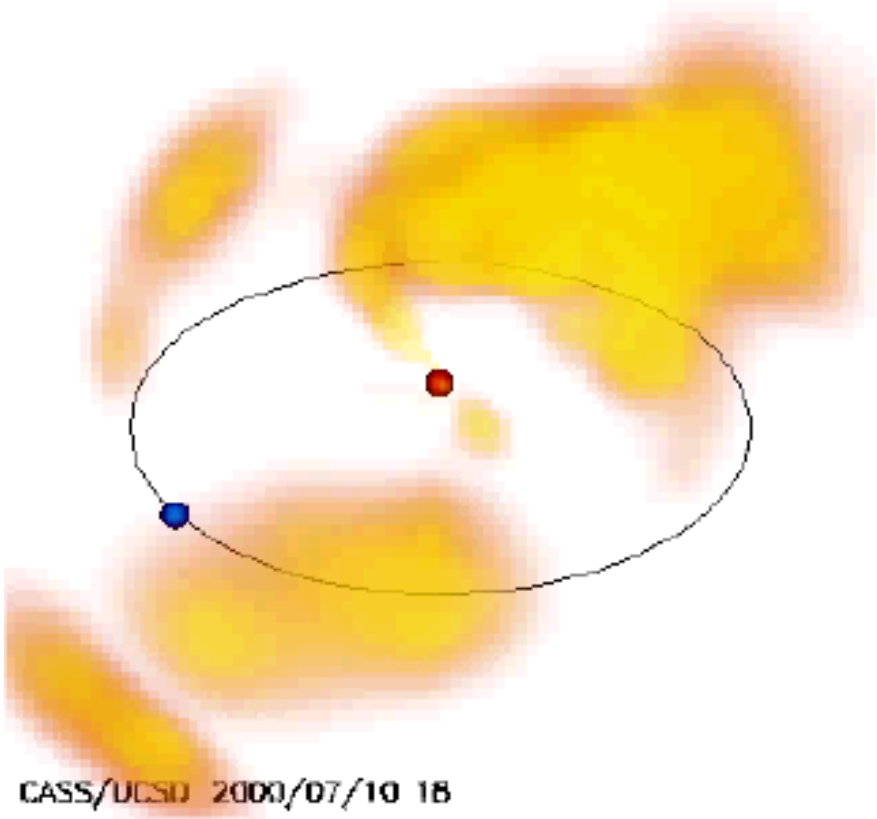

IPS Density Remote View

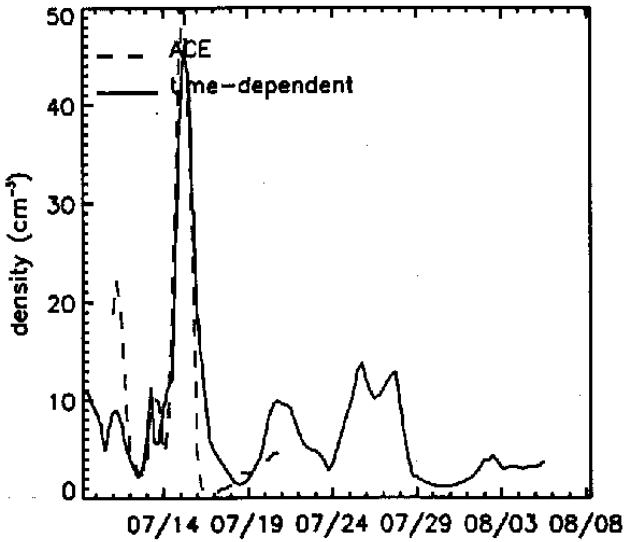

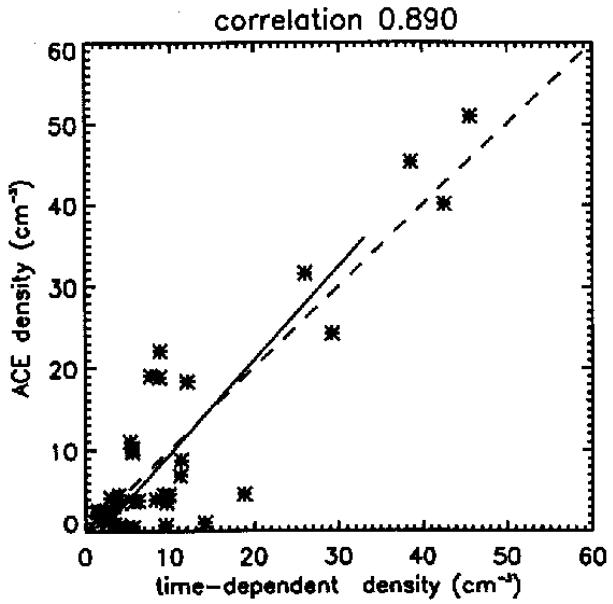

Heliospheric Tomography

Jackson, B.V., et al., 2002, *Solar Wind 10,* 31

IPS C.A.T. Analysis

Bastille Day Event

14 July 2000

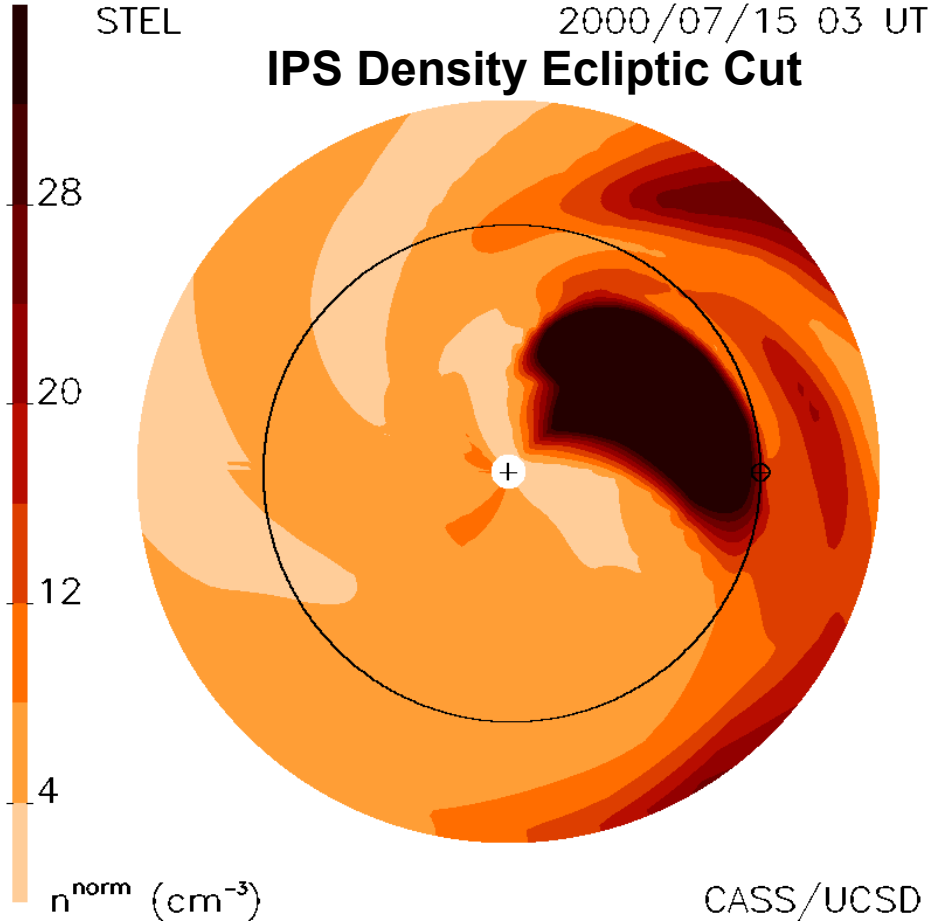

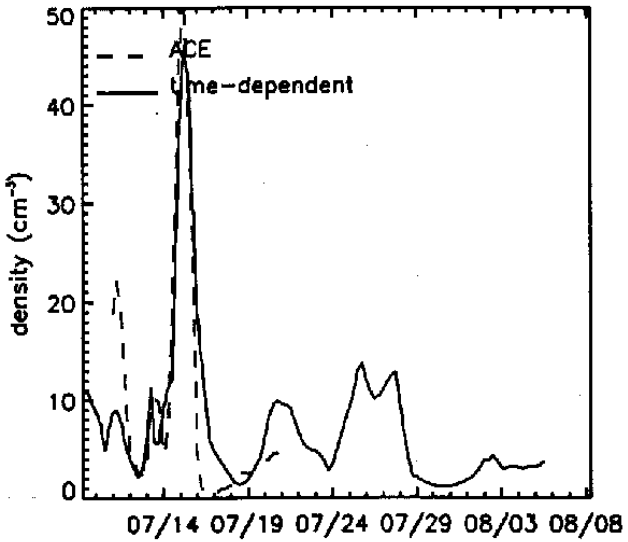

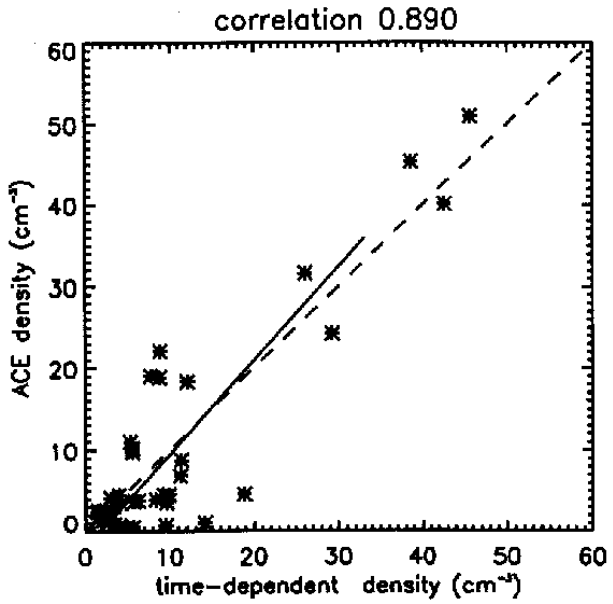

Heliospheric Tomography

Jackson, B.V., et al., 2002, *Solar Wind 10,* 31

IPS C.A.T. Analysis

Bastille Day Event

14 July 2000

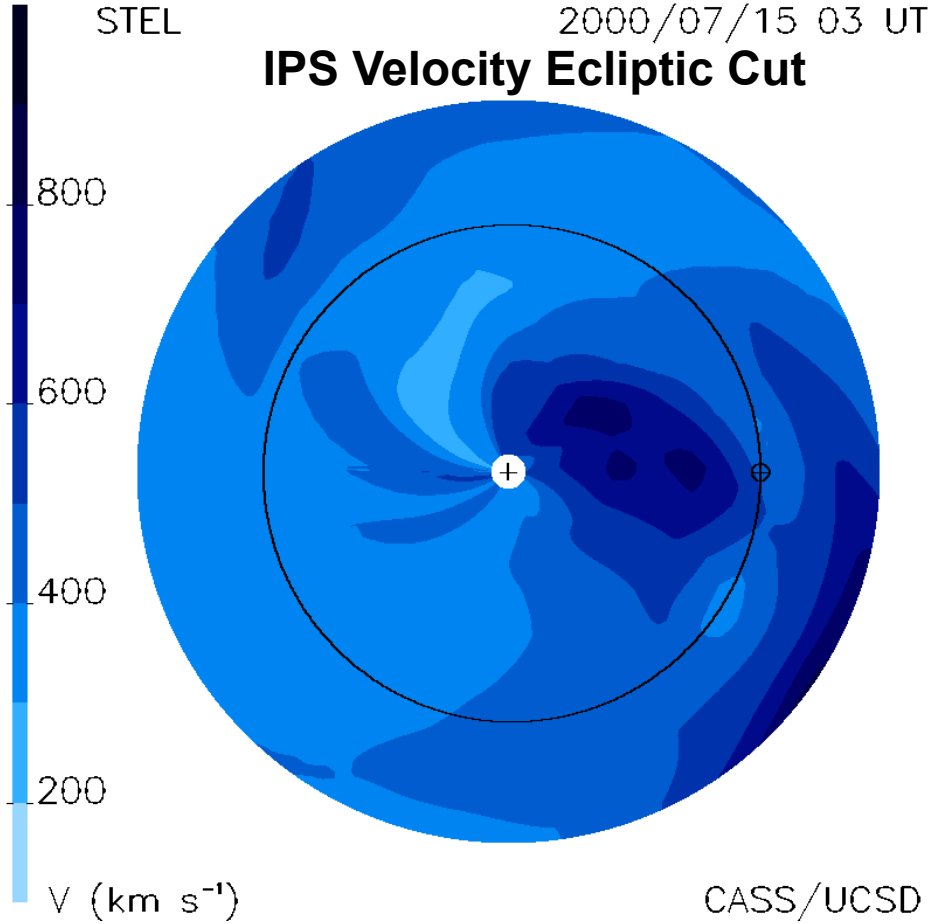

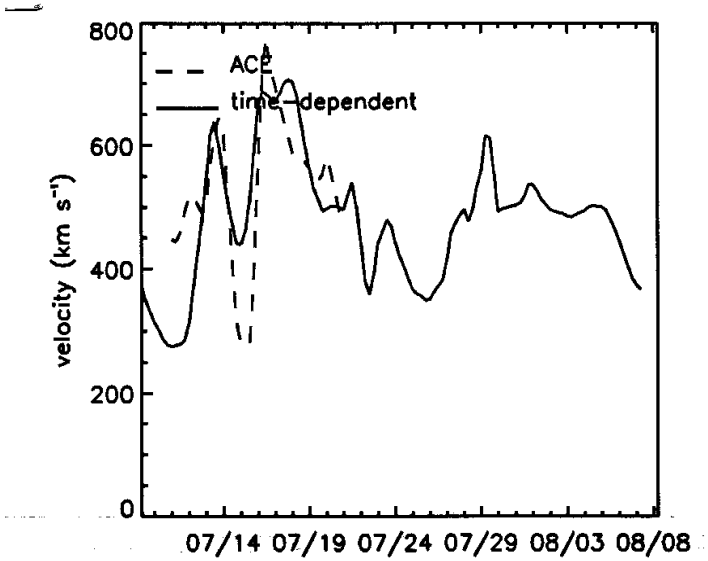

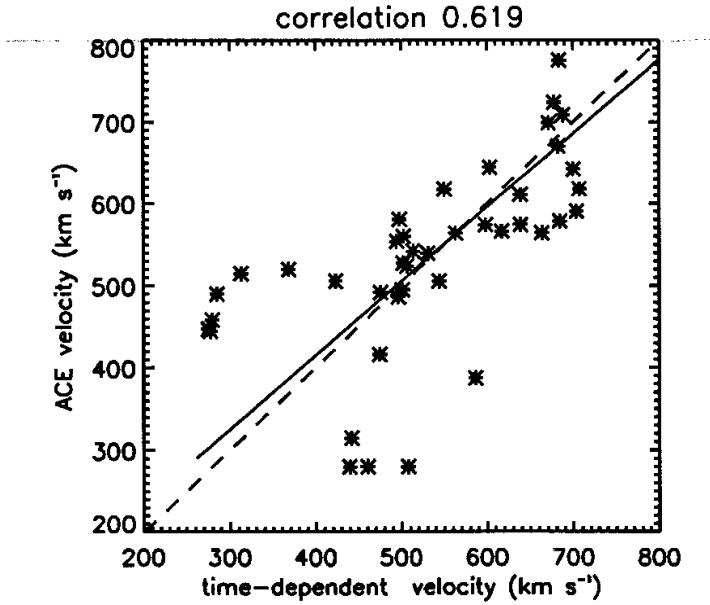

Heliospheric Tomography

Jackson, B.V., et al., 2002, *Solar Wind 10,* 31

IPS C.A.T. Analysis

Bastille Day Event 14 July 2000

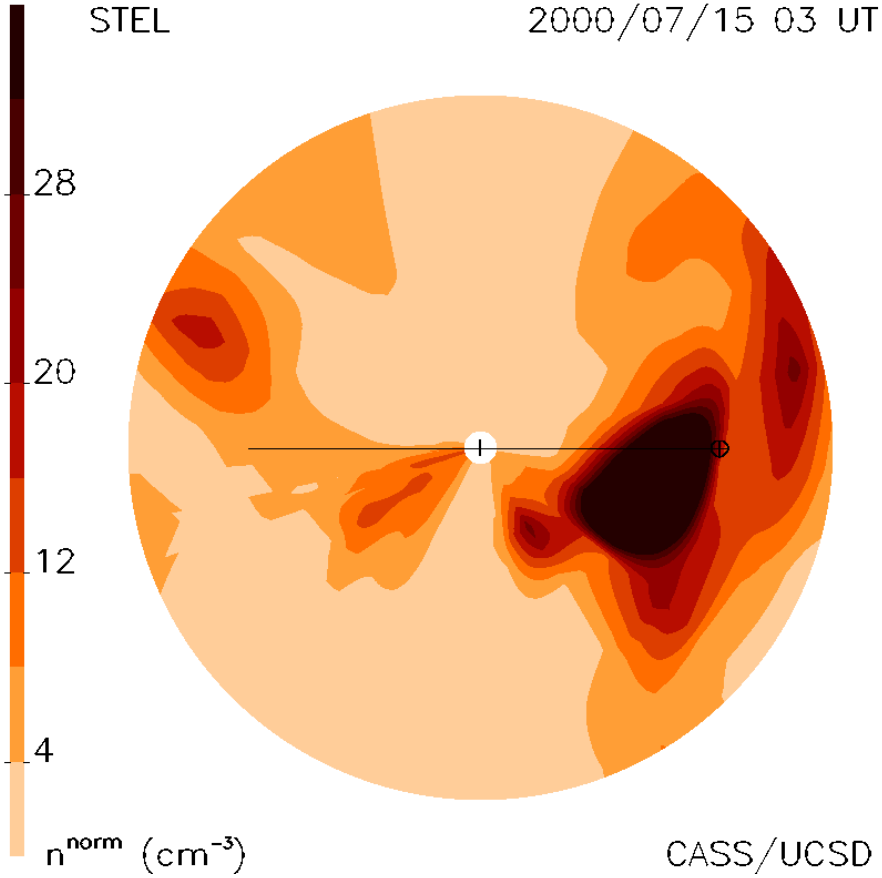

IPS Density Meridional Cut

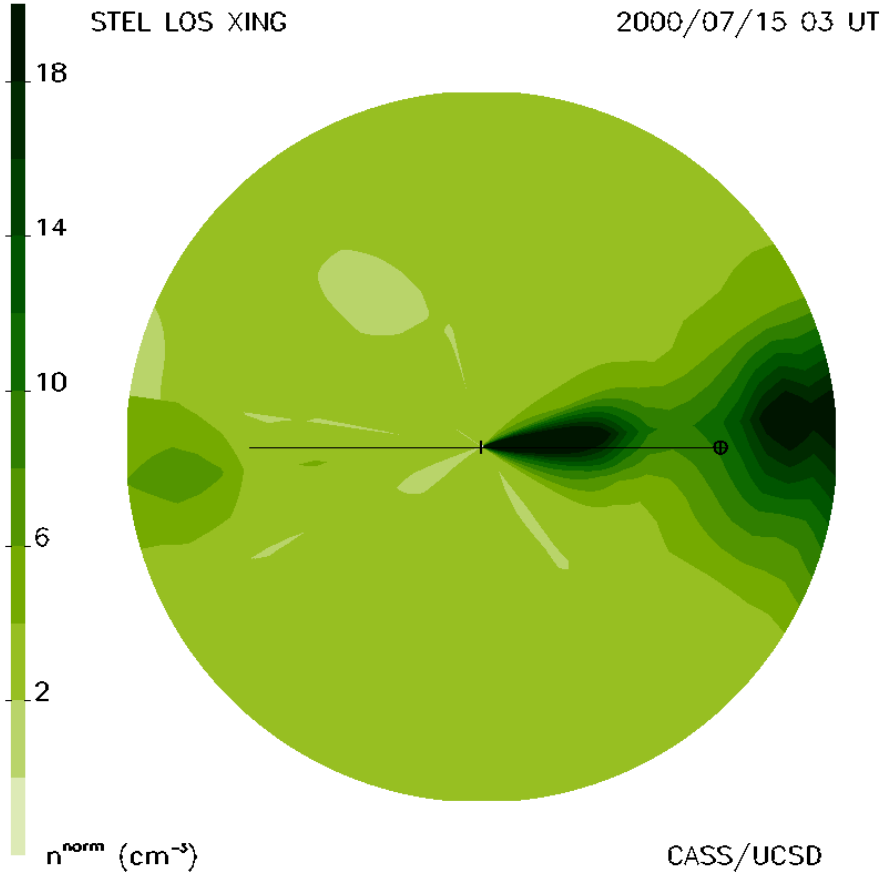

IPS Density LOS X-ing Meridional Cut

Heliospheric Tomography

IPS line-of-sight response

Jackson, B.V., *et al.*, 2010, *Solar Phys.*, 265, 245-256.

Jackson, B.V., *et al.*, 2008, *Adv. in Geosciences,* 21, 339.

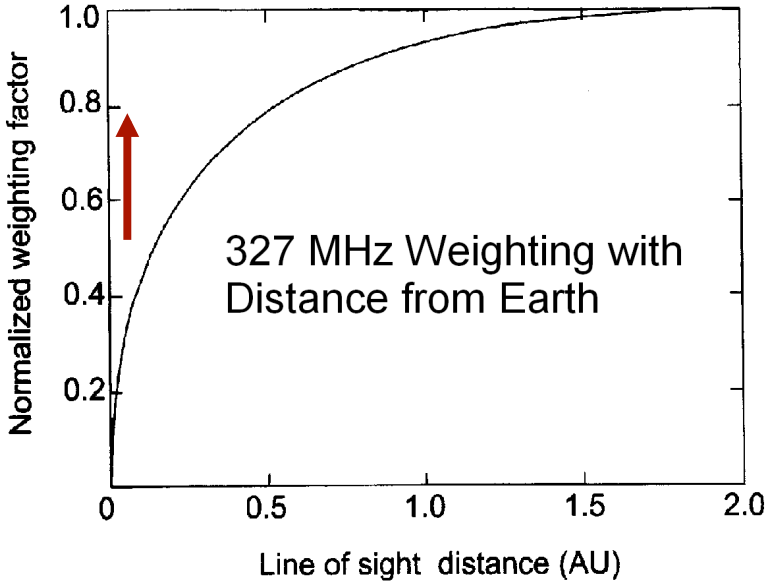

Heliospheric C.A.T. Analyses: example line-of-sight distribution for each sky location to form the source surface of the 3D reconstruction.

Innovation

STELab IPS

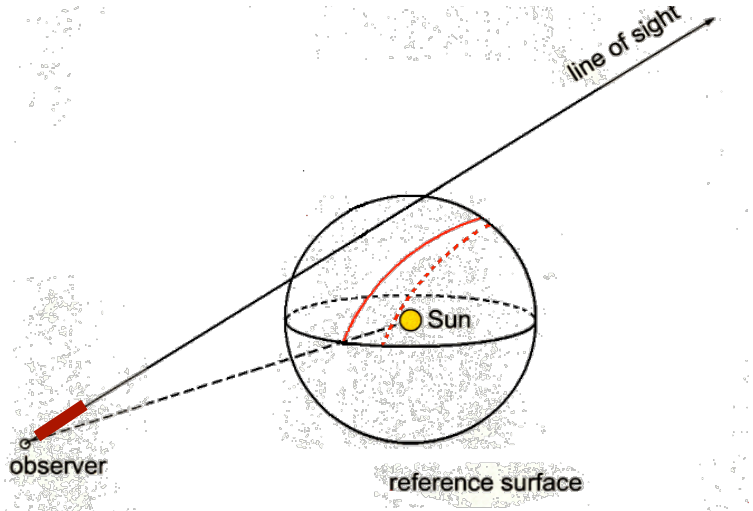

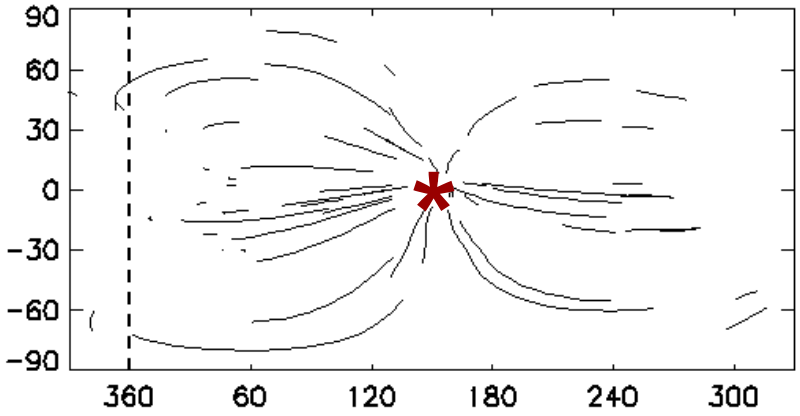

13 July 2000

Inclusion of in-situ measurements into the 3D-reconstructions

Heliospheric Tomography

Jackson, B.V., *et al*., 2010, *Solar Phys*., 265, 245-256.

Heliospheric 3D-reconstructions

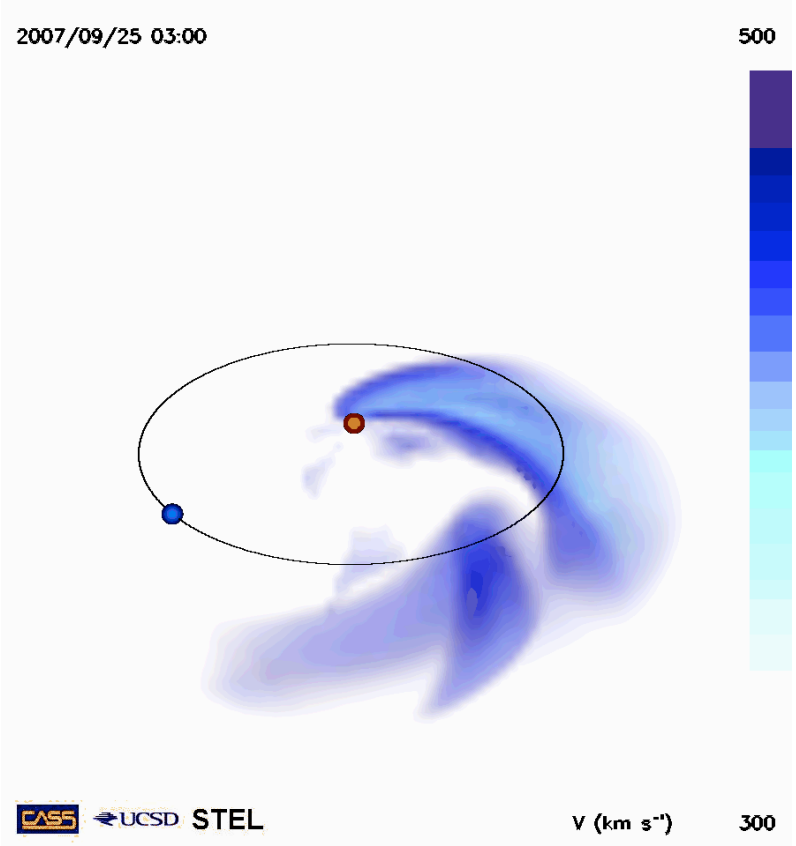

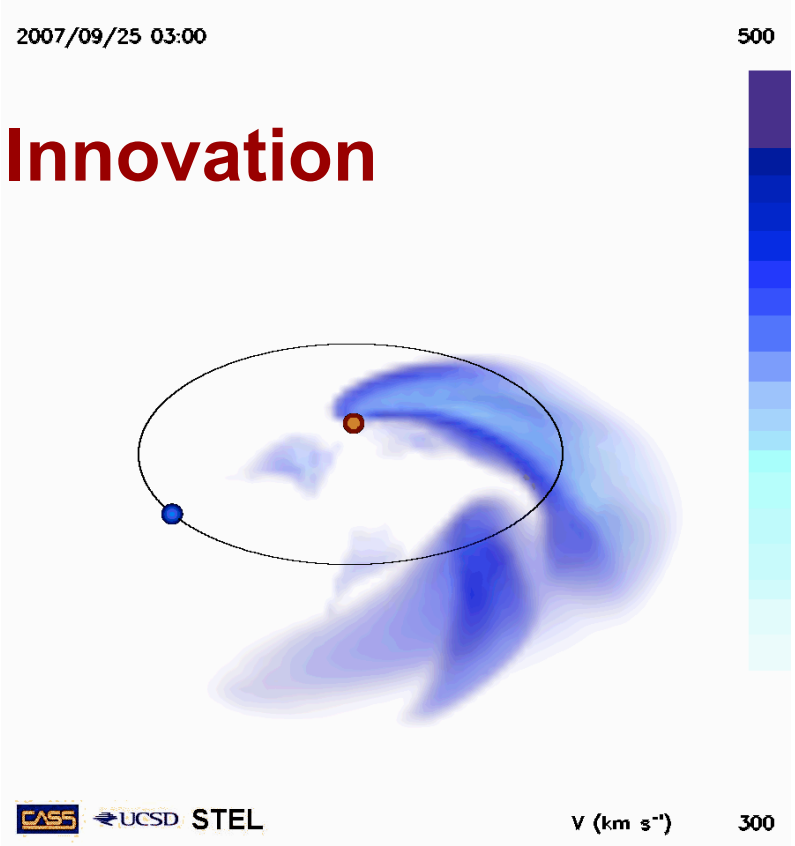

Inclusion of in-situ measurements into the 3D-reconstructions

Jackson, B.V., *et al*., 2011, *Adv. in Geosciences,* 30, 93-115.

Heliospheric Tomography

Jackson, B.V., *et al*., 2010, *Solar Phys*., 265, 245-256.

Heliospheric 3D-reconstructions

Innovation

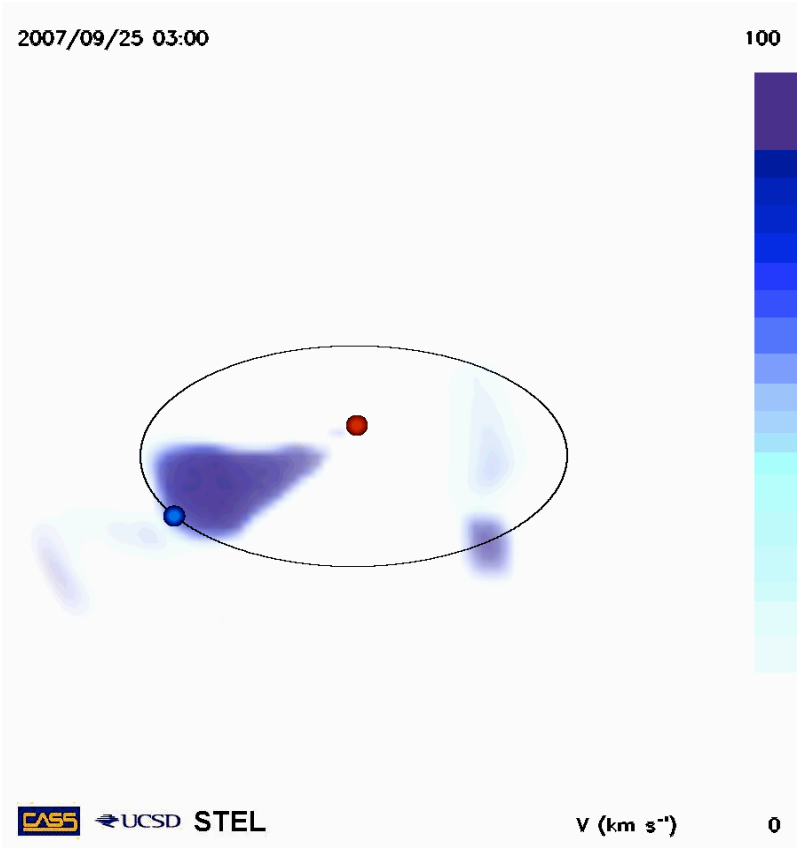

Inclusion of in-situ measurements into the 3D-reconstructions

Jackson, B.V., *et al*., 2011, *Adv. in Geosciences,* 30, 93-115.

Heliospheric Tomography

Jackson, B.V., et al., 2010, *Solar Phys.*, 265, 245-256.

Jackson, B.V., *et al.*, 2011, *Adv. in Geosciences,* 30, 93-115.

Used at the CCMC and the KSWC

Forecast

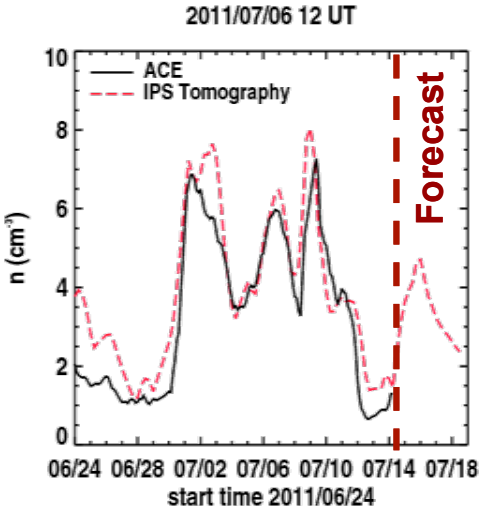

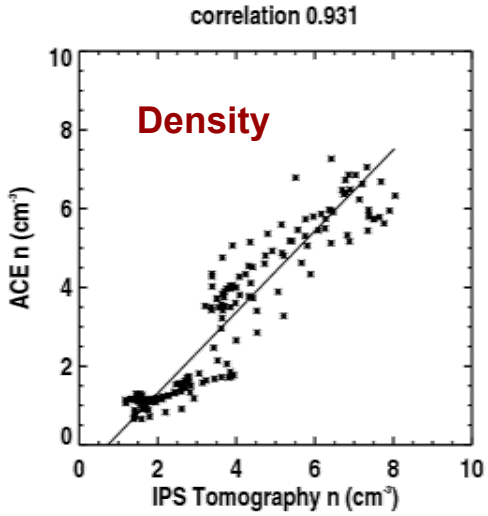

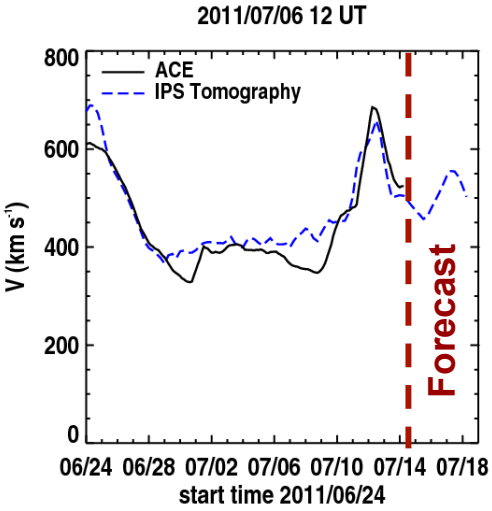

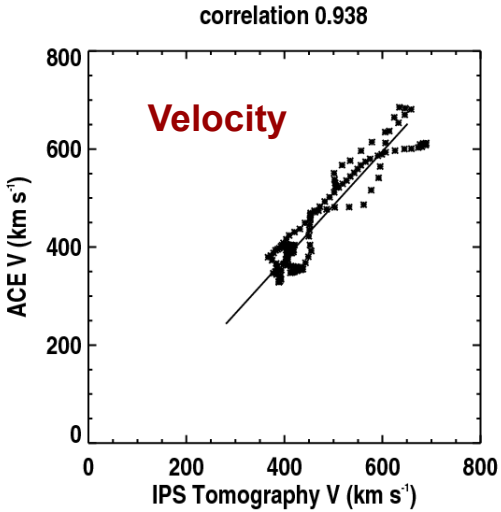

Heliospheric 3D-reconstructions

Inclusion of in-situ measurements into the 3D-reconstructions

Forecasts work better if the values match up to the present.

Heliospheric Tomography

Jackson, B.V., et al., 2010, *Solar Phys.*, 265, 245-256.

Jackson, B.V., *et al.*, 2011, *Adv. in Geosciences,* 30, 93-115.

Used at the CCMC and the KSWC

Forecast

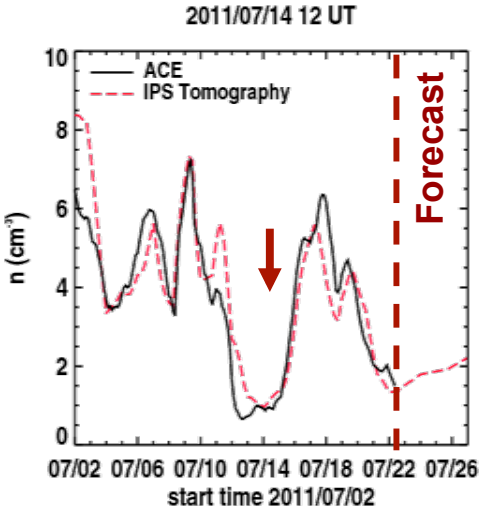

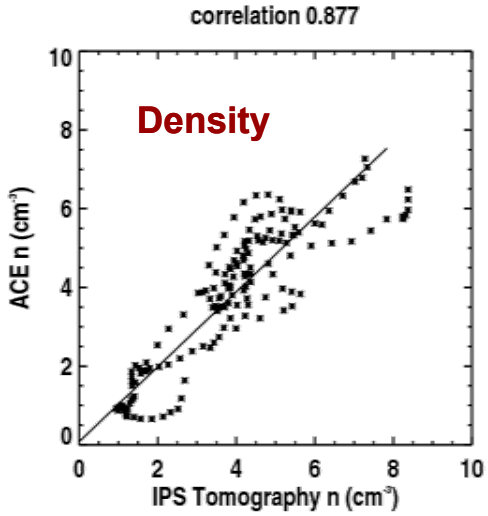

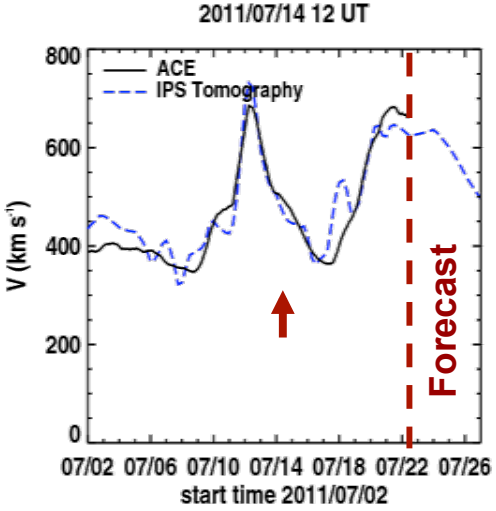

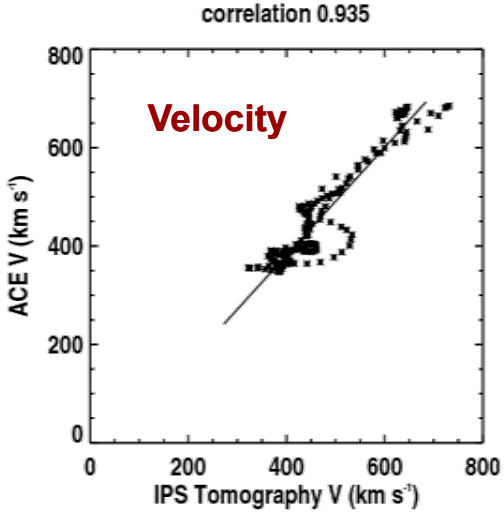

Heliospheric 3D-reconstructions

Inclusion of in-situ measurements into the 3D-reconstructions

Forecasts work better if the values match up to the present.

Heliospheric Tomography

Zhao, X. P. and Hoeksema, J. T., 1995, *J. Geophys. Res.,* 100 (A1), 19.

http://ips.ucsd.edu/

Magnetic Field Extrapolation

Dunn et al., 2005, *Solar Physics* 227: 339–353.

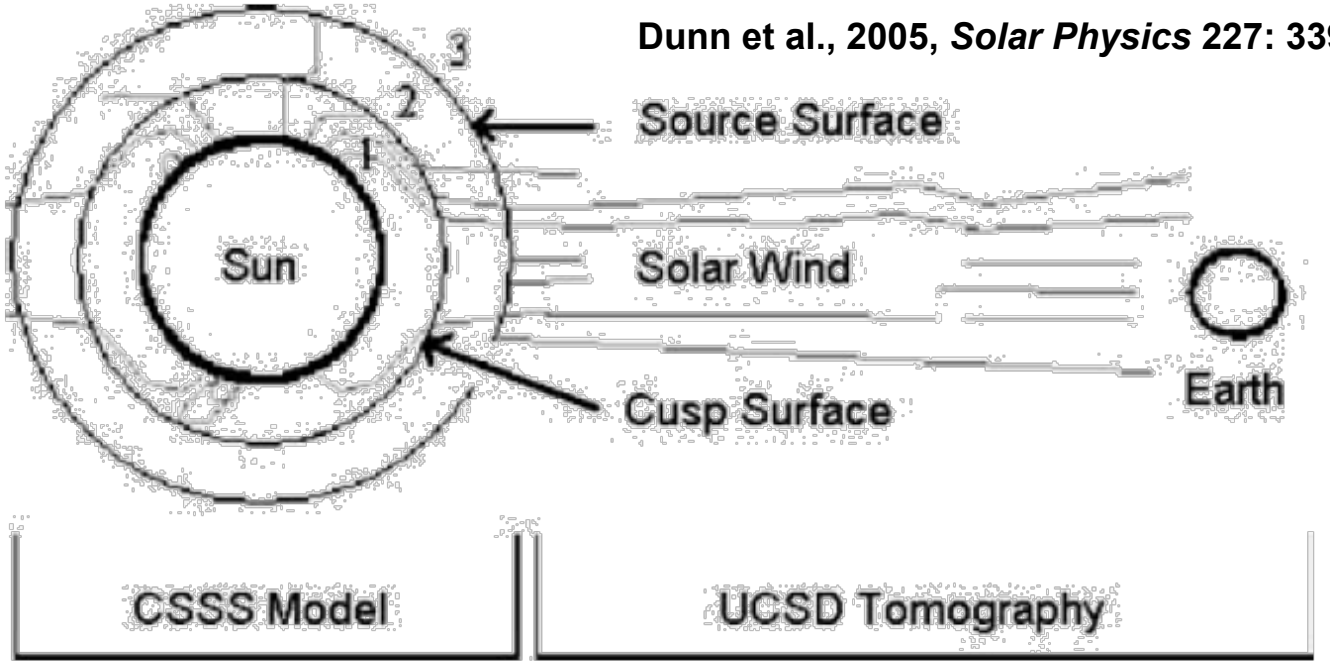

1. Inner region: the CSSS model calculates the magnetic field using photospheric measurements and a horizontal current model.

2. Middle region: the CSSS model opens the field lines. In the outer region.

3. Outer region: the UCSD tomography convects the magnetic field along velocity flow lines.

Jackson, B.V., et al., 2012, *Adv. in Geosciences,* 30, 93-115.

Heliospheric Tomography

IPS Forecasts

Heliospheric Tomography

Jackson, B.V., *et al.*, 2011, *Adv. in Geosciences,* 30, 93-115.

http://ips.ucsd.edu/ Real-Time Forecasts

UCSD IPS analysis

UCSD Web pages

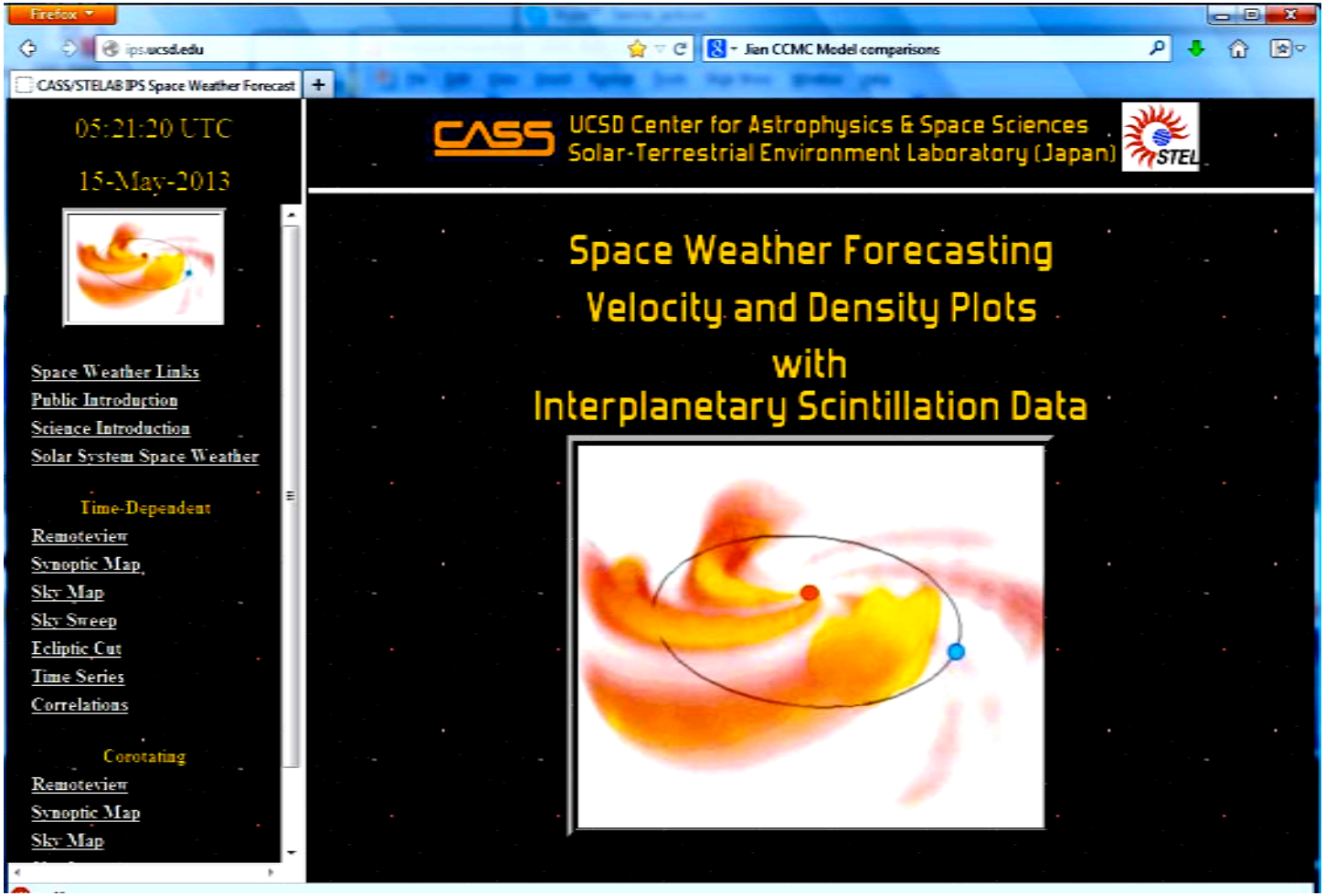

Web Analysis Runs Automatically Using Linux on a P.C.

Heliospheric Tomography

http://ips.ucsd.edu/ Skymap view

Jackson, B.V., *et al.*, 2011, *Adv. in Geosciences,* 30, 93-115.

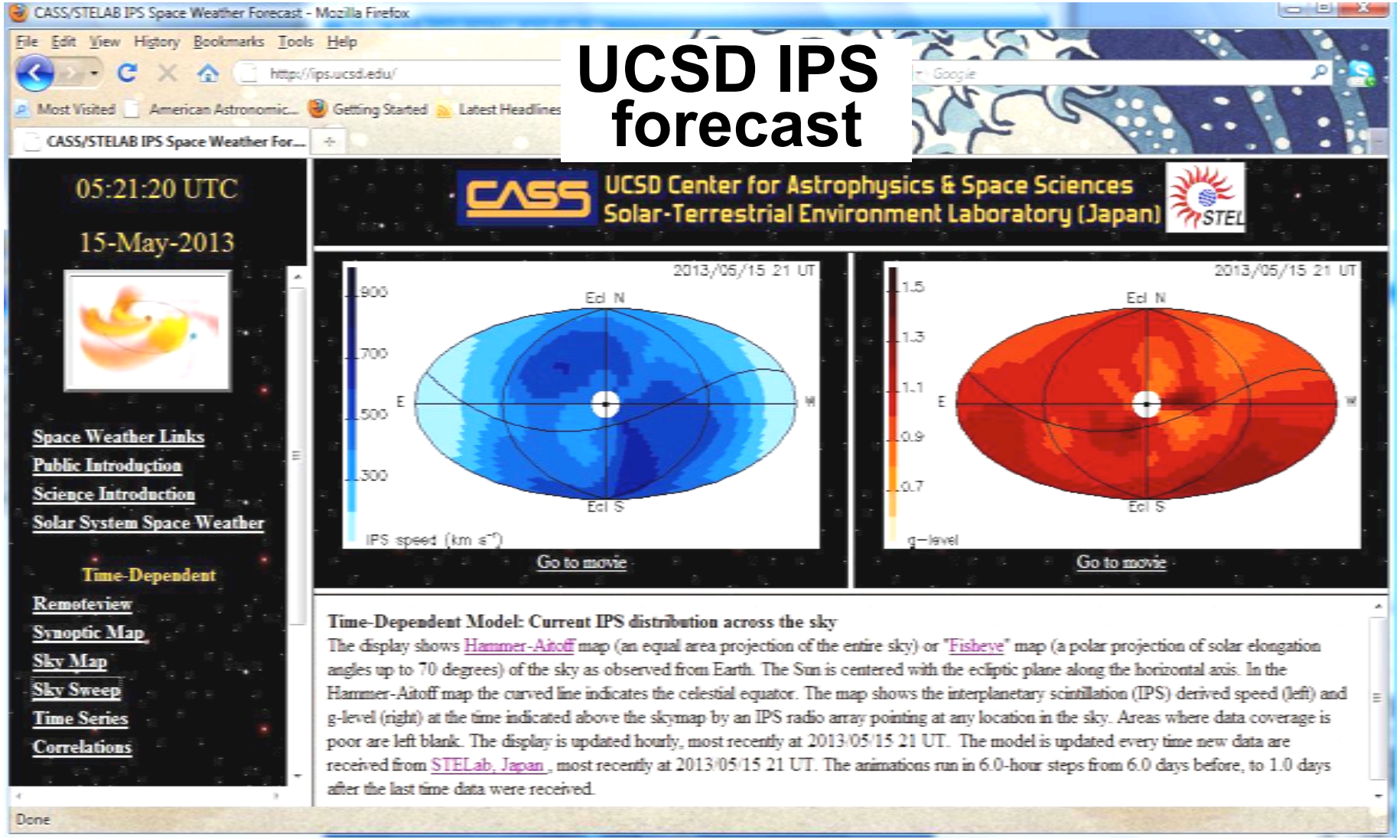

Web analysis runs automatically using Linux on a P.C.

Heliospheric Tomography

http://ips.ucsd.edu/ Skysweep view

Jackson, B.V., *et al.*, 2011, *Adv. in Geosciences,* 30, 93-115.

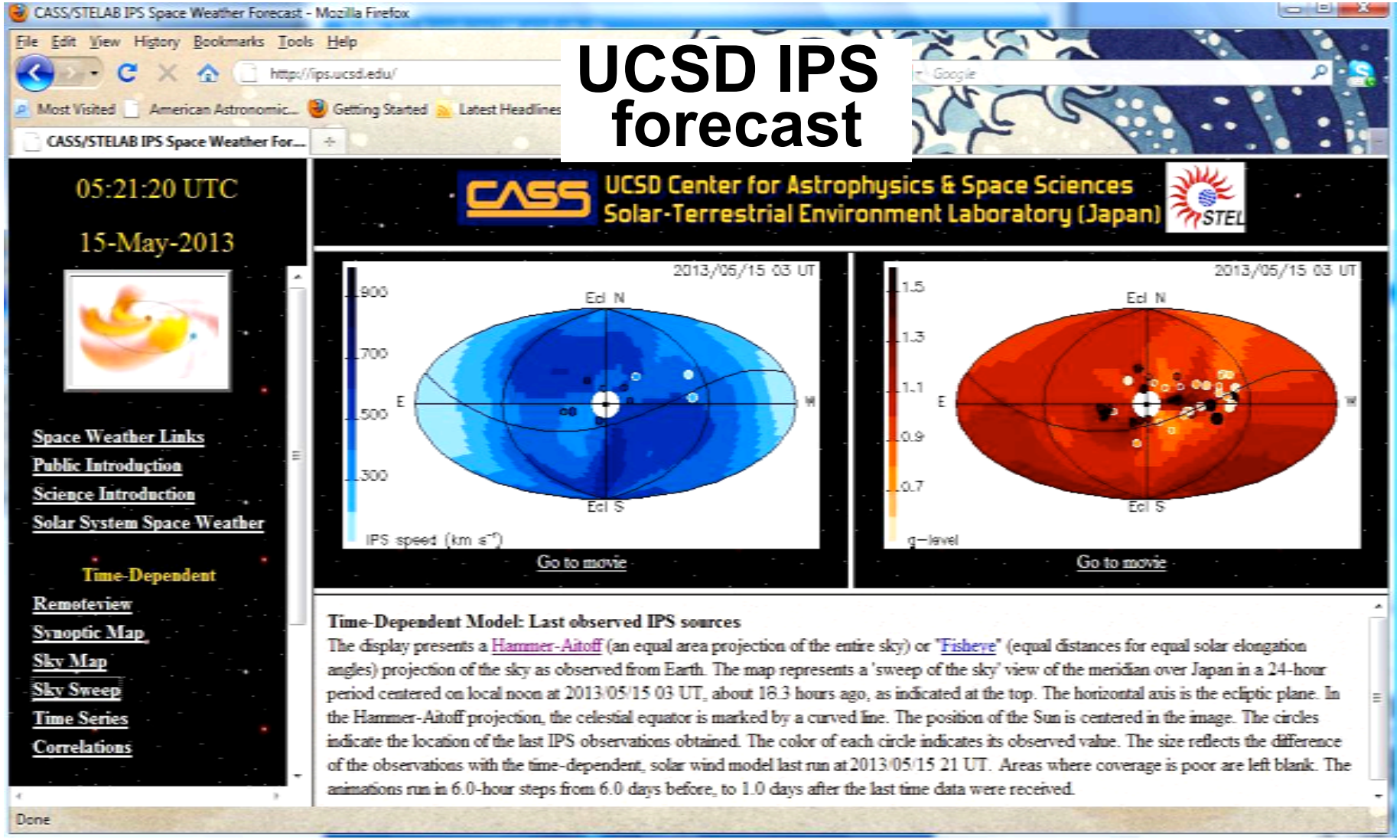

Web analysis runs automatically using Linux on a P.C.

Heliospheric Tomography

http://ips.ucsd.edu/ **Skymap view**

Jackson, B.V., *et al.*, 2011, *Adv. in Geosciences,* 30, 93-115.

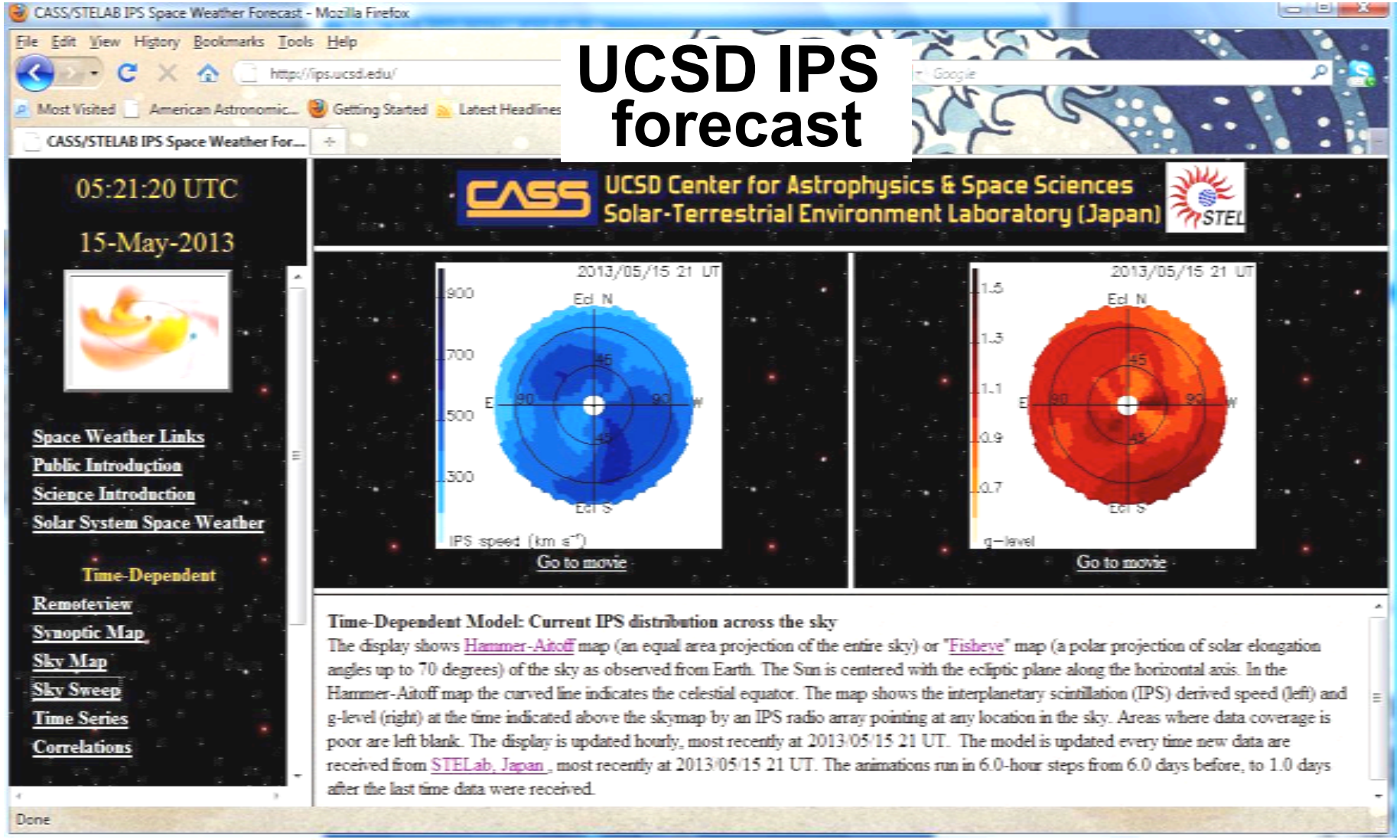

Web analysis runs automatically using Linux on a P.C.

Heliospheric Tomography

http://ips.ucsd.edu/

Jackson, B.V., *et al.*, 2011, *Adv. in Geosciences,* 30, 93-115.

Forecast **Fit to CELIAS data**

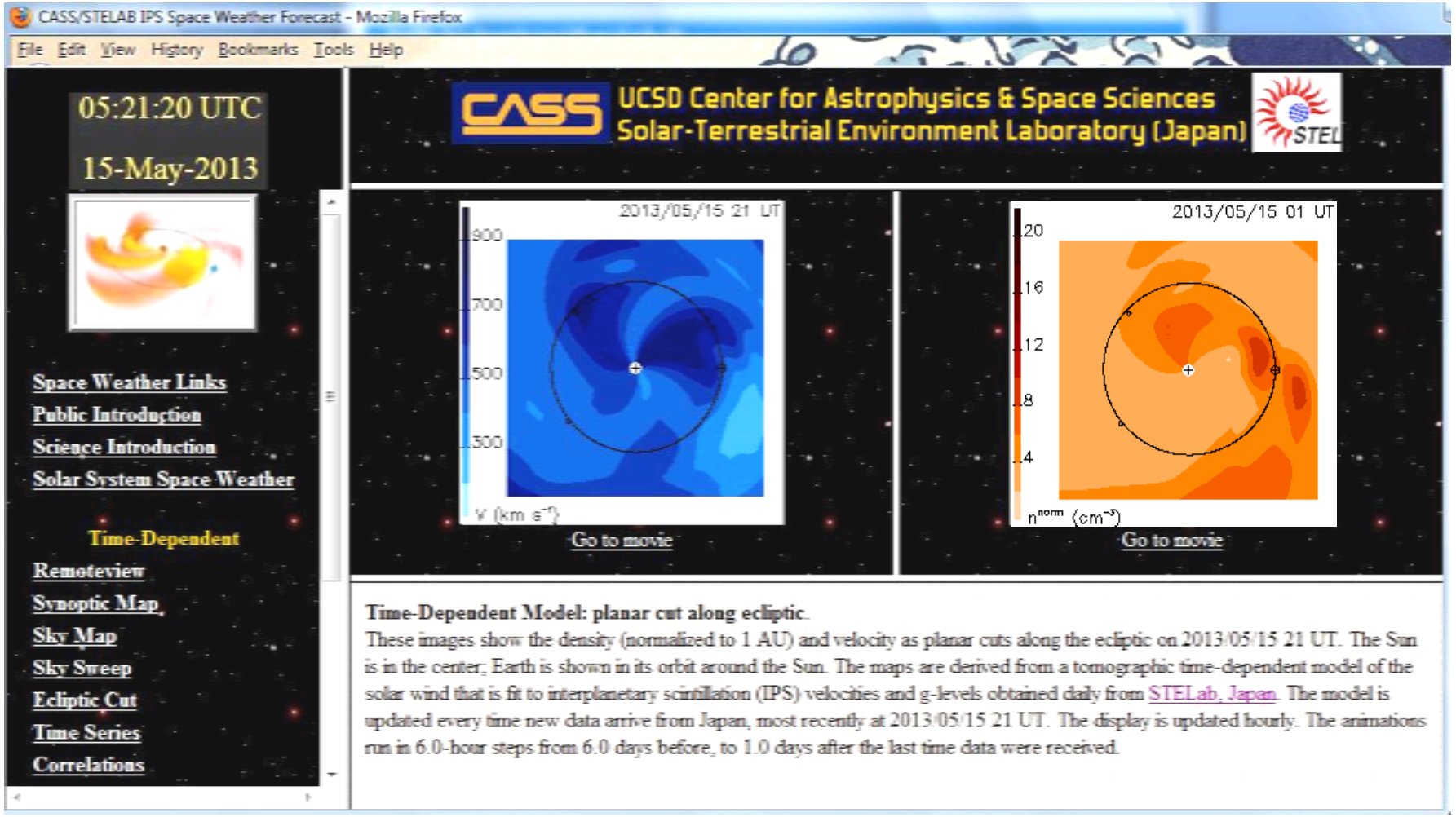

One CME just passed 2013/05/14 4-6 UT increase by ~8 Np/cc

Web Analysis Runs Automatically Using Linux on a P.C.

Heliospheric Tomography

http://ips.ucsd.edu/

Jackson, B.V., *et al.*, 2011, *Adv. in Geosciences,* 30, 93-115.

Forecast **Fit to CELIAS data**

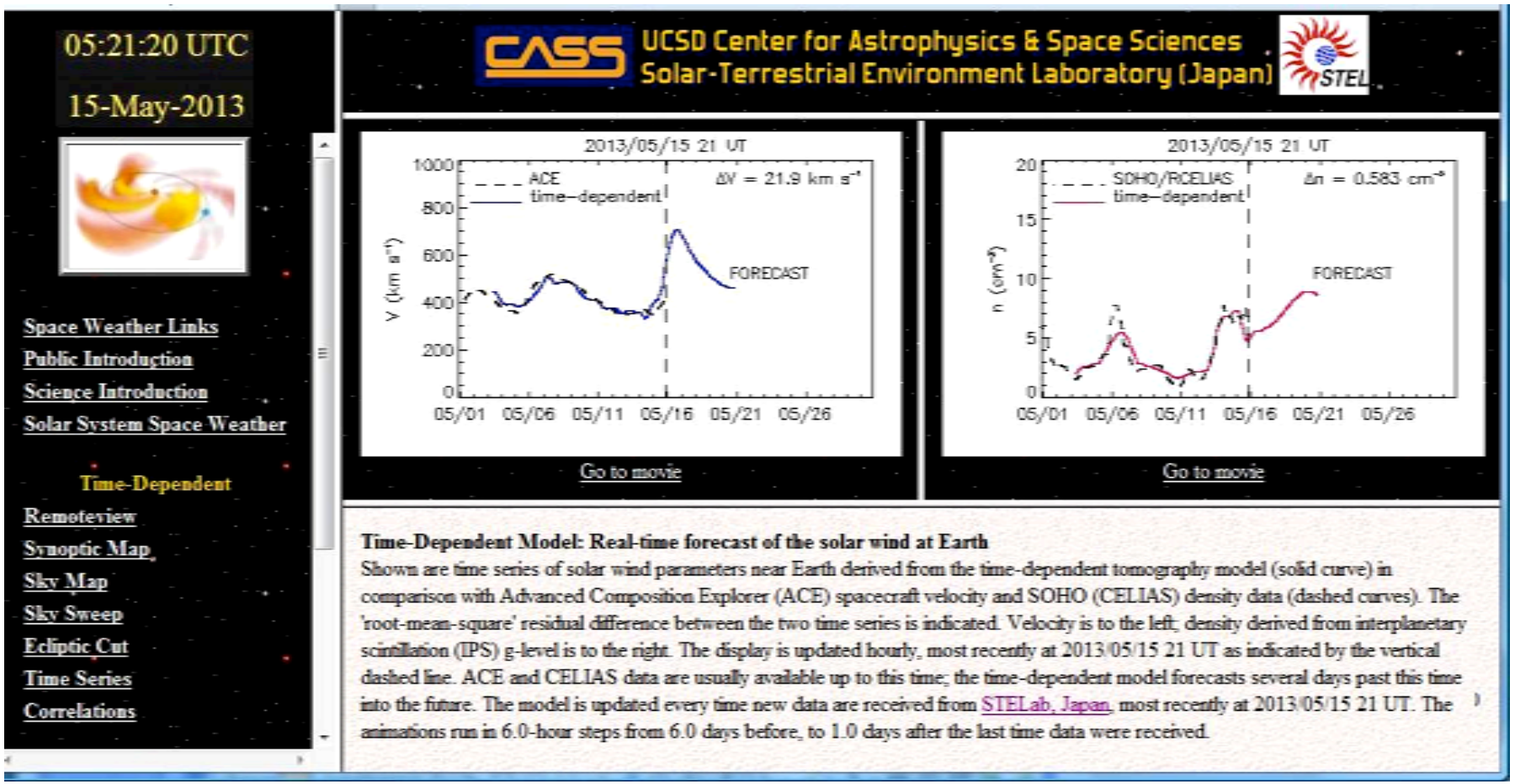

One CME just passed 2013/05/14 4-6 UT increase by ~8 Np/cc

Web Analysis Runs Automatically Using Linux on a P.C.

Heliospheric Tomography

Jackson, B.V., *et al*., 2010, *Solar Phys*., 265, 245-256.

Jackson, B.V., *et al*., 2011, *Adv. in Geosciences,* 30, 93-115.

Correlations (from UCSD forecast)

Pearson's r correlation coefficient, day to day forecast verification

Five day behind forecast

Velocity

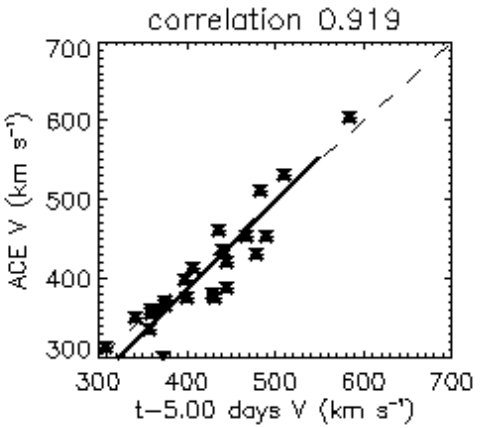

Density

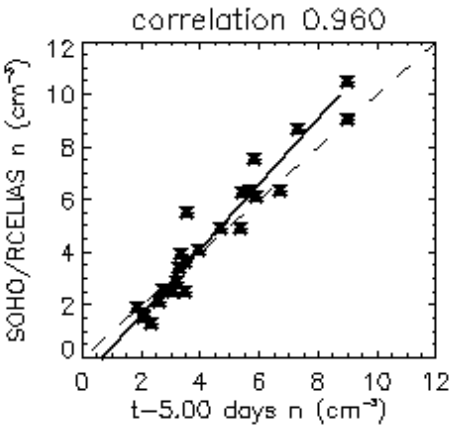

One day ahead forecast

Velocity

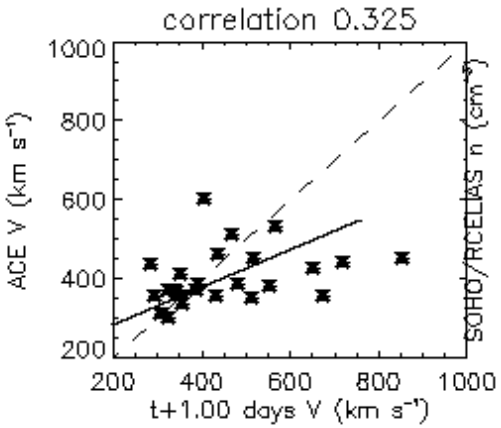

Density

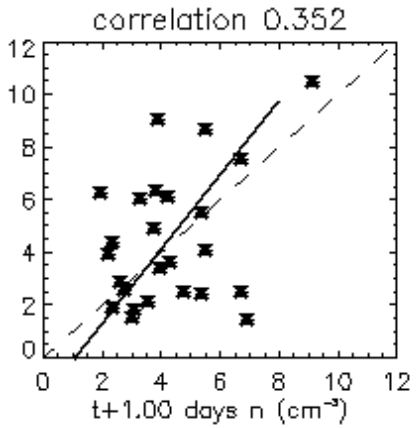

Velocity matched to ACE, density matched to CELIAS

Remote velocity from STELab IPS three-site

Remote density from STELab IPS *g*-level

Heliospheric Tomography

Fit to CELIAS Current Forecasts Fit to ACE L0

UCSD

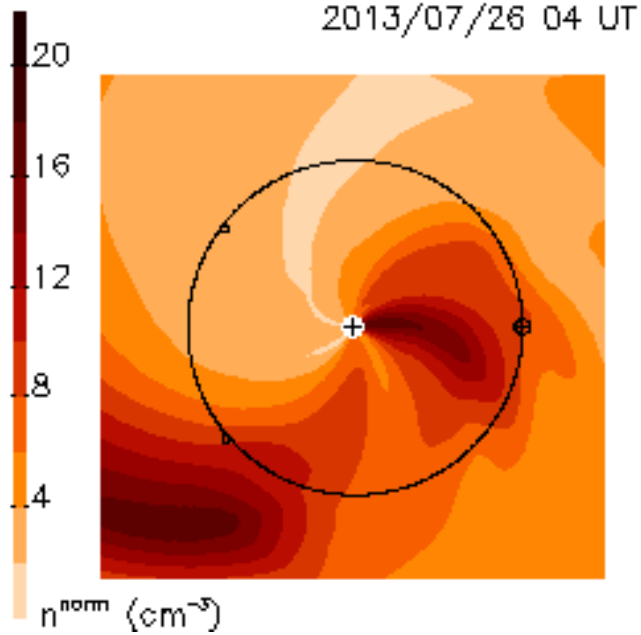

KSWC

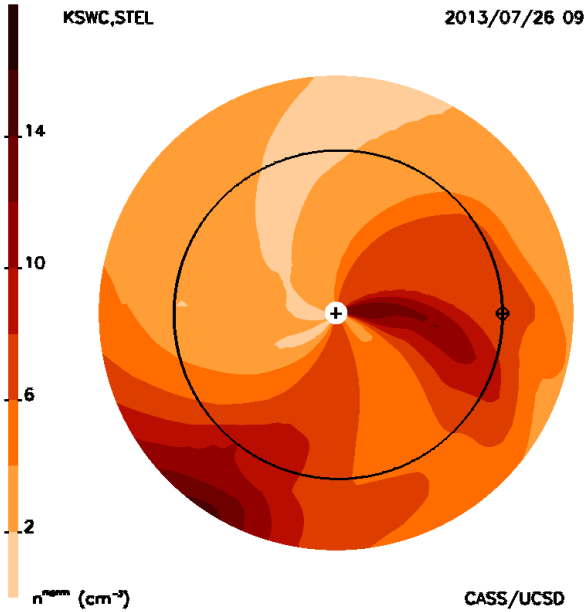

http://ips.ucsd.edu/

http://www.spaceweather.go.kr/models/ips

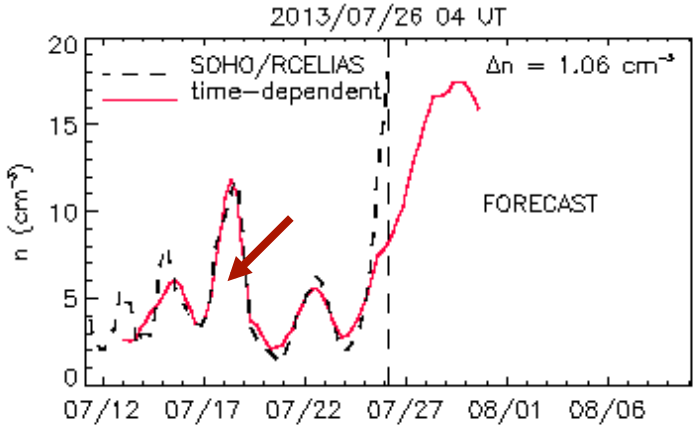

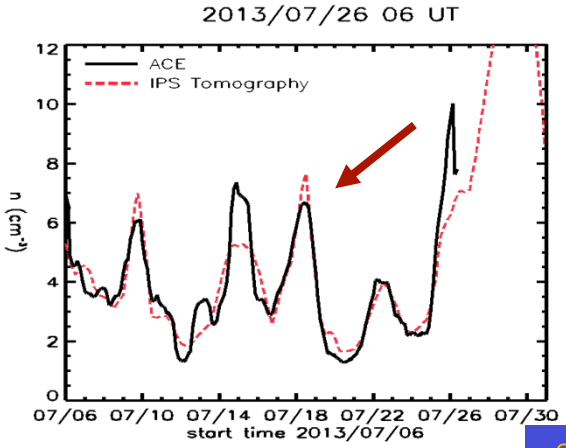

Heliospheric Tomography

Jackson, B.V., *et al.*, 2012, *Adv. in Geosciences,* (in press).

http://ips.ucsd.edu/ **Earth** **Radial and Tangential Magnetic Field**

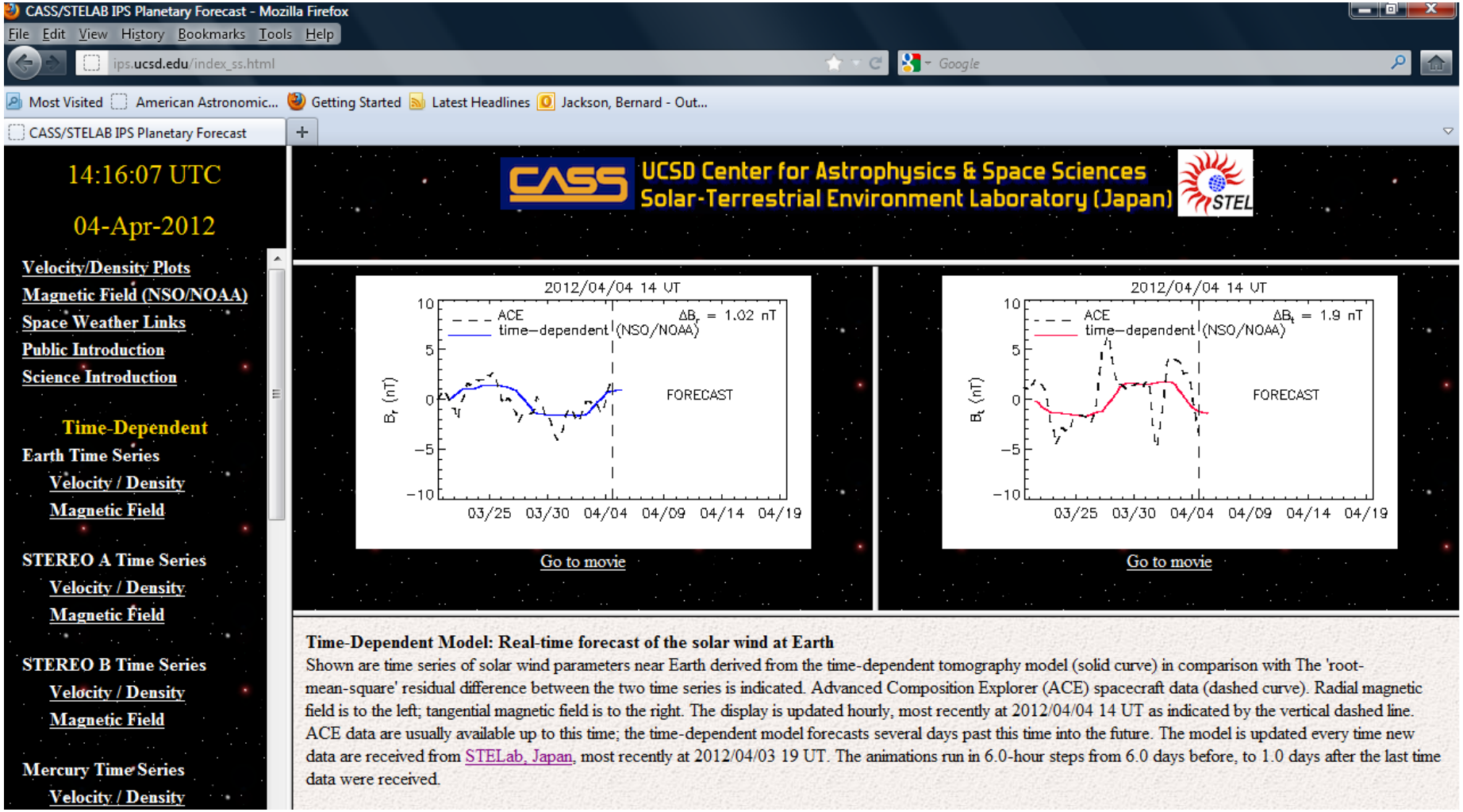

Web Analysis Runs Automatically Using Linux on a P.C.

Heliospheric Tomography

Jackson, B.V., *et al.*, 2011, *Adv. in Geosciences,* 30, 93-115.

Correlations (from UCSD forecast)

Pearson's r correlation coefficient, day to day forecast verification

Five day behind forecast

One day ahead forecast

B_{radial}

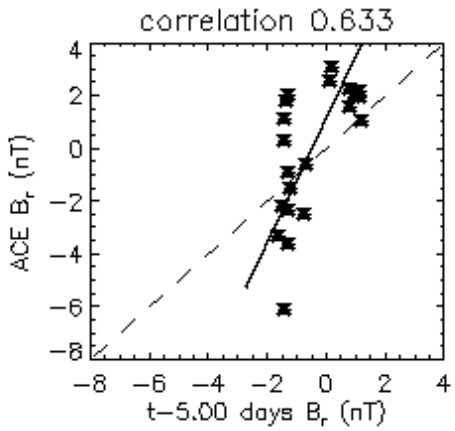

$B_{tangential}$

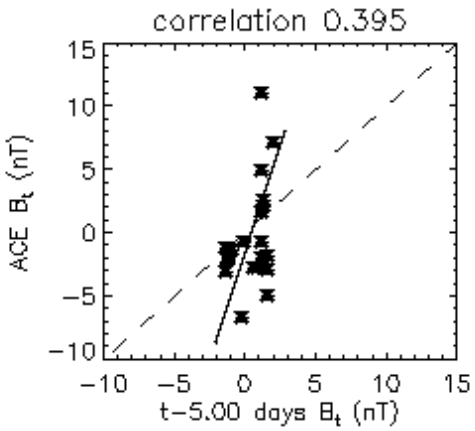

B_{radial}

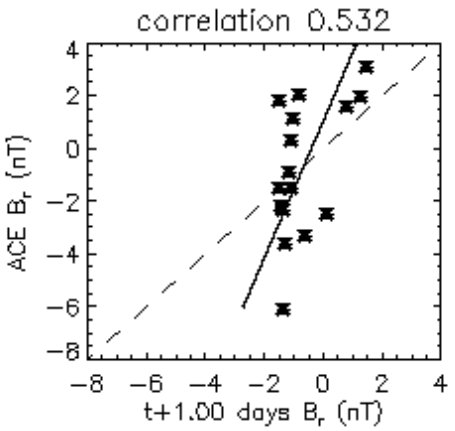

$B_{tangential}$

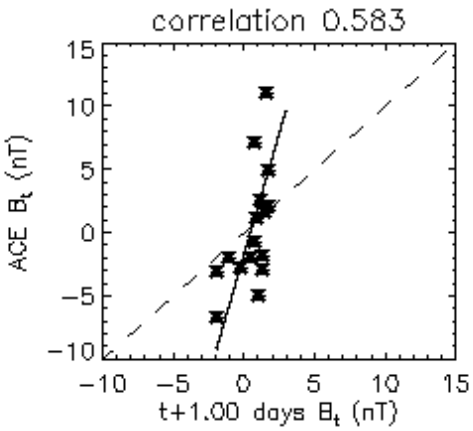

RTN coordinates

Heliospheric Tomography

Jackson, B.V., *et al.*, 2011, *Adv. in Geosciences,* 30, 93-115.

Correlations (from UCSD forecast)

Pearson's r correlation coefficient, day to day forecast verification

Five day behind forecast

One day ahead forecast

B_{radial}

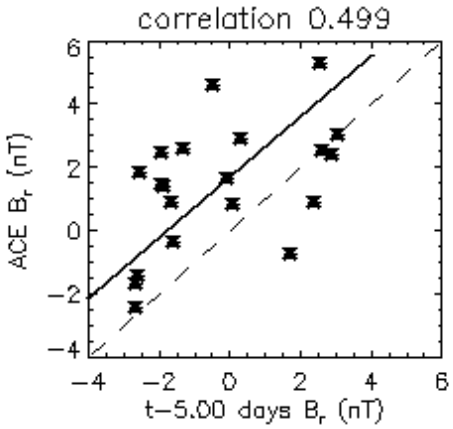

$B_{tangential}$

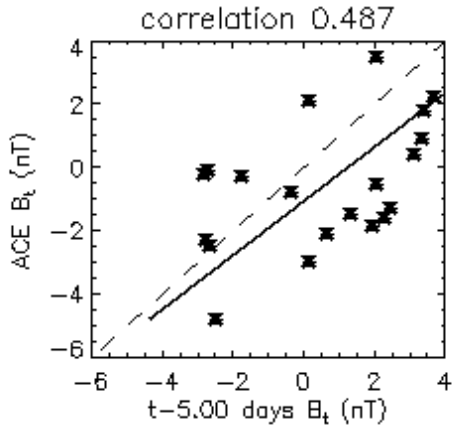

B_{radial}

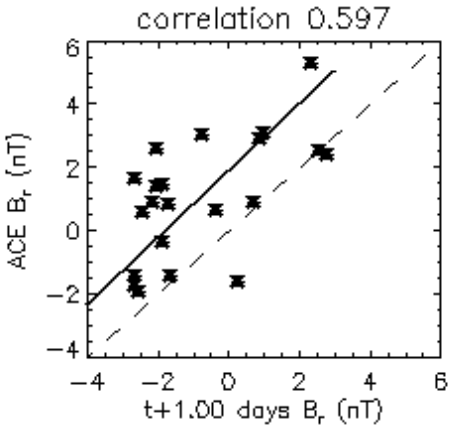

$B_{tangential}$

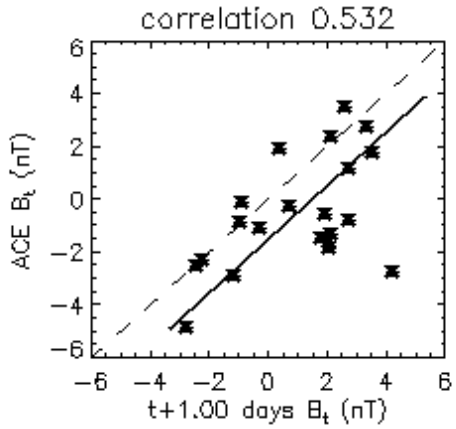

RTN coordinates

Heliospheric Tomography

Towards
a Comprehensive Model
that Includes 3D-MHD

UCSD Heliospheric Tomography

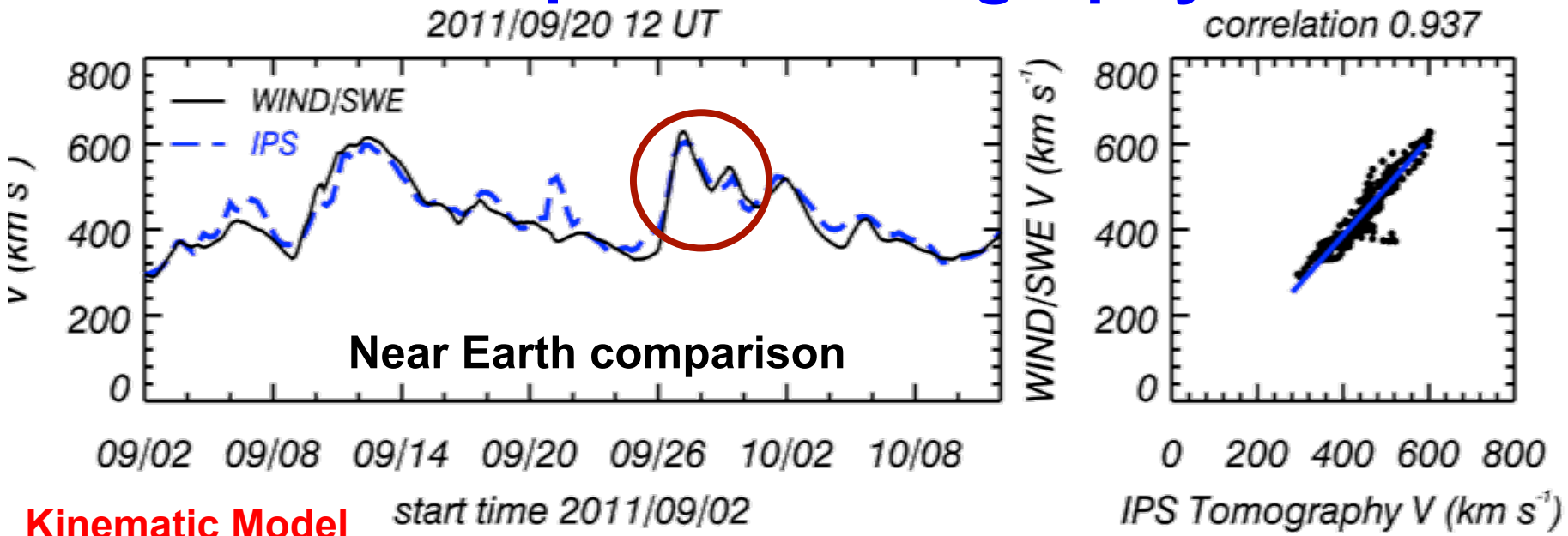

Kinematic Model
Iterative Data Fit

Interesting Event

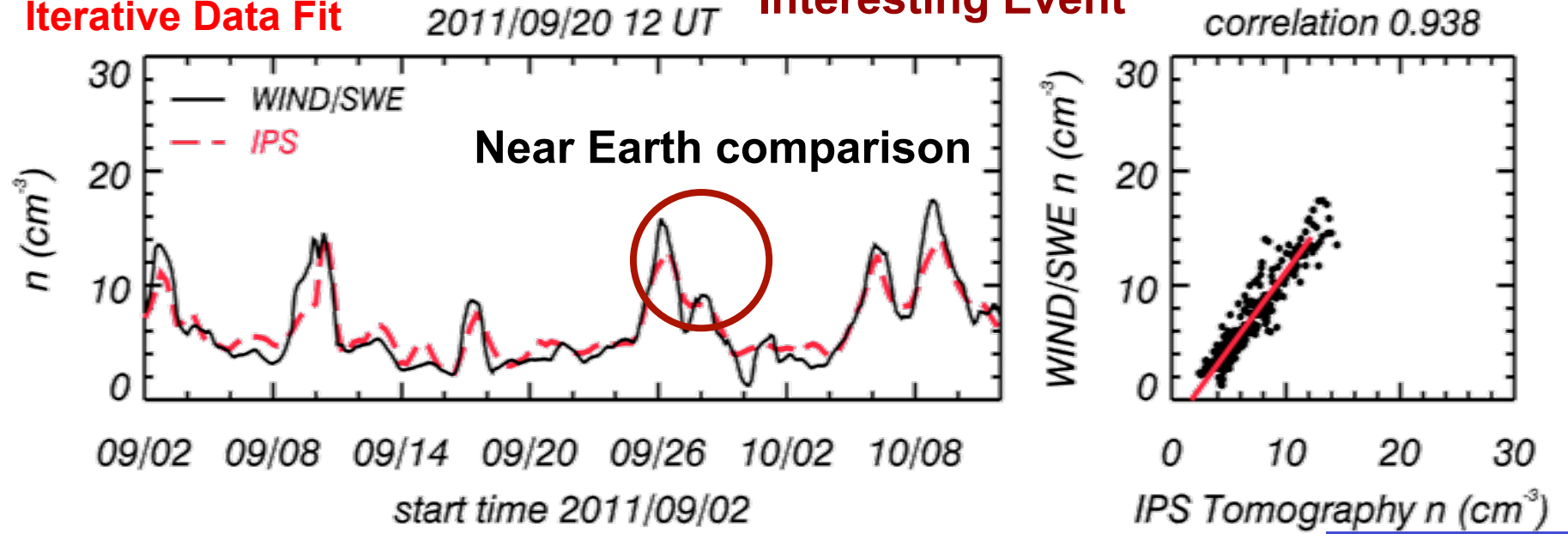

Heliospheric Tomography

(Yu, H-S., et al., 2012, *AIP Conference Proc. 1500*, pp. 147-152.)

IPS-Derived 3D-MHD Model Boundaries

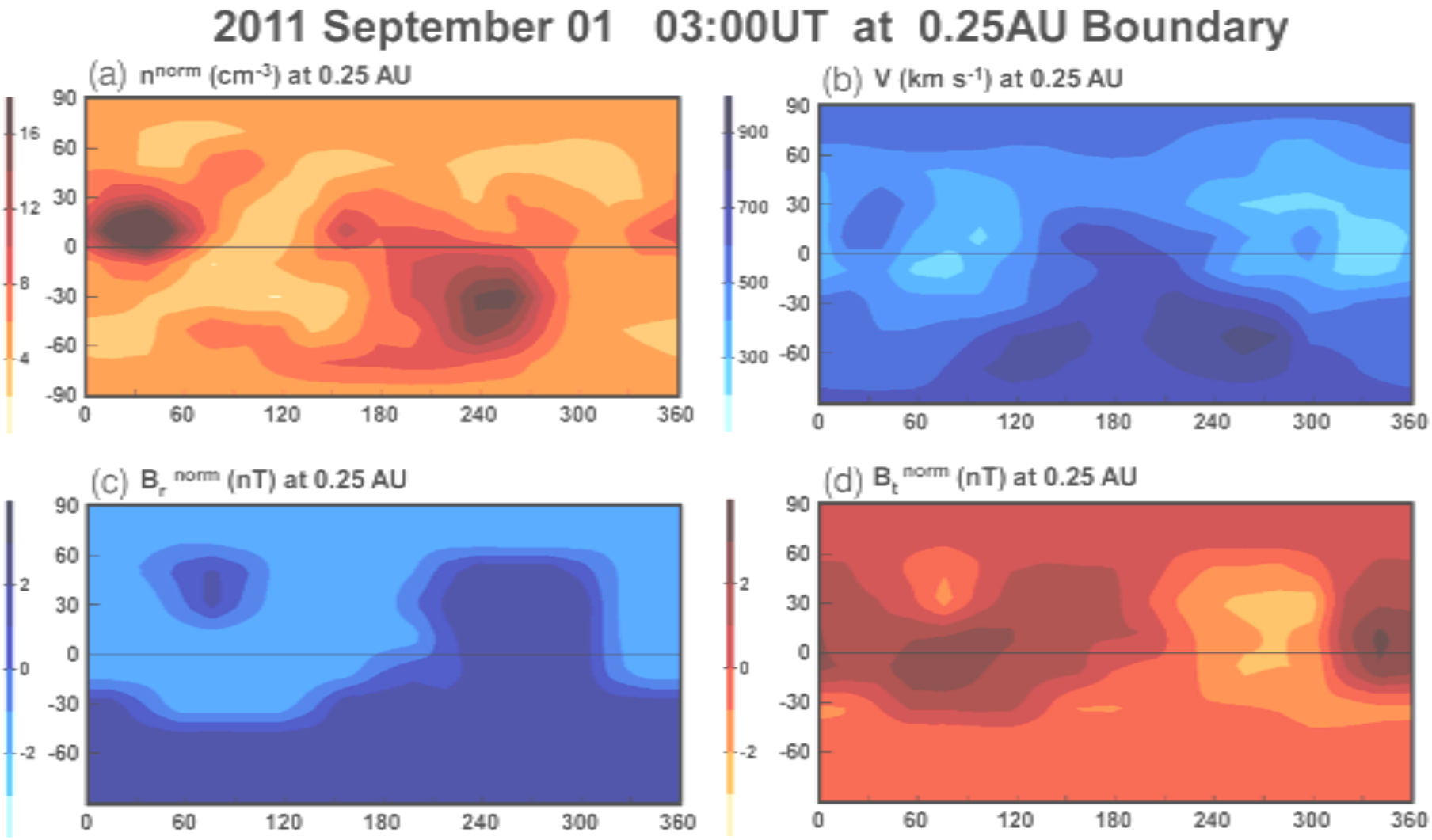

MS-FLUKSS (UAH) Heliospheric Tomography

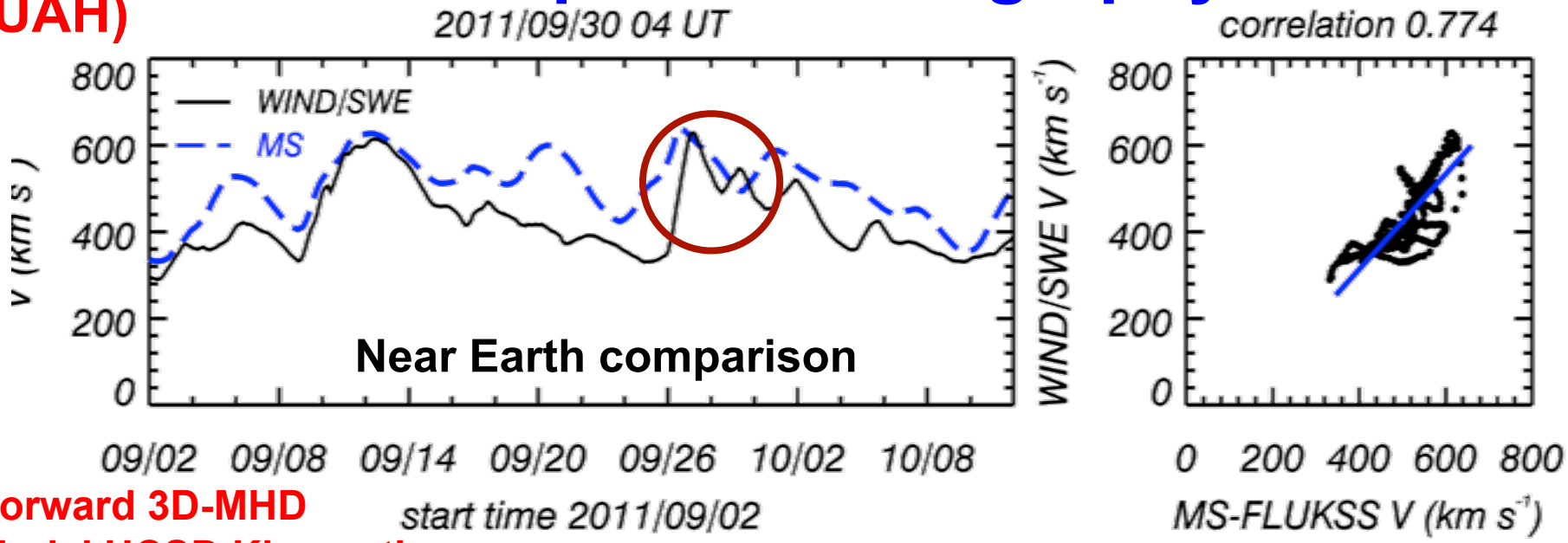

Forward 3D-MHD Model UCSD Kinematic Inner Boundary

Interesting Event

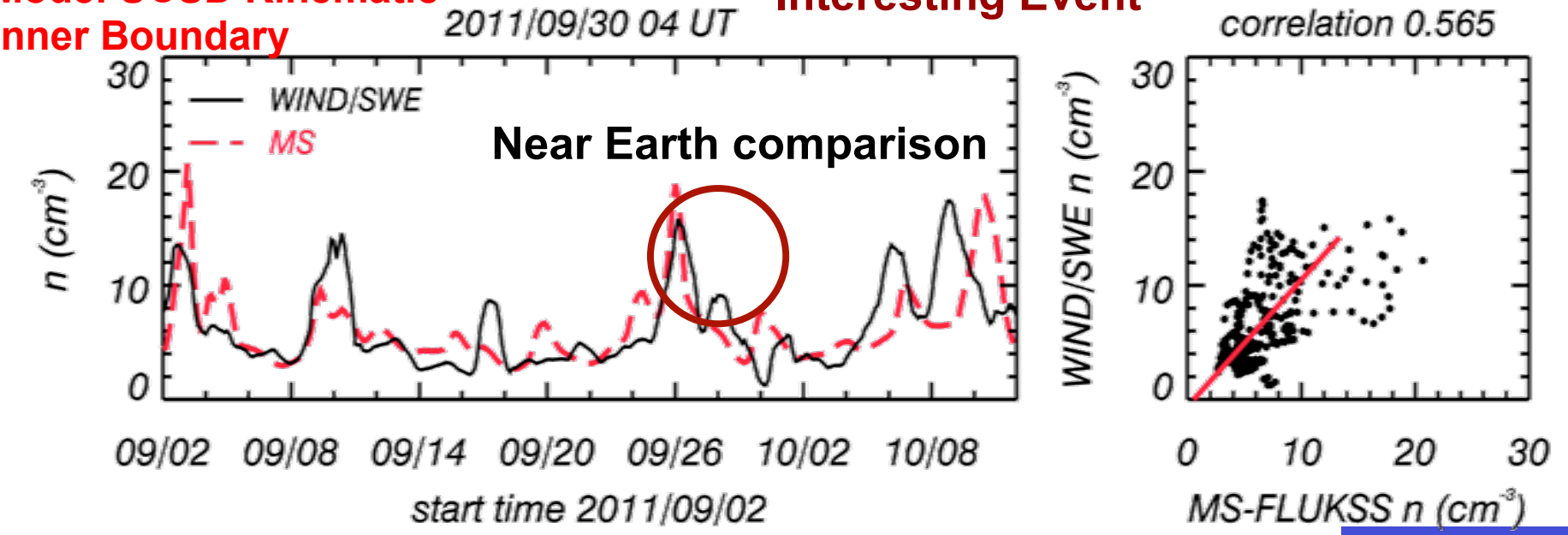

H-3D-MHD (NRL) Heliospheric Tomography

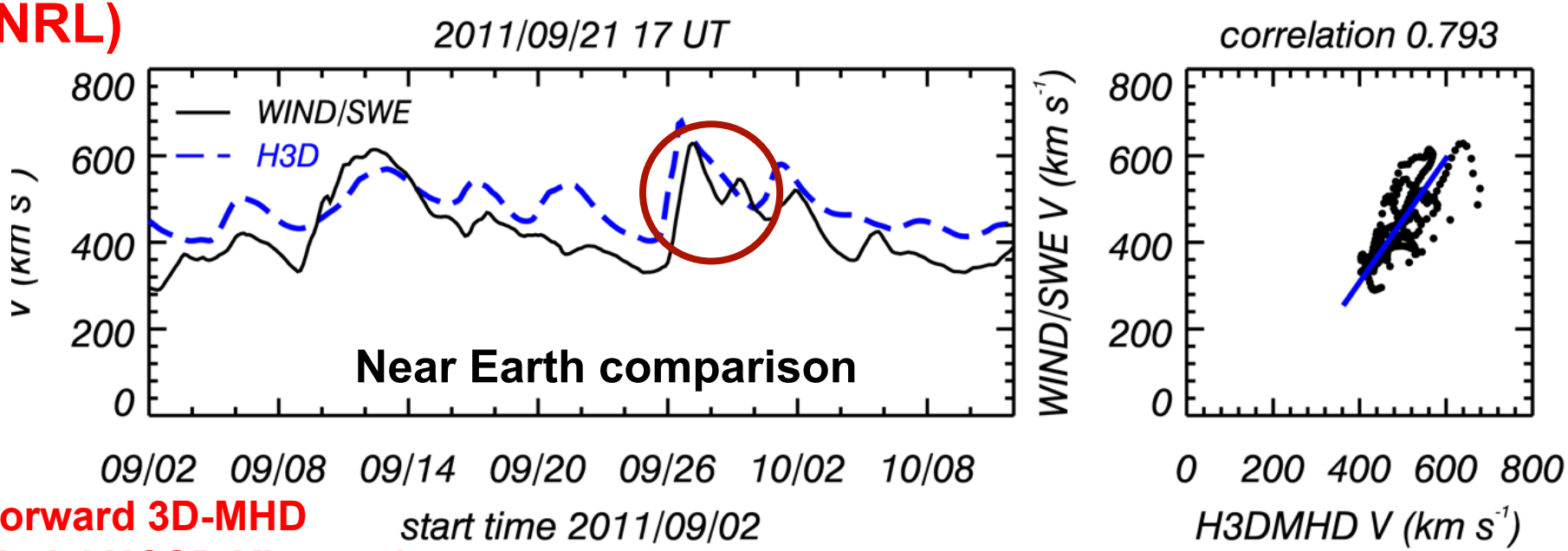

Forward 3D-MHD Model UCSD Kinematic Inner Boundary

Interesting Event

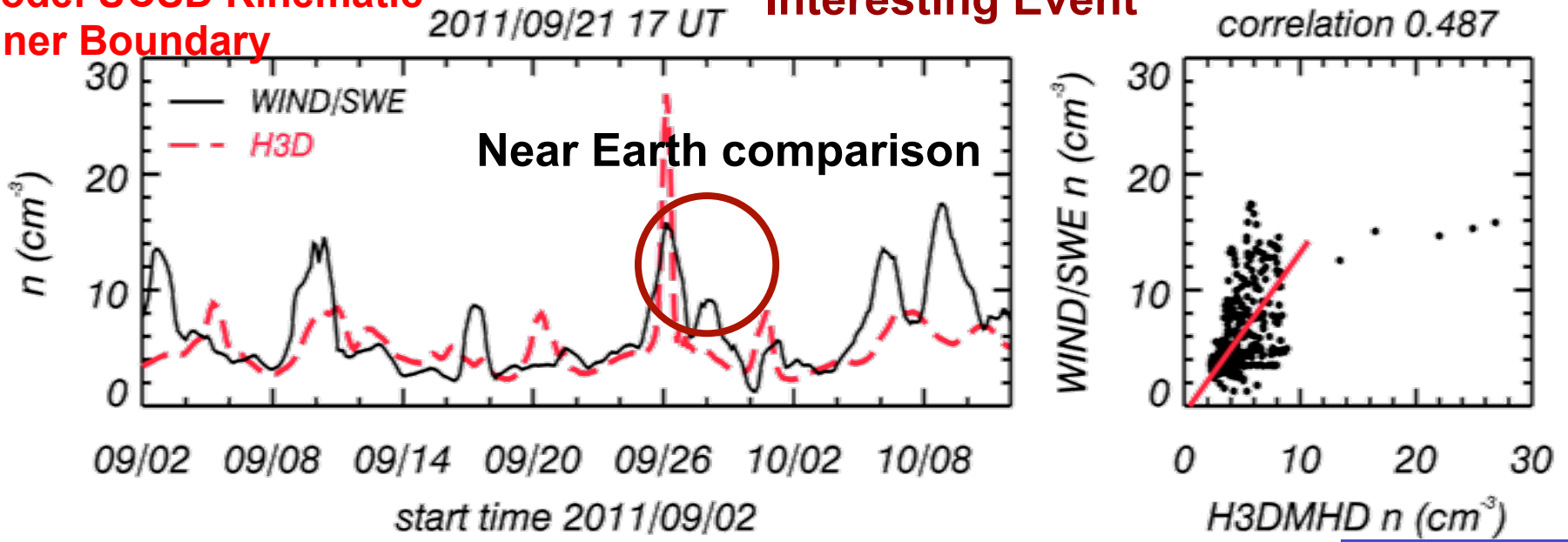

ENLIL (D. Odstrcil)

Heliospheric Tomography

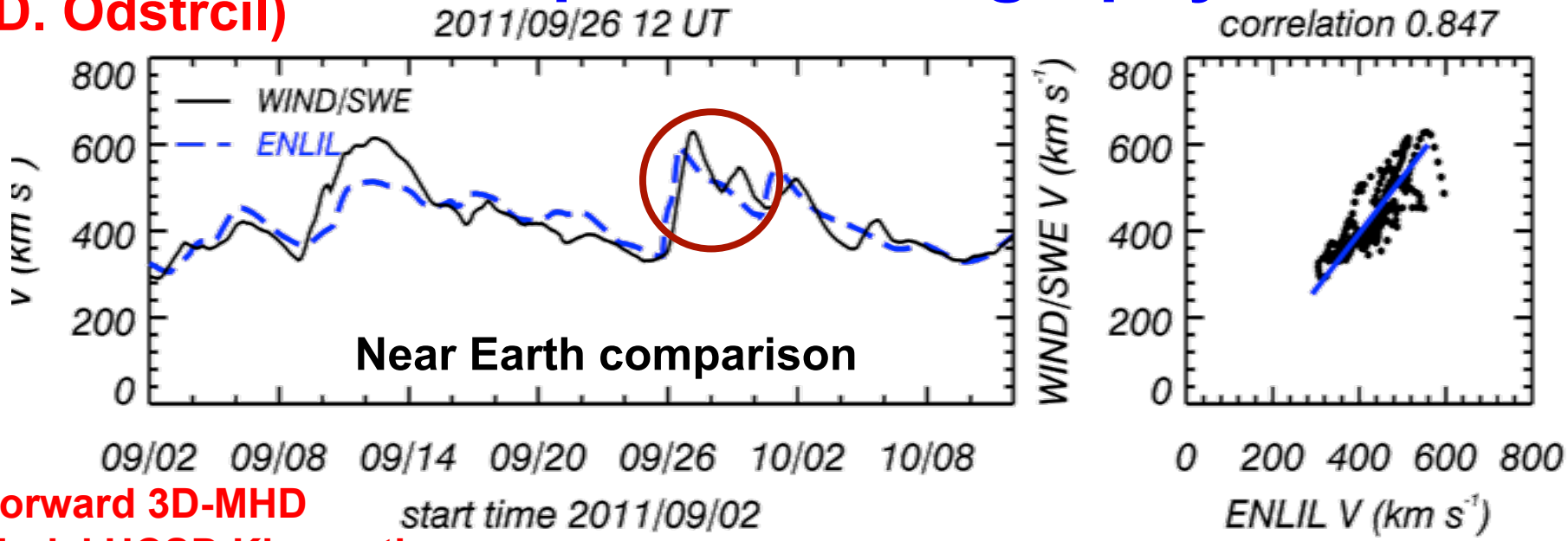

Forward 3D-MHD Model UCSD Kinematic Inner Boundary

Interesting Event

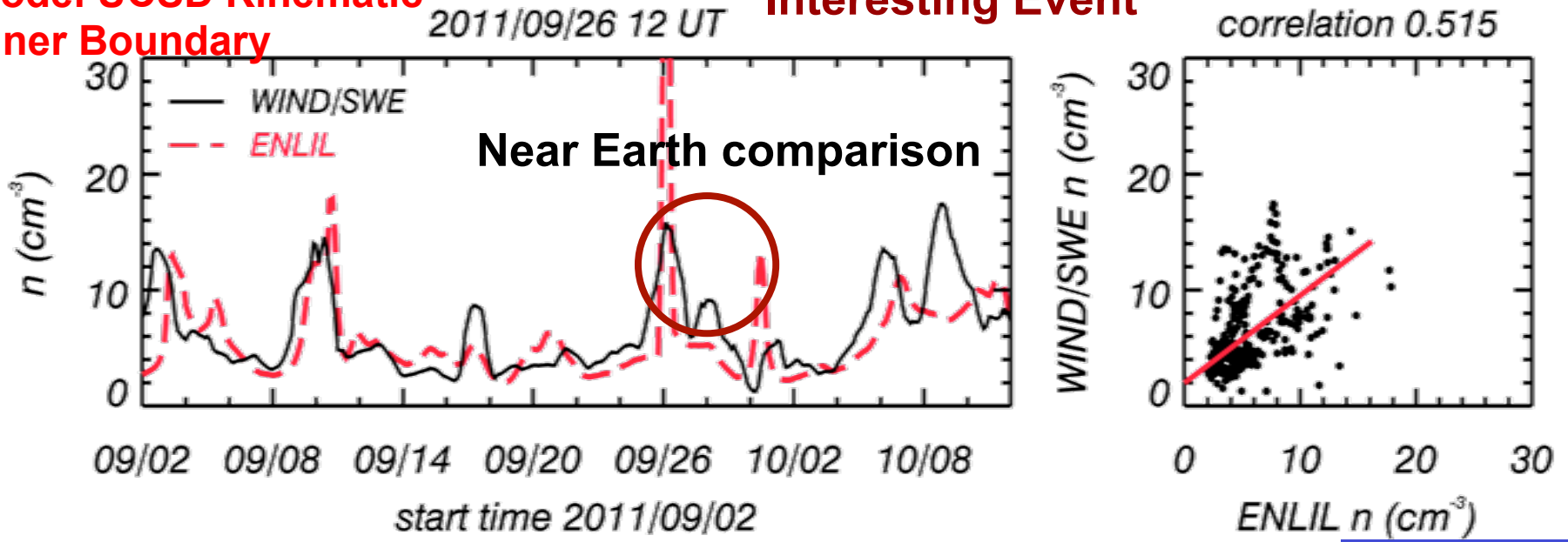

Kinematic Model
Iterative Data Fit

Heliospheric Tomography

UCSD IPS Data Fit Model

UCSD kinematic modeling from a 15.0 Rs
3D time-dependent IPS tomography boundary.

(Yu, H-S., et al., 2014, *NOAA Space Weather Week*, poster.)

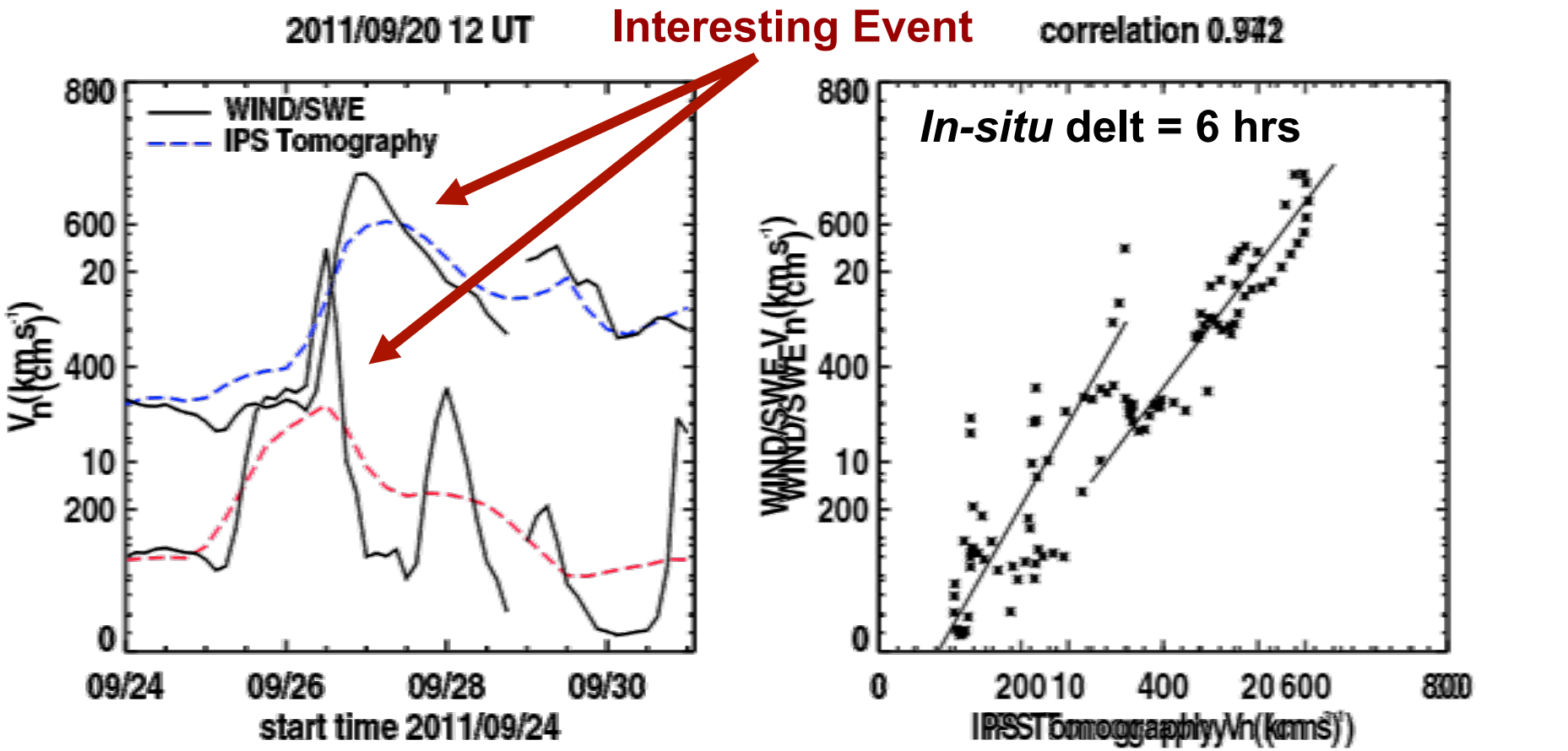

ENLIL
(D. Odstrcil)

Heliospheric Tomography

UCSD IPS Data Fit Model

ENLIL forward modeling from a 21.0 Rs
3D time-dependent IPS tomography boundary.

(Yu, H-S., et al., 2014, *NOAA Space Weather Week*, poster.)

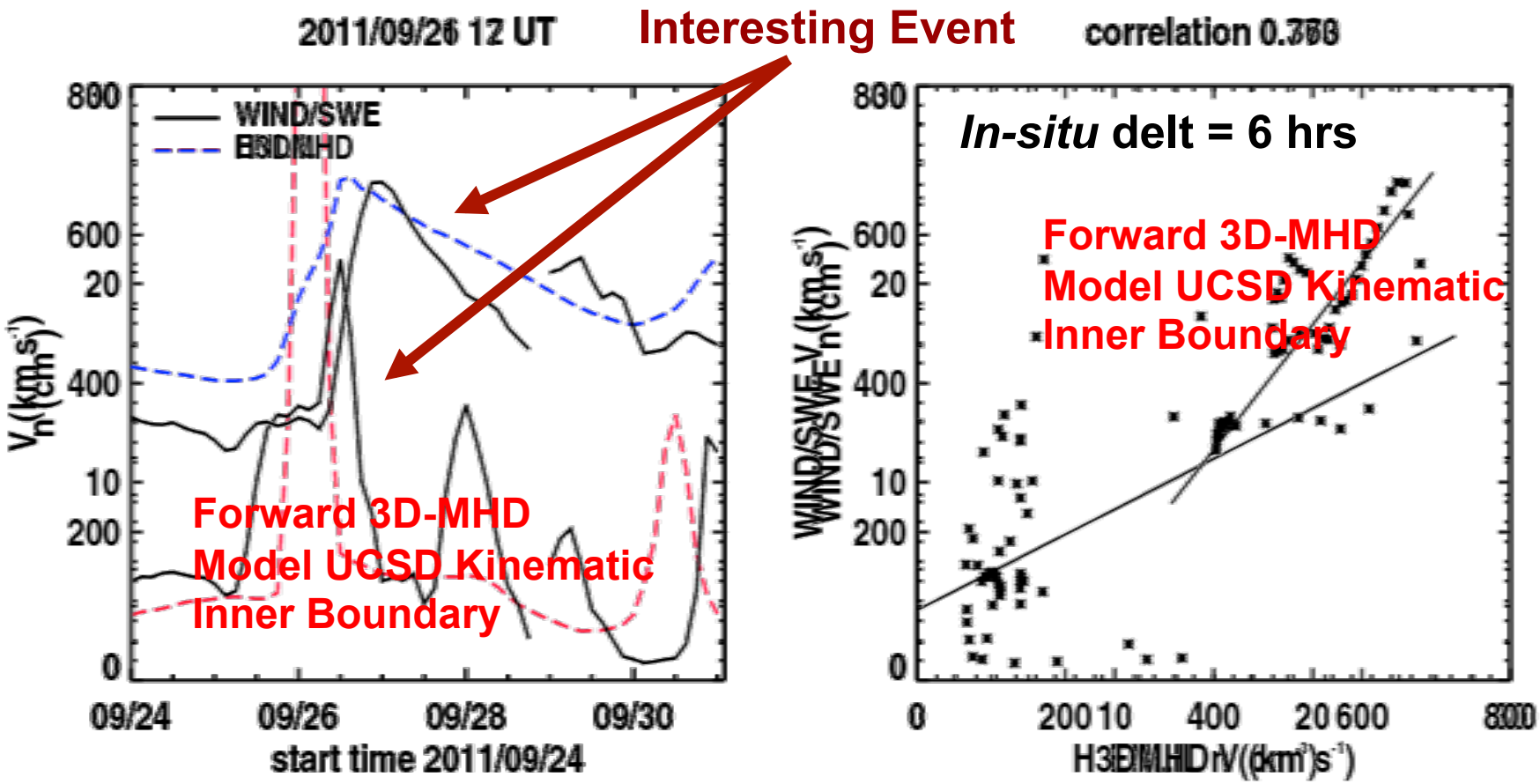

Kinematic Model
Iterative Data Fit

Heliospheric Tomography

UCSD IPS Data Fit Model

ENLIL forward modeling from a 21.0 Rs
3D time-dependent IPS tomography boundary.

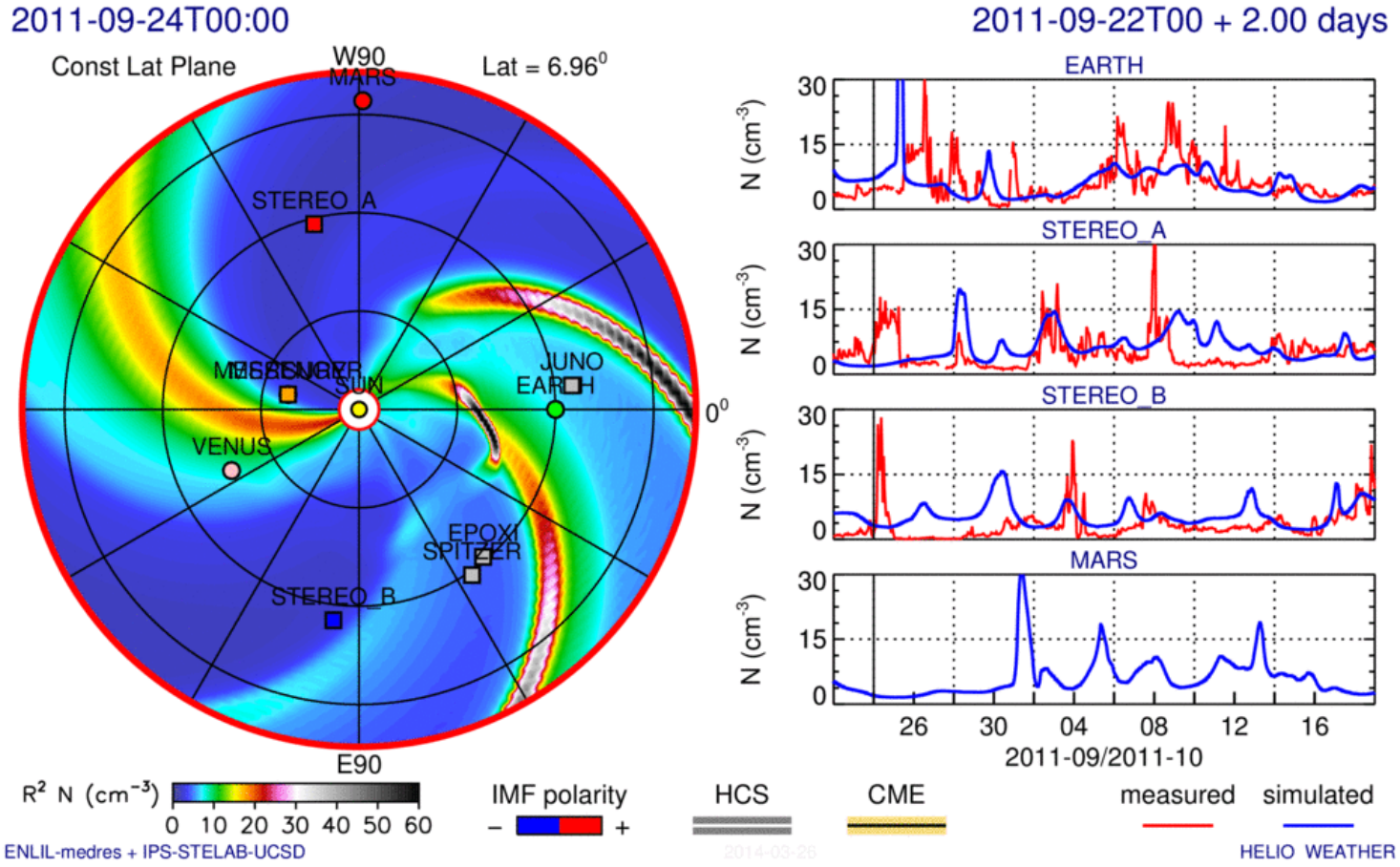

Density

Kinematic Model
Iterative Data Fit

Heliospheric Tomography

UCSD IPS Data Fit Model

Ecliptic Cuts

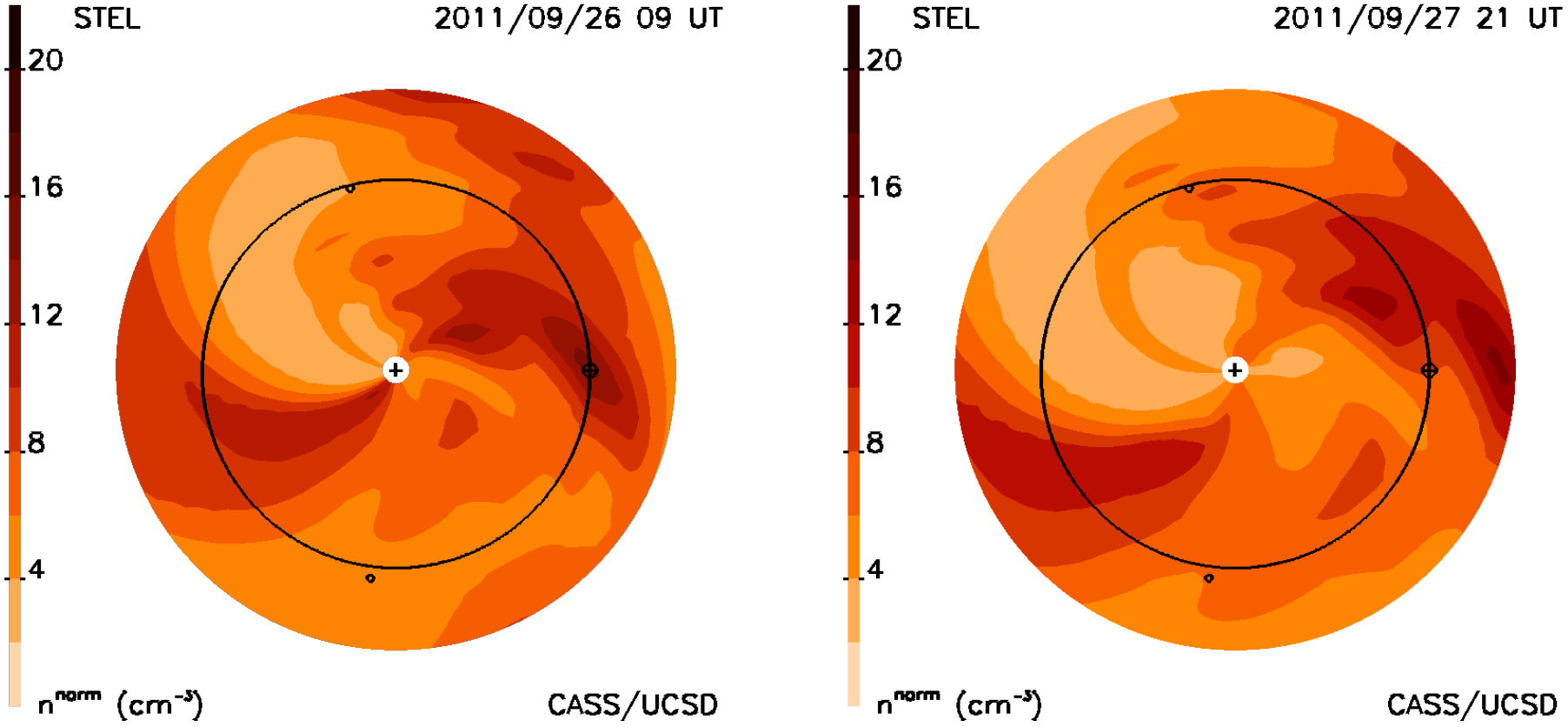

Density

Heliospheric Tomography

Observations

CMEs Observed by C2 STEREO HI-A,B

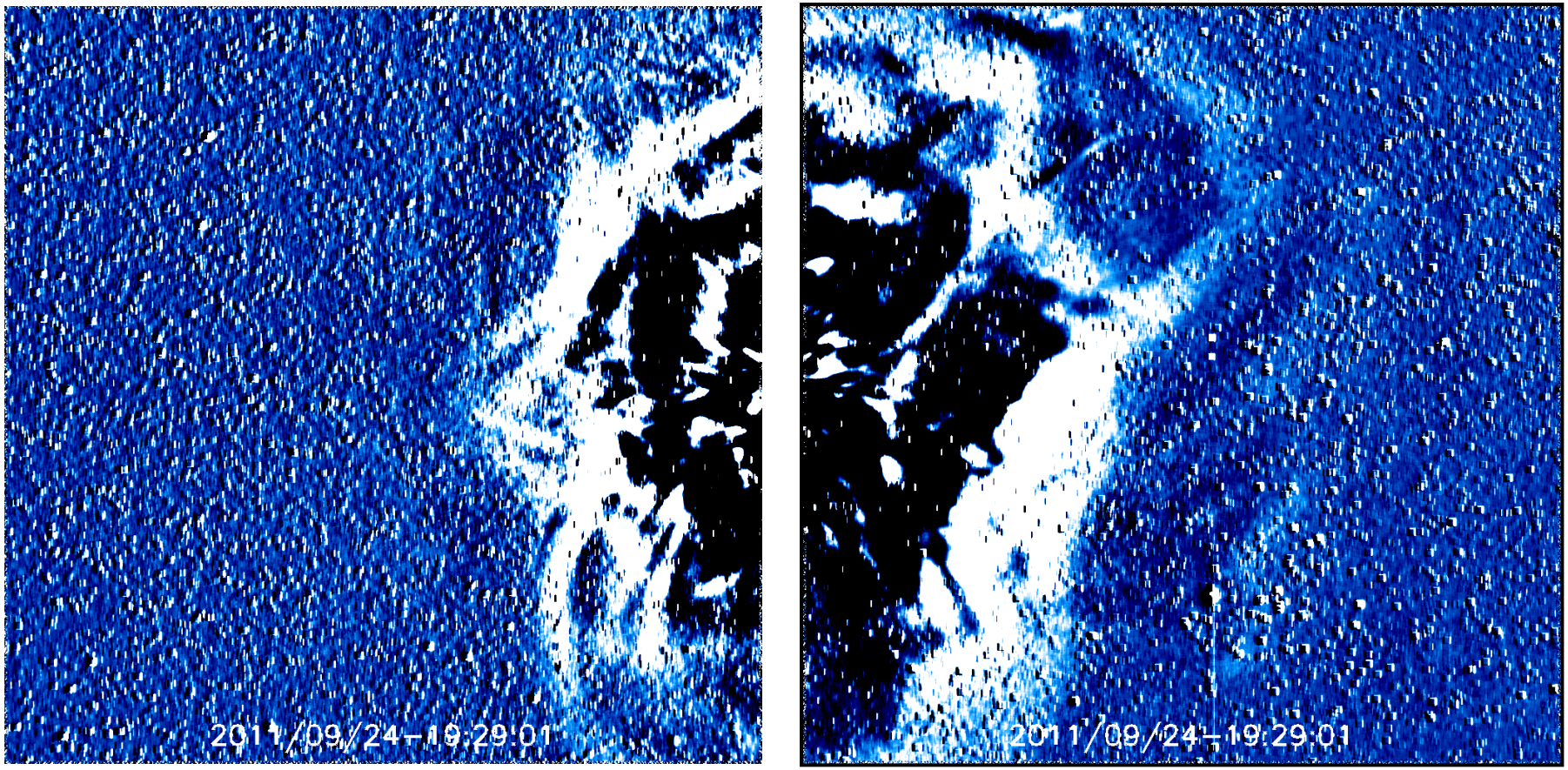

HI-A CME 1 HI-B

Heliospheric Tomography

Observations

CMEs Observed by C2 STEREO HI-A,B

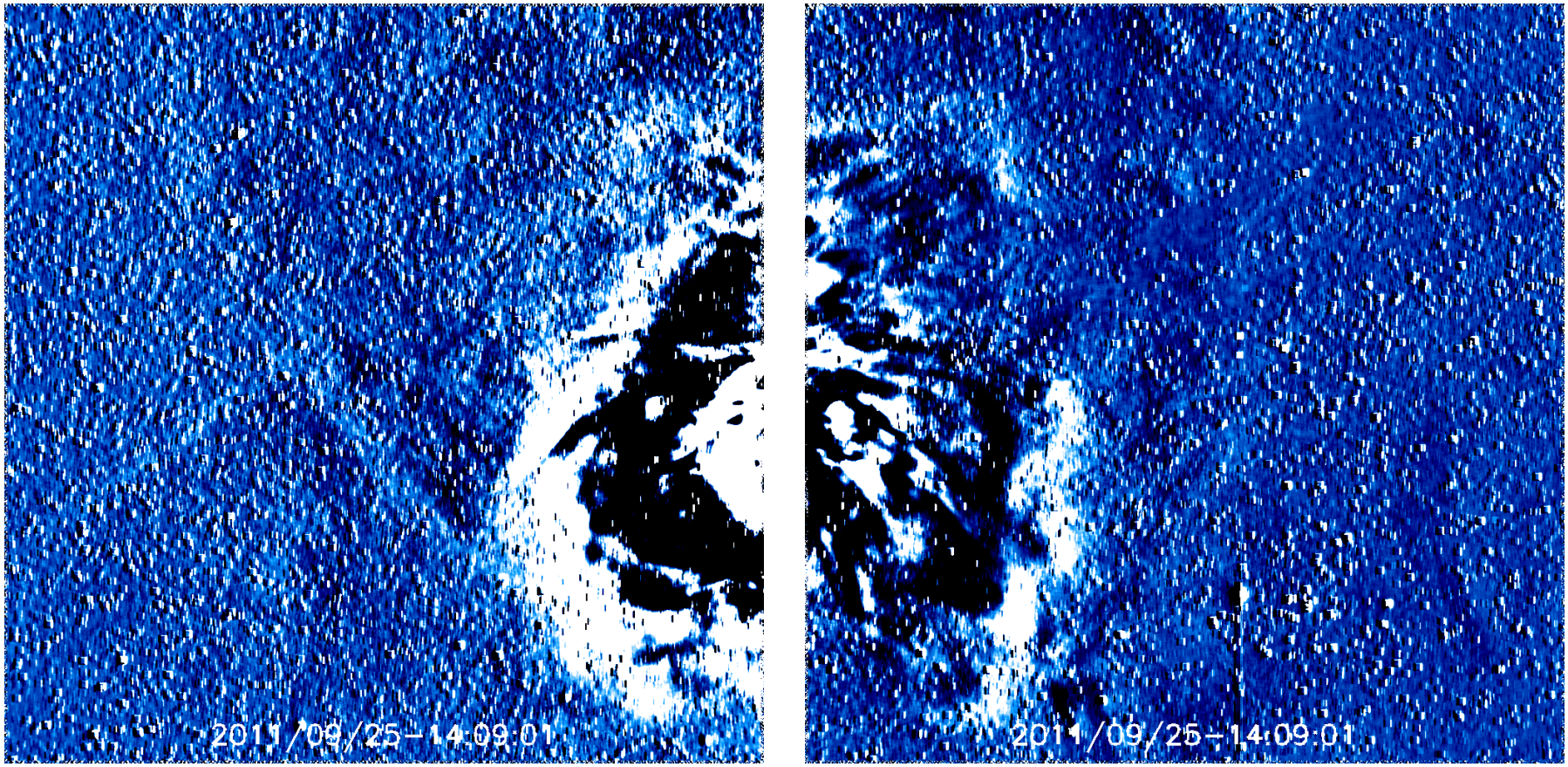

HI-A CME 2 HI-B

Heliospheric Tomography

Observations

CMEs Observed by C2 STEREO HI-A,B

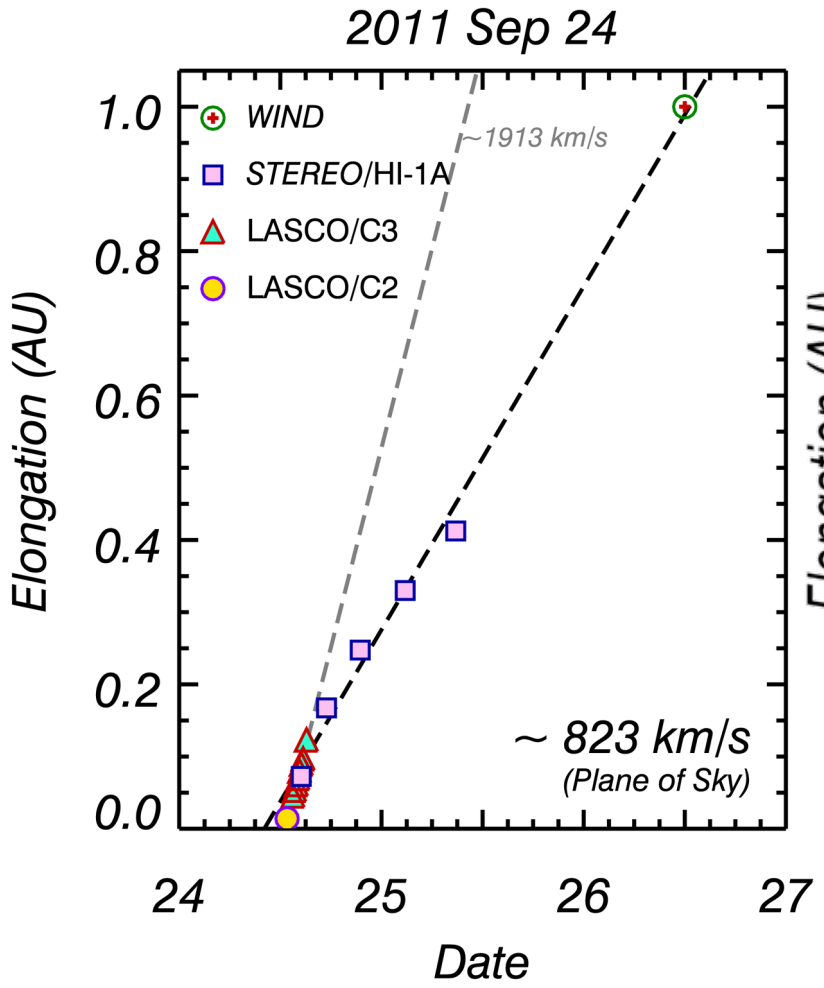

CME 1

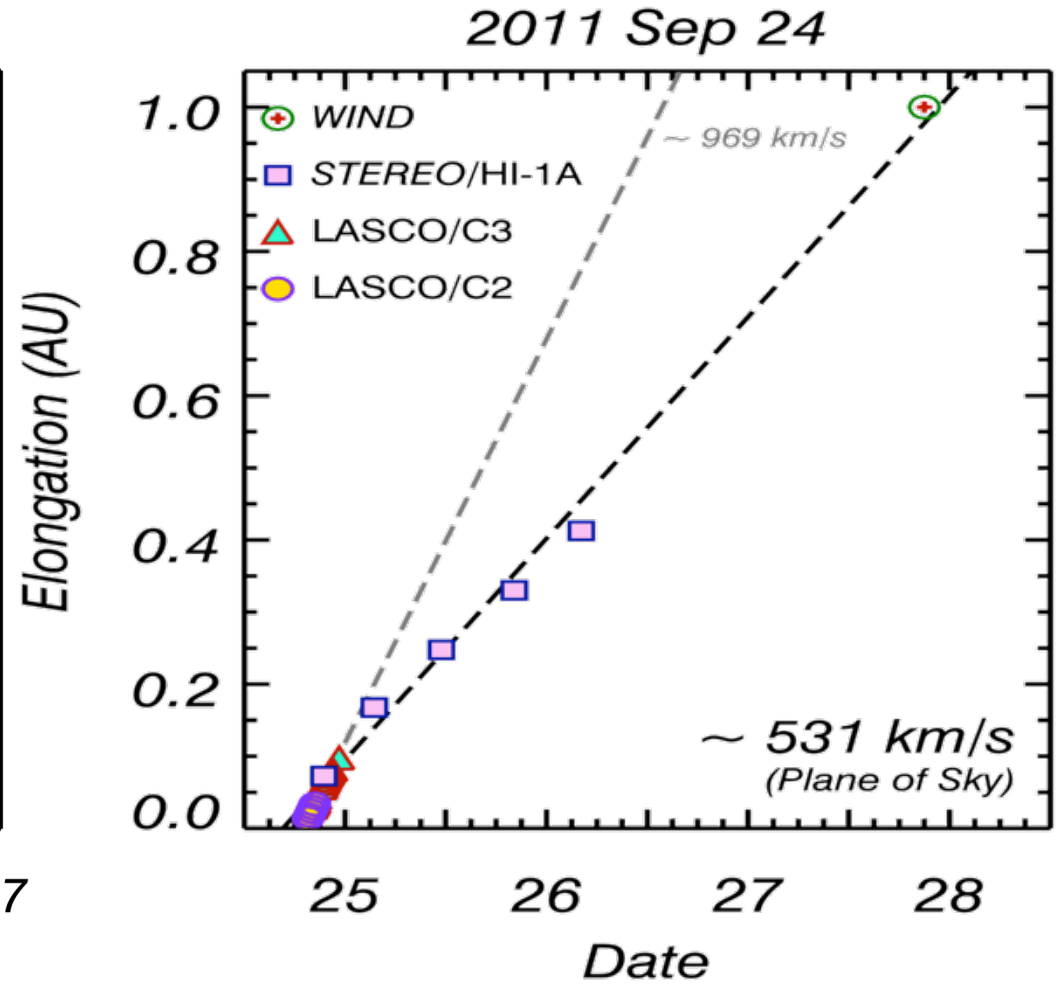

CME 2

ENLIL
(D. Odstrcil)

Heliospheric Tomography

UCSD IPS Data Fit Model

ENLIL forward modeling from a 21.0 Rs
3D time-dependent IPS tomography boundary.

(Yu, H-S., et al., 2014, *NOAA Space Weather Week*, poster.)

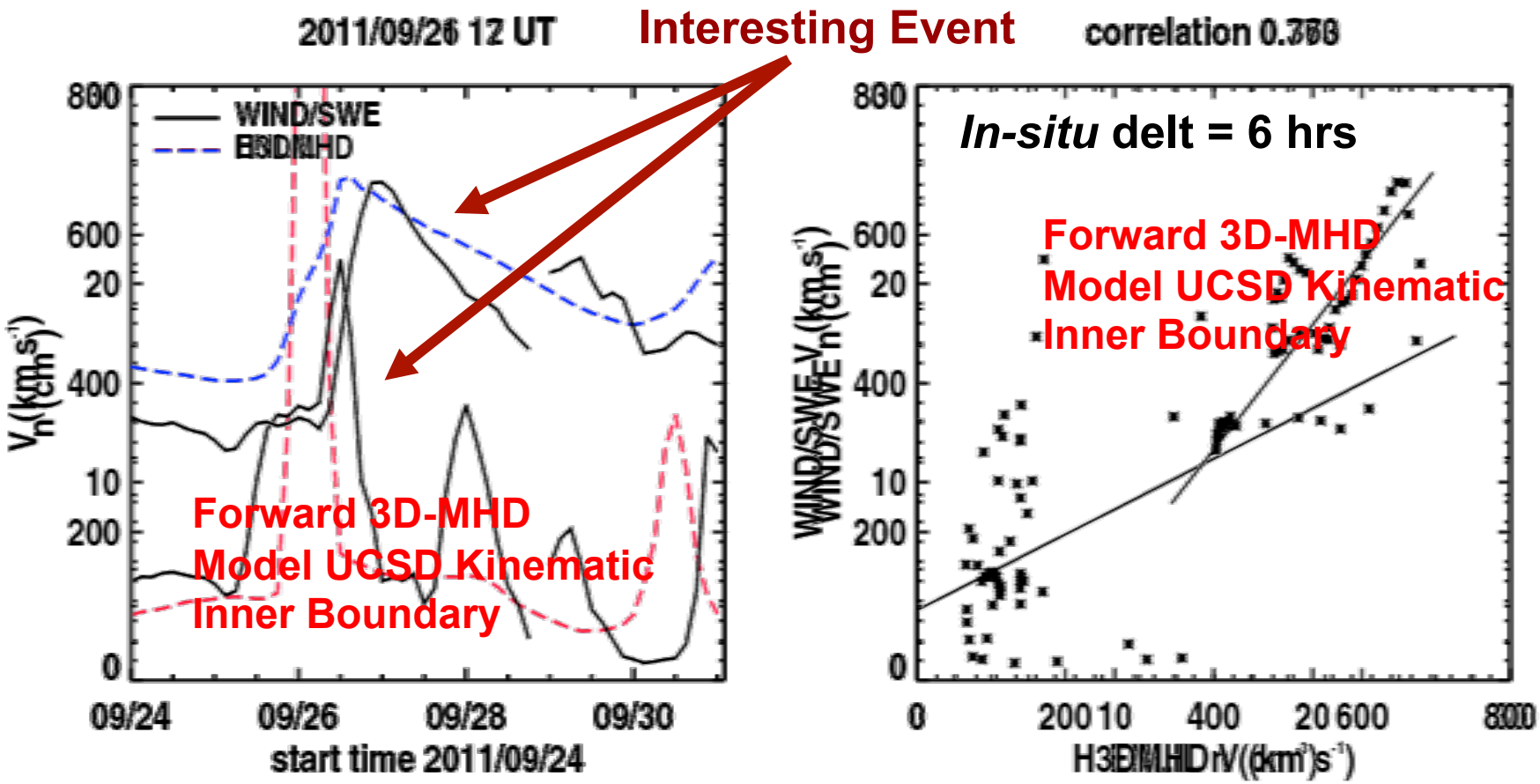

Heliospheric Tomography
ENLIL Model Drivers

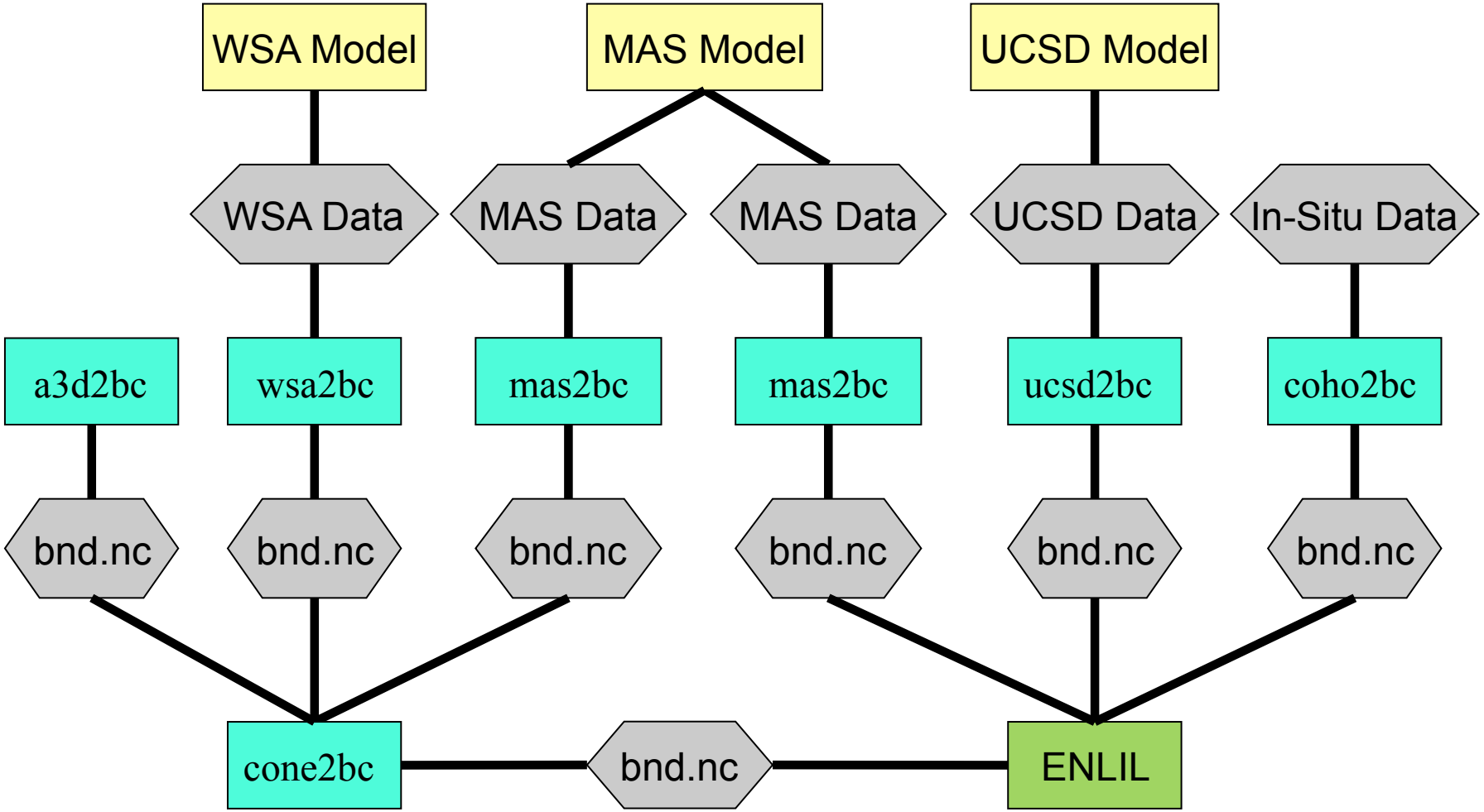

- Currently, there are three models (yellow) that can be used to drive ENLIL (green)
- Computational system shares data sets (grey) and uses couplers (blue)

Heliospheric Tomography

Summary:

IPS analysis:

A ground-based technique. Can provide low-resolution velocity and density analysis, and accurate forecasts of time-variable heliospheric structure.

The IPS analysis can provide input to 3D-MHD models. Better, and more abundant IPS data, should be available in the near future.

Heliospheric Tomography

More Details

Faraday Rotation

Heliospheric Tomography

$$\Phi = \lambda^2 \int n_e \overline{B} \bullet \overline{ds}$$

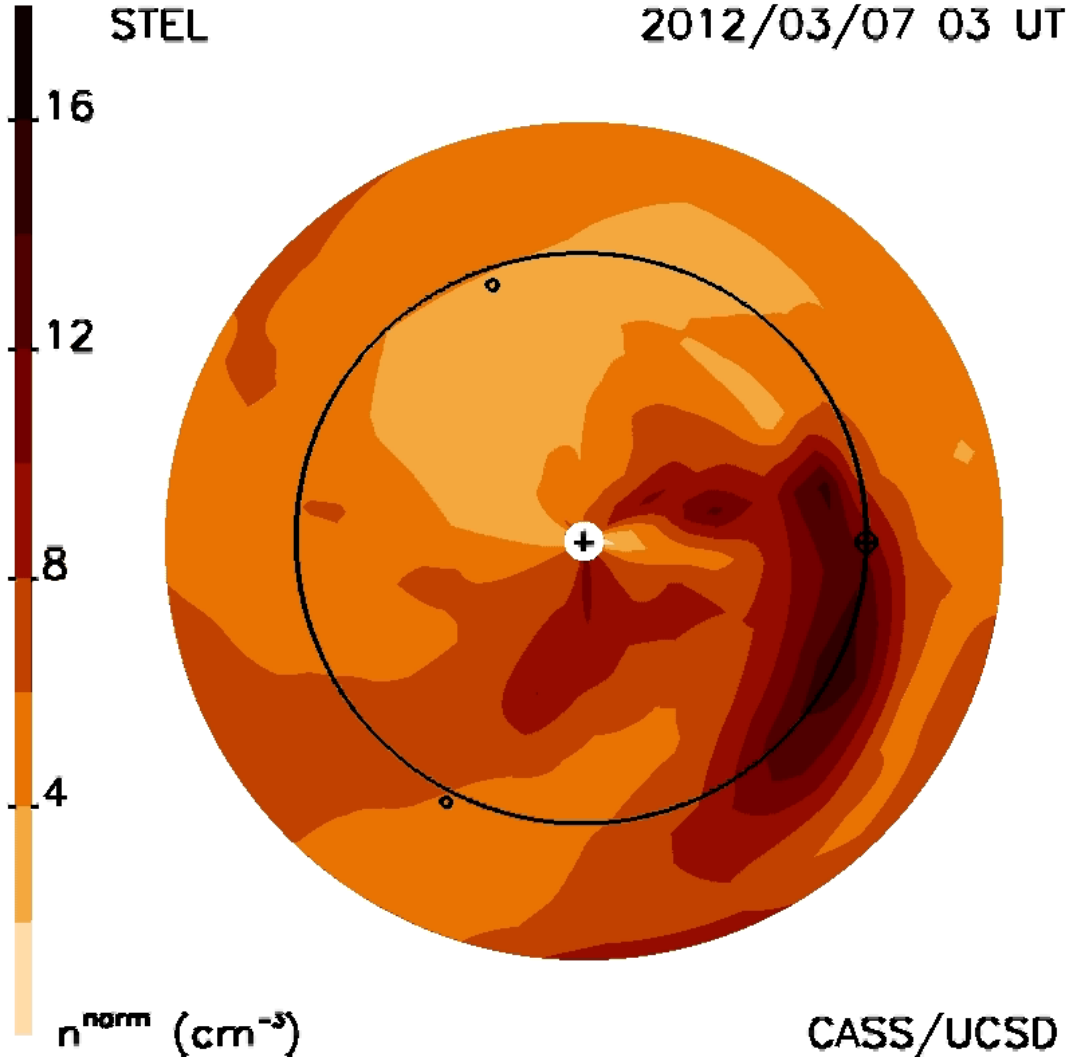

3-D reconstructions of Carrington rotation (CR) 2121 showing a CME of interest from 07 March 2012 launched around 01:00UT.

Heliospheric Tomography

$$\Phi = \lambda^2 \int n_e \overline{B} \cdot \overline{ds}$$

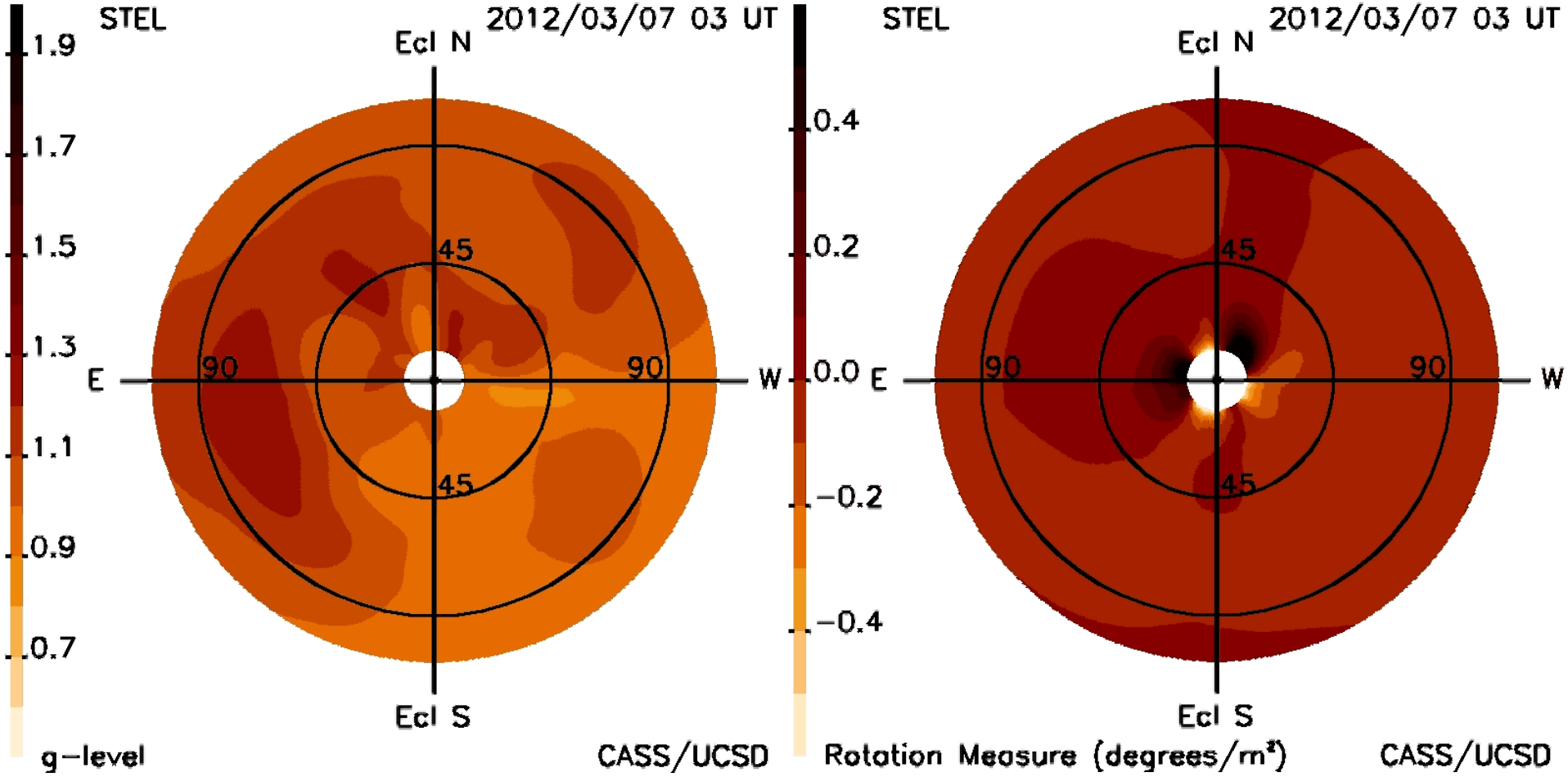

The same period extracted from CR2121 comparing IPS *g*-level fisheye sky map (left) with that of reconstructed RM from ambient magnetic fields (right) perturbed by the CME.

Heliospheric Tomography

Oberoi and Lonsdale, 2012, *Radio Science,* 47, RS0K08, doi:10.1029/2012RS004992.

Faraday rotation signals at low frequency

$$\Phi = \lambda^2 \int n_e \overline{B} \bullet \overline{ds}$$

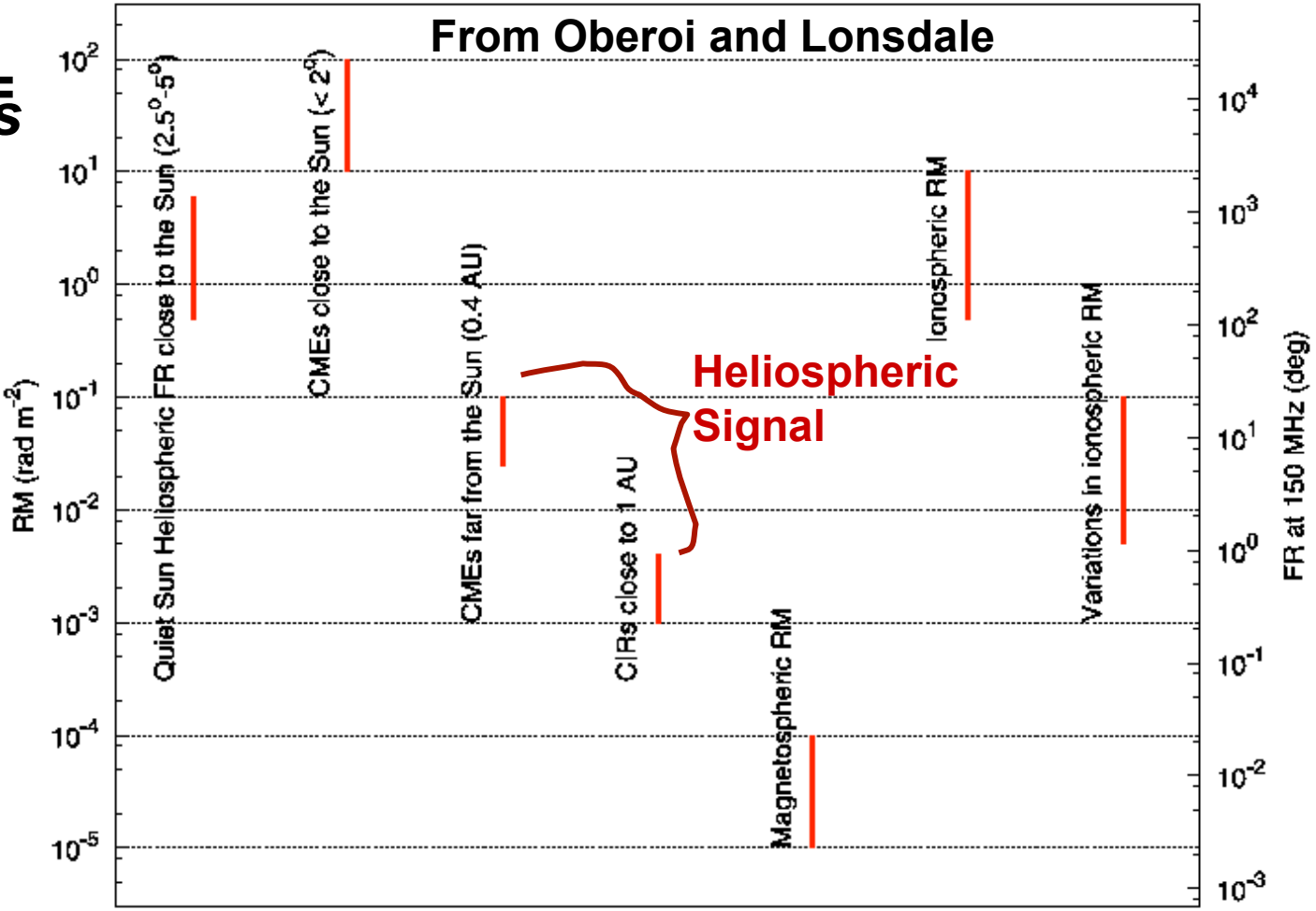

Heliospheric Tomography

Better IPS data

Heliospheric Tomography

Future Potential – Better IPS Data

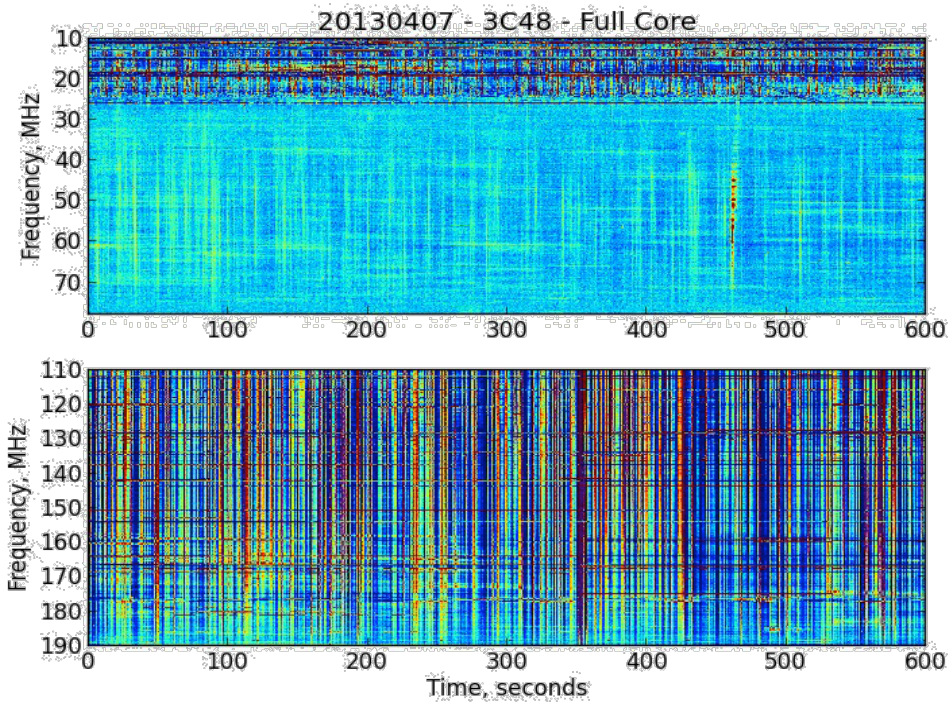

LOFAR IPS 3C48 Signal

LOFAR (Western Europe)

(Some parts of the LOFAR system are now operating - Richard Fallows, Mario Bisi are involved. IPS tests are ongoing.)

Heliospheric Tomography

KSWC and IPS array

Heliospheric Tomography

IPS Workshop 2013

(November 23-24, 2013, STELab, Japan following CAWSES II)

Objectives:

1) Standardize the IPS measurement output for external use.

2) Discuss the best way to provide IPS velocities and g-level from a single site IPS system

3) Discuss current progress on heliospheric Faraday rotation measurement.

Heliospheric Tomography

DATA

IPS Heliospheric Analyses (STELab)

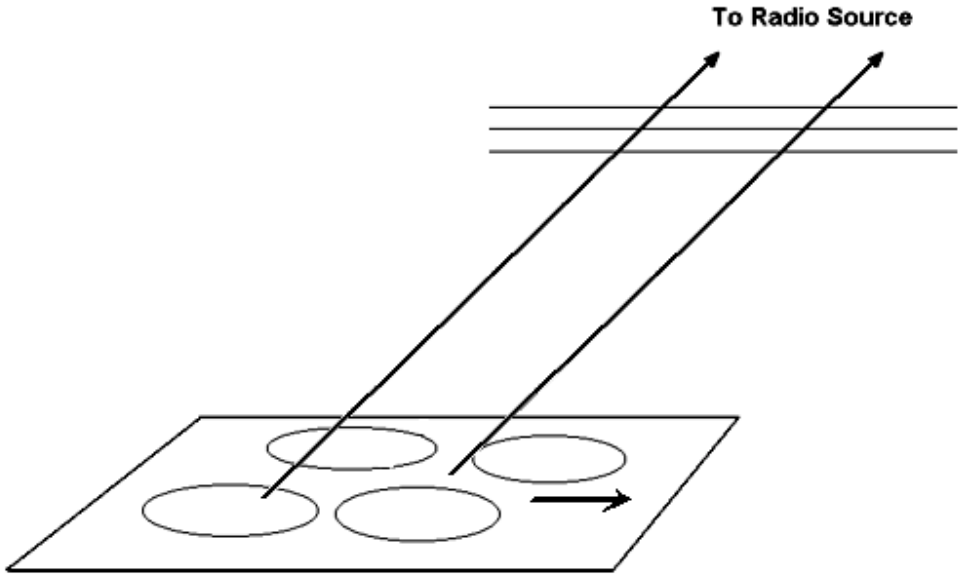

IPS line-of-sight response

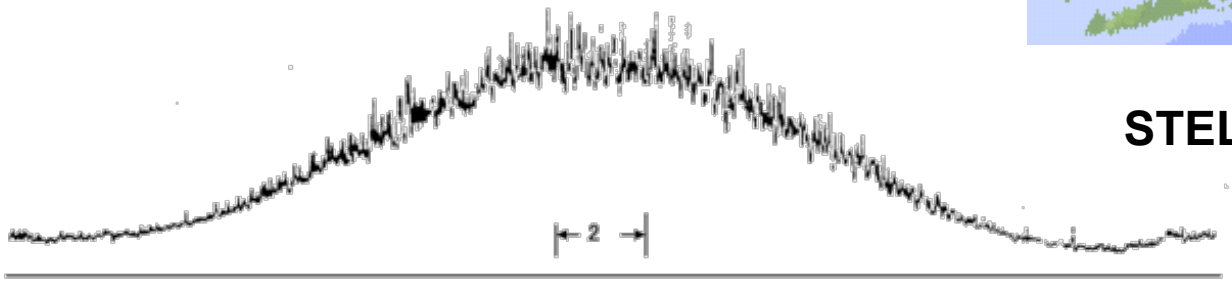

STELab IPS array systems

Heliospheric Tomography

Cross Correlation Analysis with Upgraded STEL IPS System

(Courtesy of M. Tokumaru)

Tokumaru, M., *et al.*, 2013, *AOGS 2013 Presentation* , June, Brisbane, Australia.

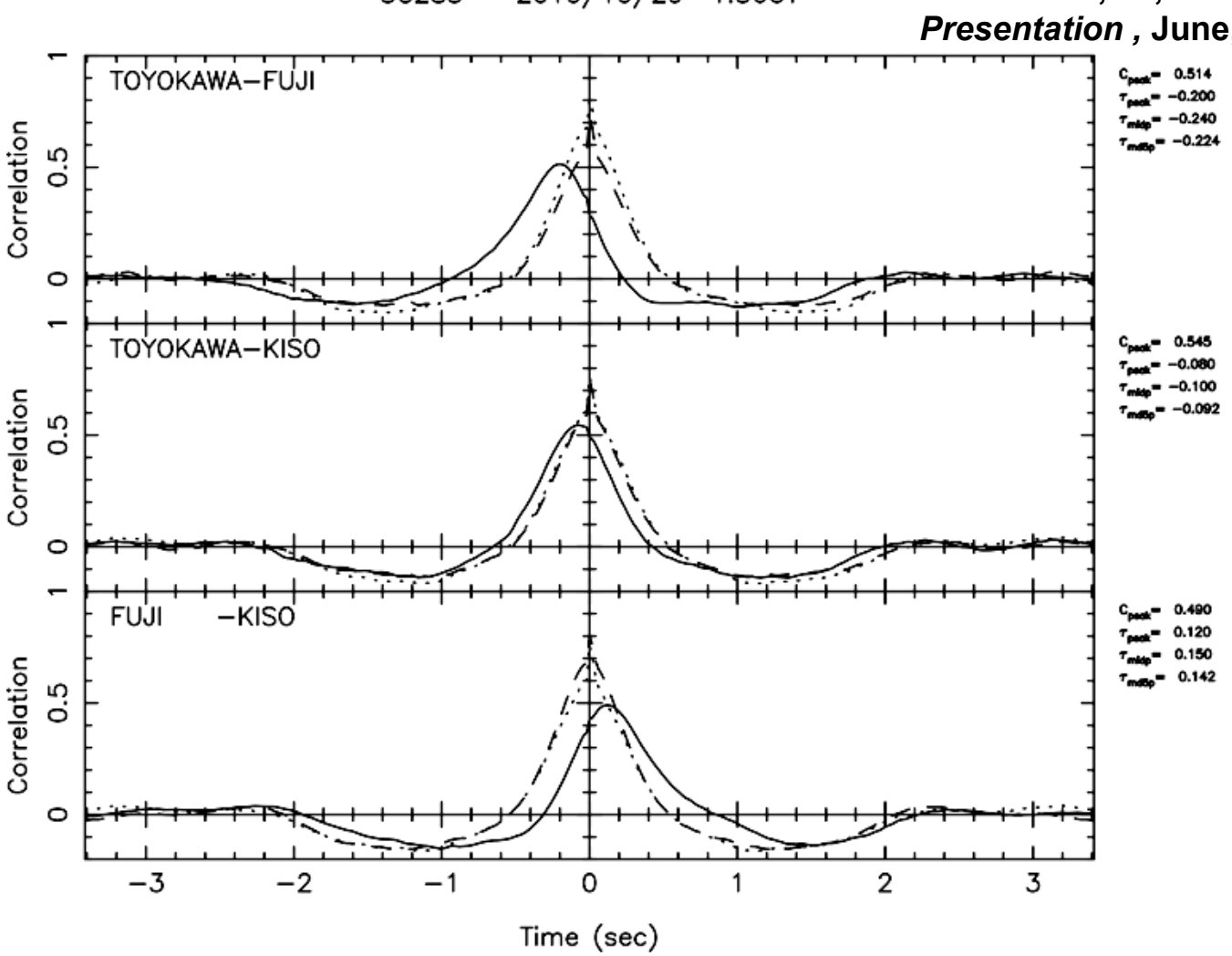

Solid lines: Cross Correlation
Dashed/Dotted lines: Auto Correlation

Taking account of the baseline geometry, we determine the solar wind speed. For this case, we obtain **V=522+/-3 km/s**. Here, we assume radial flow and the anisotropy.

Heliospheric Tomography

A model of the power spectra of density fluctuations

To calculate solar wind velocities using a single IPS station, we use a theoretical power spectrum: an integration of scattering layers along the line of sight (z).
The spectrum depends on: **λ, ε, v, Θ, α** (isotropic medium).

Mejía-Ambriz, J., *et al.*, 2013, *AGU 2013 Presentation*, May, Cancoon, Mexico.

$$P(f) = c \int_{-\infty}^{\infty} \frac{dz}{V_x(z)} \int_{-\infty}^{\infty} dq_y \sin^2\left(\frac{q^2 z_0 \lambda}{4\pi}\right) e^{-\left(\frac{q r_0 \Theta}{2.35}\right)^2} R^{-4} q^{-\alpha}$$

- Frequency of intensity fluctuations
- Solar wind velocity
- Diffractive function (Fresnel function)
- Visibility function of the source
- Heliocentric distance at the region of IPS (point P)
- Wave number of solar wind irregularities $q_x^2 + q_y^2 = q^2$

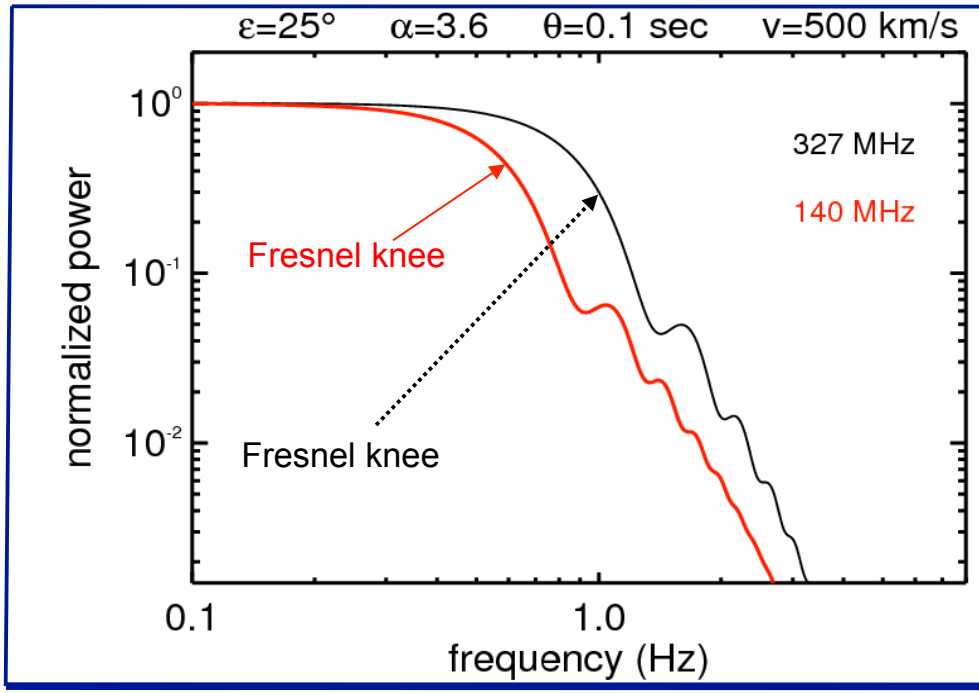

α ≈ 3.5 ± 0.5
Turbulence spectrum follows a potential law

Example of the model (log-log): **MEXART** and **STEL** observing frequencies.

Heliospheric Tomography

A model of the power spectra of density fluctuations

To calculate solar wind velocities using a single IPS station, we use a theoretical power spectrum: an integration of scattering layers along the line of sight (z).
The spectrum depends on: **λ, ε, v, Θ, α** (isotropic medium).

Mejía-Ambriz, J., *et al.*, 2013, *AGU 2013 Presentation* , May, Cancoon, Mexico.

$$P(f) = c \int_{-\infty}^{\infty} \frac{dz}{V_x(z)} \int_{-\infty}^{\infty} dq_y \sin^2\left(\frac{q^2 z_0 \lambda}{4\pi}\right) e^{-\left(\frac{q\Theta}{2.35}\right)^2} R^{-4} q^{-\alpha}$$

- Frequency of intensity fluctuations
- Solar wind velocity
- Diffractive function (Fresnel function)
- Visibility function of the source
- Heliocentric distance at the region of IPS (point P)
- Wave number of solar wind irregularities $q_x^2 + q_y^2 = q^2$

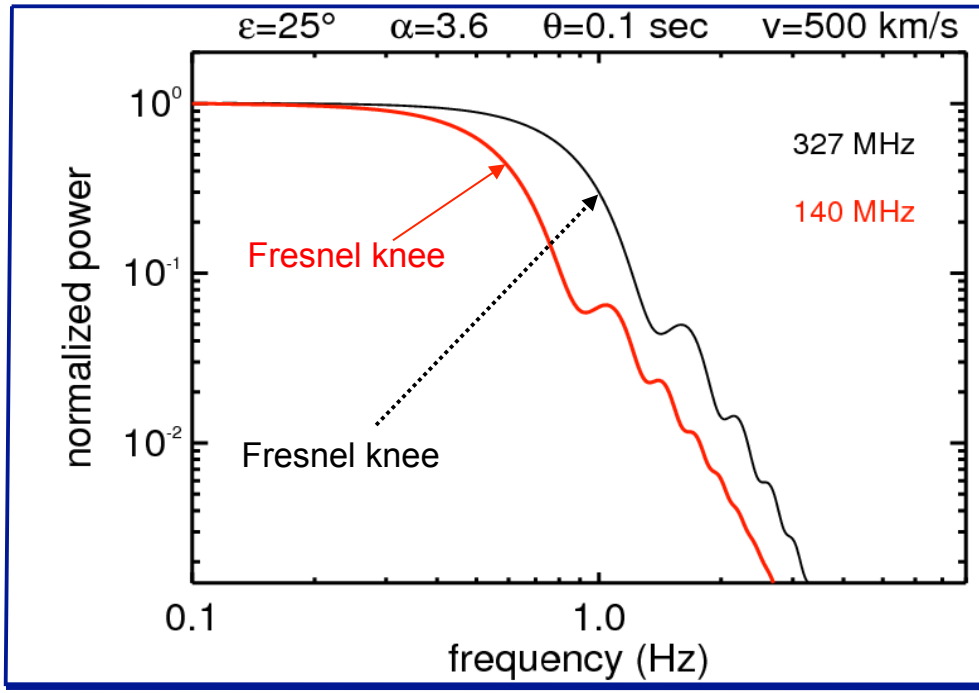

α ≈ 3.5 ± 0.5
Turbulence spectrum follows a potential law

Example of the model (log-log): **MEXART** and **STEL** observing frequencies.

Heliospheric Tomography
Comparison between Spectrum Fitting and Cross Correlation Methods

3C273 2012/9/3

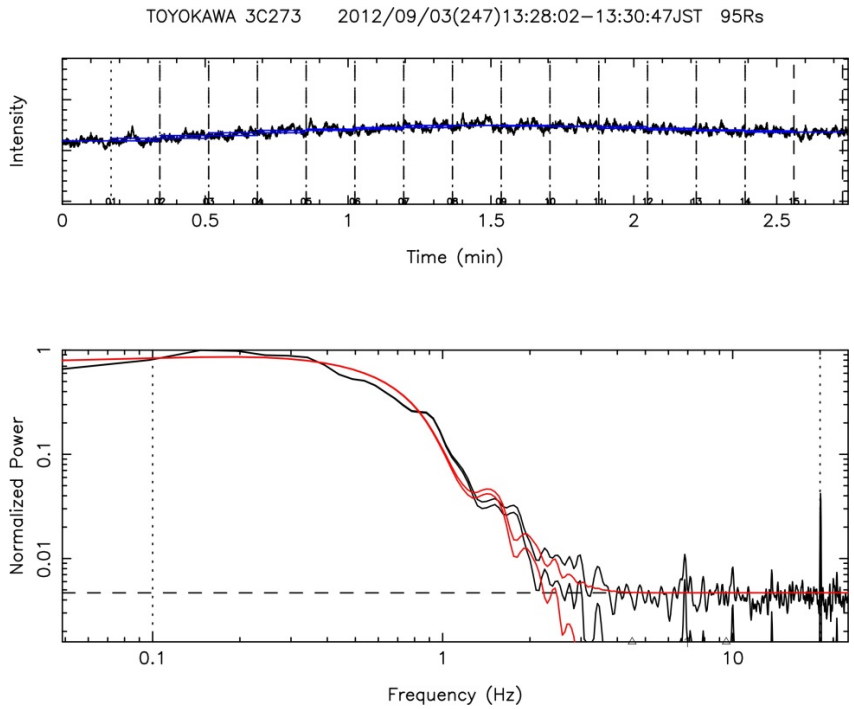

from IPS obs. for 3C273 in 2012

Correlation ~0.47

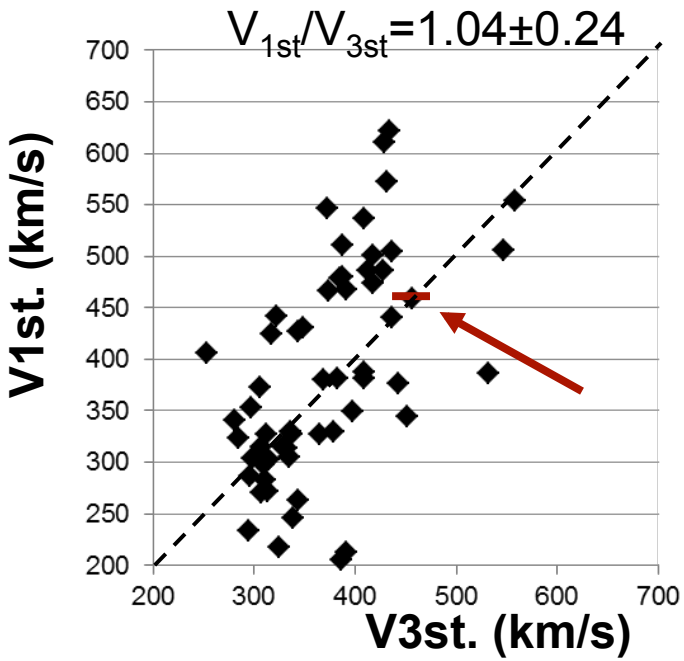

Spectrum Fitting Method
(Single-station meas.)
Speed $V_{1st.}$=459km/s
Axial Ratio=1.07
Spectral Index=3.8

⇔ **Cross Correlation Method**
(3-station meas.)
Speed $V_{3st.}$= 457±13 km/s

(Courtesy of M. Tokumaru)

Tokumaru, M., *et al.*, 2013, *AOGS 2013 Presentation* , June, Brisbane, Australia.

Heliospheric Tomography

Summary:

IPS analysis:

A ground-based technique. Can provide low-resolution velocity and density analysis, and accurate forecasts of time-variable heliospheric structure.

Other ground-based analyses such as heliospheric Faraday rotation can possibly be provided from the same radio systems.
The IPS analysis can provide input to 3D-MHD models.
Better, and more abundant IPS data, should be available in the near future.

Heliospheric Tomography

Jackson, B.V., et al., 2008, *Adv. in Geosciences*, 21, 339-360.

The UCSD 3D-reconstruction program

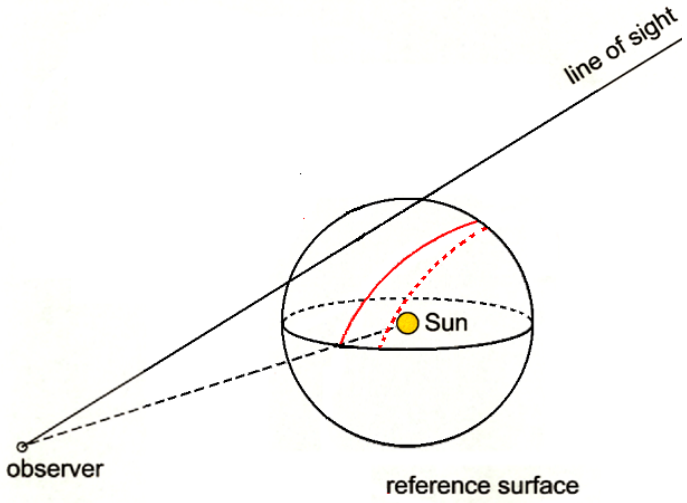

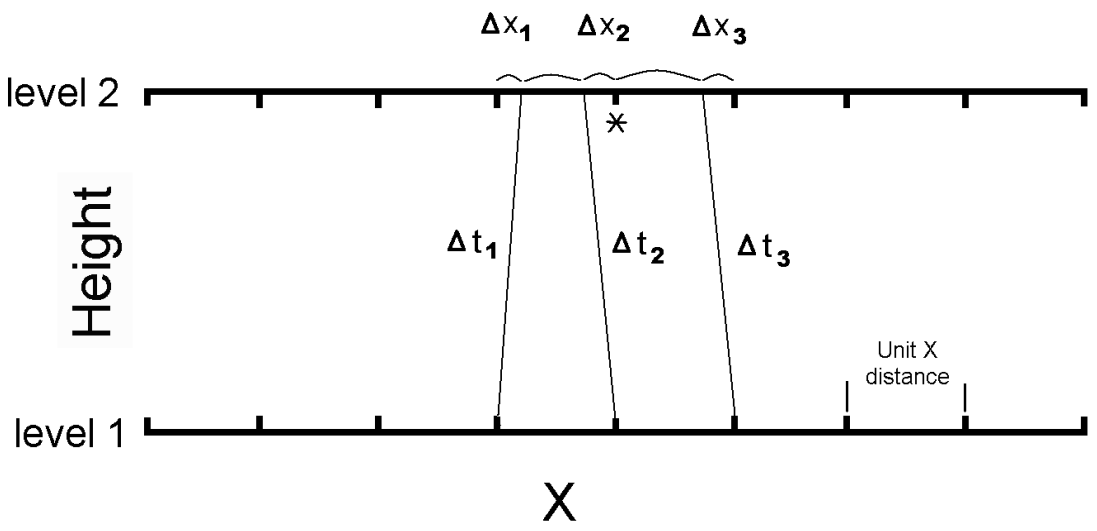

The "traceback matrix" (any solar wind model works)

In the traceback matrix the location of the upper level data point (starred) is an interpolation in x of Δx2 and the unit x distance – Δx3 distance or (1 – Δx3). Similarly, the value of Δt at the starred point is interpolated by the same *spatial* distance. Each 3D traceback matrix contains a regular grid of values ΣΔx, ΣΔy, ΣΔt, ΣΔv, and ΣΔm that locates the origin of each point in the grid at each time and its change in velocity and density from the heliospheric model.

Heliospheric Tomography used to Provide Velocities, Densities, and Vector Magnetic Fields

B.V. Jackson
and
H.-S. Yu, P.P. Hick, A. Buffington, D. Odstrcil
Center for Astrophysics and Space Sciences,
University of California at San Diego, LaJolla, CA, USA

http://smei.ucsd.edu/ **http://ips.ucsd.edu/**

Heliospheric Tomography

Solar Mass Ejection Imager (SMEI) Analysis

Heliospheric Tomography

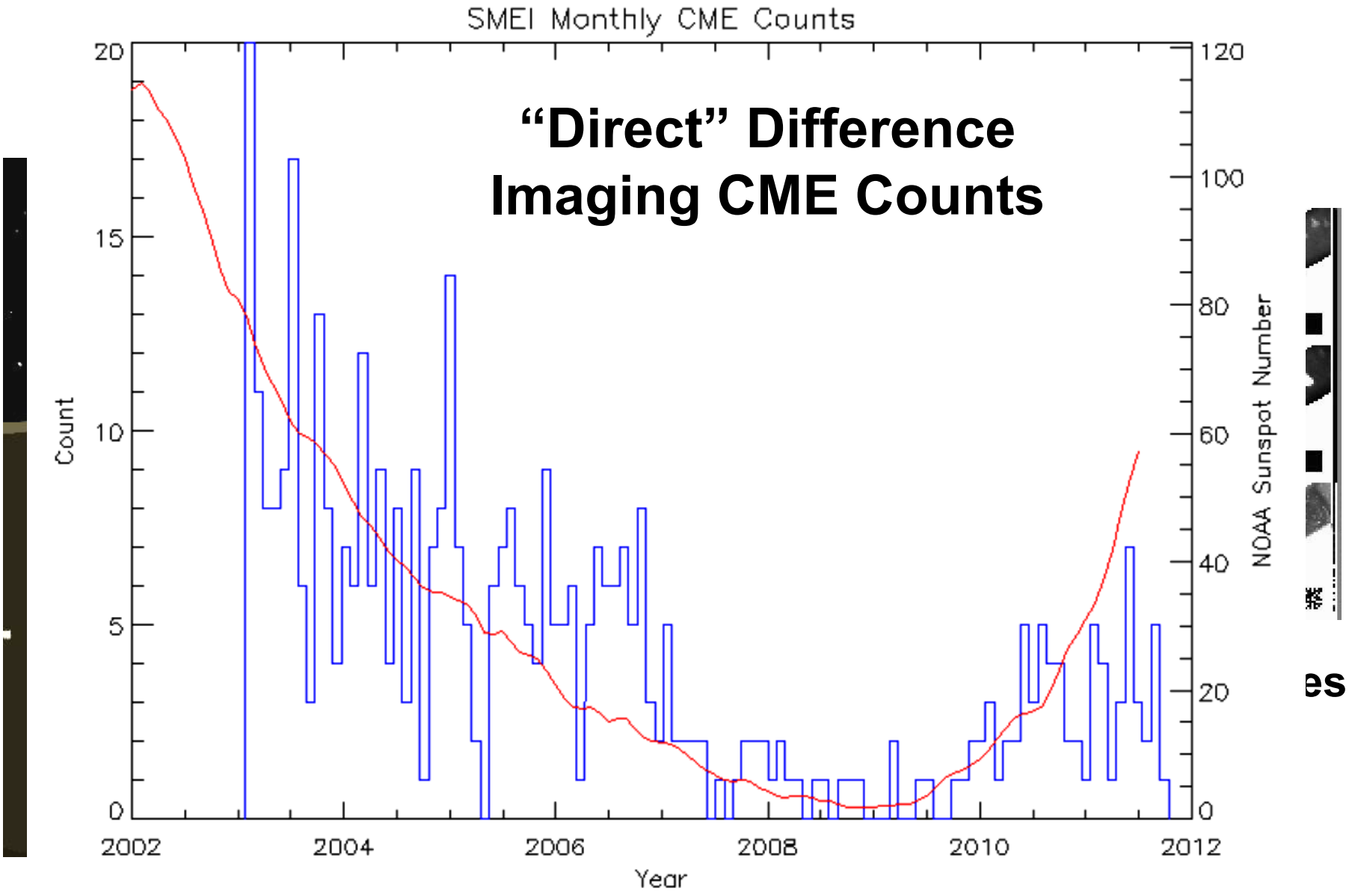

Heliospheric Tomography

SMEI

2003 May 27-28 CMEs

Brightness from the 28 May 2003 halo CMEs: Direct difference (top), 3D-reconstruction (bottom).

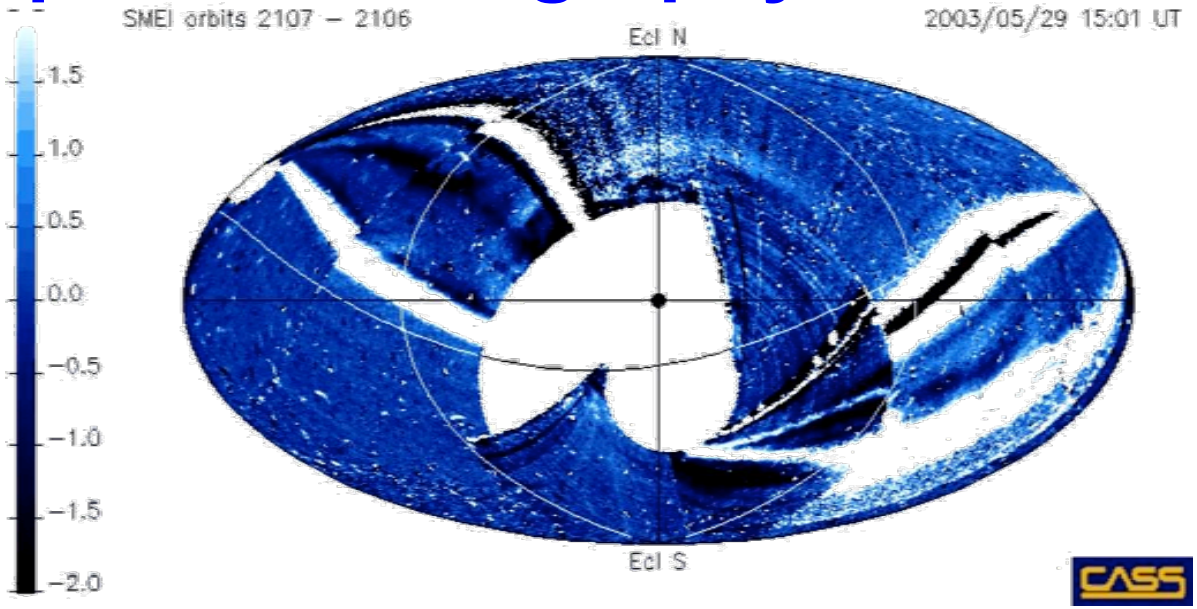

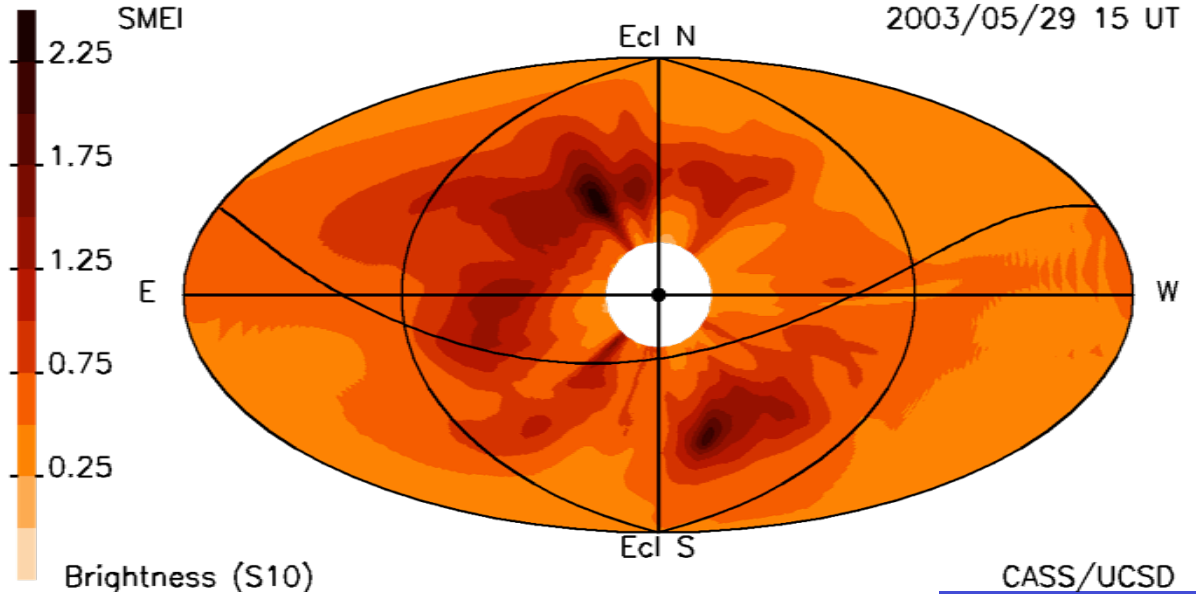

Heliospheric Tomography

Jackson, B.V., *et al.*, 2008, *J. Geophys Res.*, 113, A00A15, doi:10.1029/2008JA013224

2003 May 27-28 CME events

SMEI density 3D reconstruction of the 27-28 May 2003 halo → CMEs as viewed from 30º above the ecliptic plane about 30º west of the Sun-Earth line.

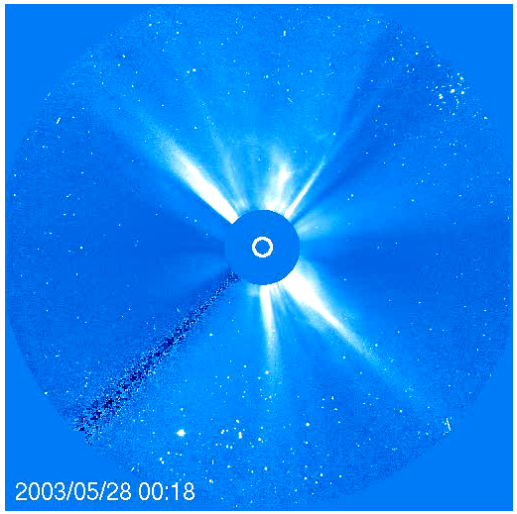

LASCO C3

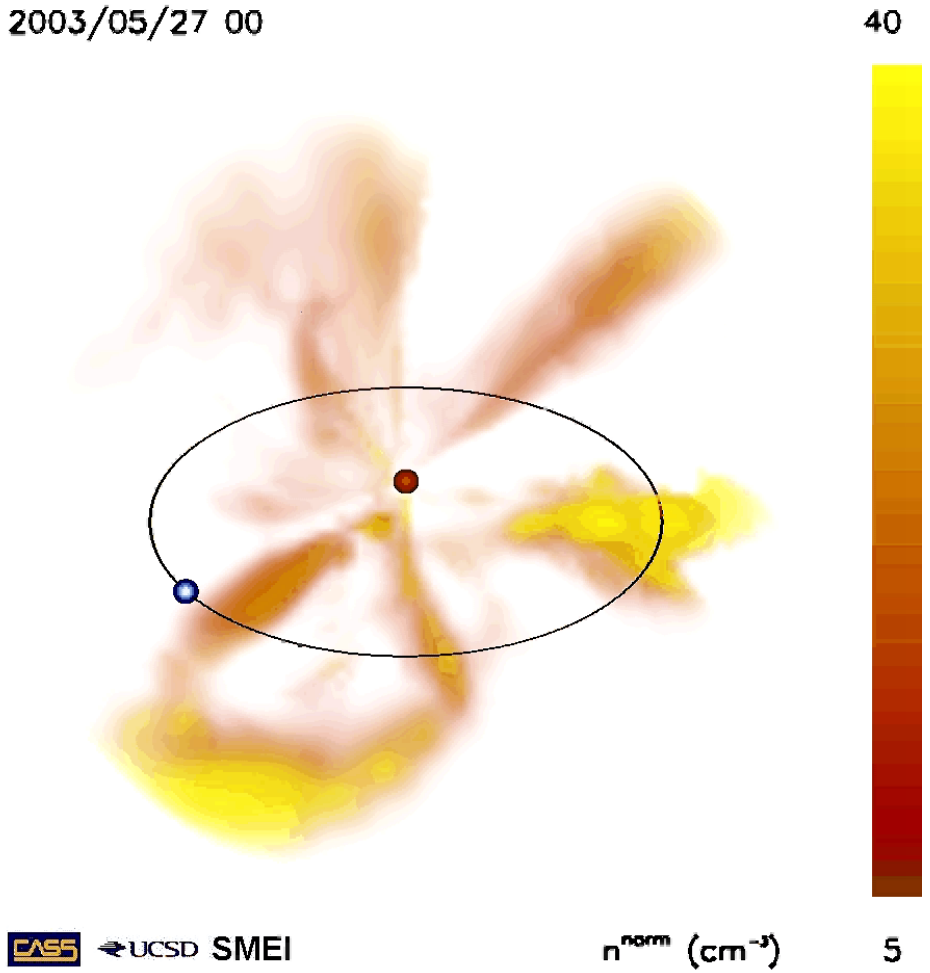

SMEI density (remote observer view) of the 27-28 May 2003 halo CMEs

Heliospheric Tomography

Jackson, B.V., *et al*., 2008, *J. Geophys Res*., 113, A00A15, doi:10.1029/2008JA013224

27-28 May 2003 CME event period

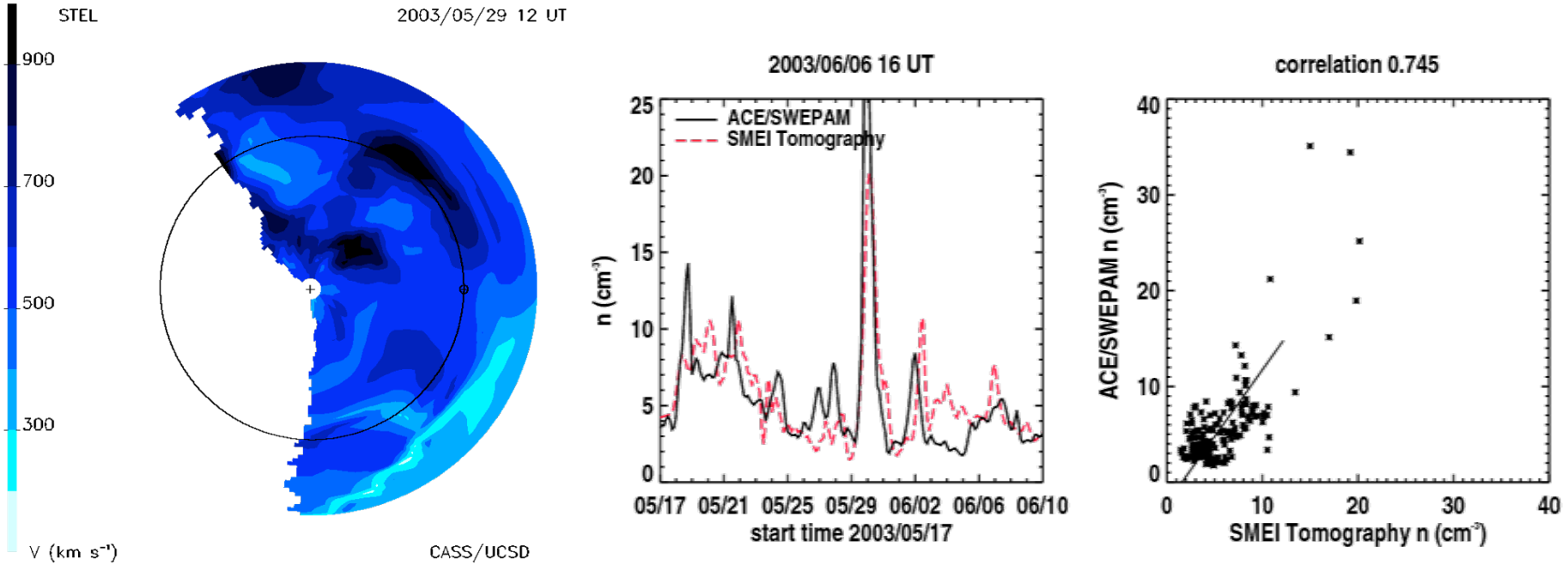

Full SMEI data set, 6-hour cadence, 3º x 3º lat, long

SMEI proton density reconstruction for the 27-28 May 2003 halo CME sequence. Reconstructed and ACE L2 *in-situ* densities are compared over one Carrington rotation.

Heliospheric Tomography

Jackson, B.V., *et al.*, 2008, *J. Geophys Res.*, 113, A00A15, doi:10.1029/2008JA013224

2003 May 27-28 CME events

CME mass

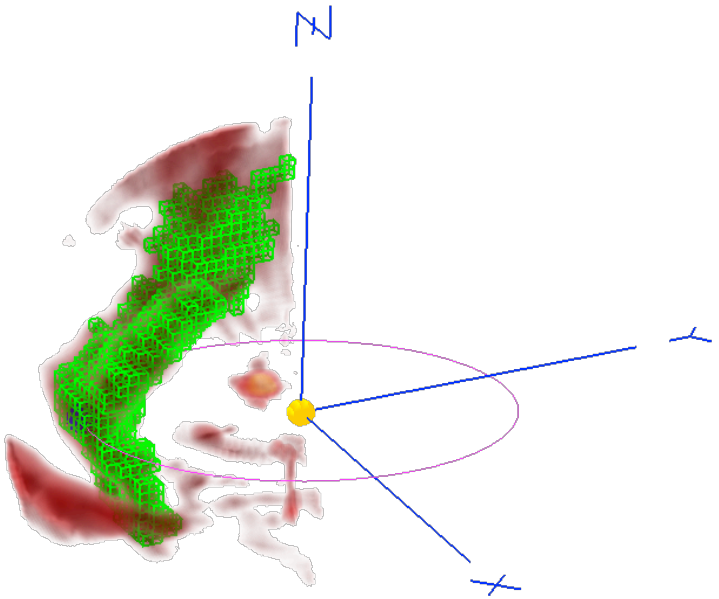

Excess Mass(g): 1.844E+016
Total Mass(g): 2.491E+016
Ambient (g): 6.470E+015
Energy (ergs): 3.448E+031

2003/05/30 00:00 UT

Volume: 0.144 AU^3

Heliospheric Tomography

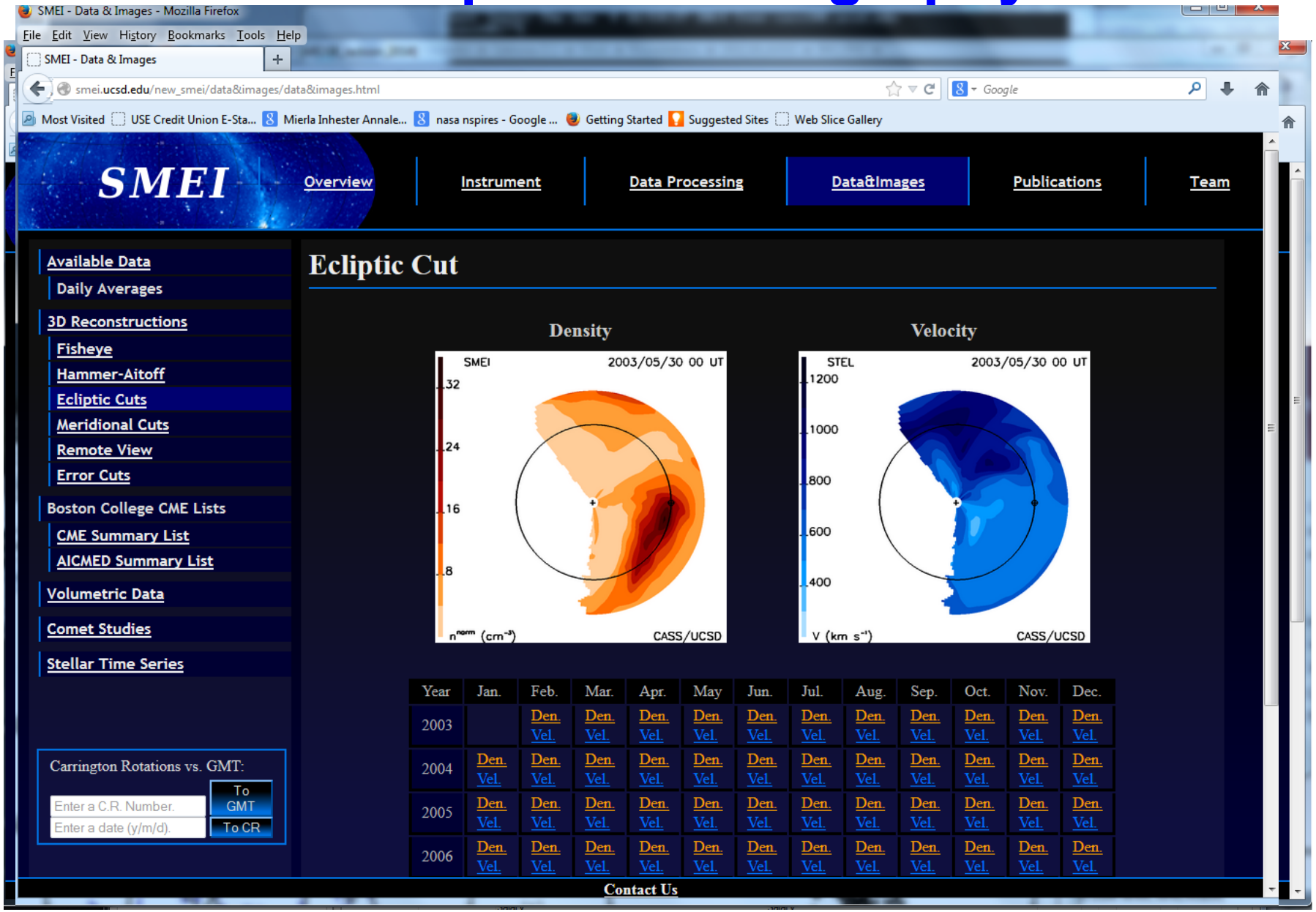

SMEI Webpages - http://smei.ucsd.edu